

# Times are changing

*Implications of climate change for the occurrence and predictability of tipping points*



Bregje van der Bolt

## Propositions

1. Safe rates of change need to be determined in order to keep the planet within the safe operating space. (This thesis)
2. Slowing down can be both a driver of, and an indicator for critical transitions. (This thesis)
3. Theoretical ecologists stay largely shielded from real-world problems, by tending to only offer proof-of-principles and synthetic examples, leaving the rest of the field with little guidance on how to apply their methods.
4. Most ecological research is not replicable, and never will be.
5. The incentives of academic research are at sharp odds with the need for data-driven, highly collaborative interdisciplinary research.
6. Both the level of PhD students and the quality of science improves when one of the chapters must be a replicate study that challenges the results of a previous study.
7. Scientists should not participate in the public debate.

Propositions belonging to the thesis, entitled,  
*'Times are changing.  
Implications of climate change for the occurrence and  
predictability of tipping points'*  
Bregje van der Bolt  
Wageningen, 10 January 2020

# **Times are changing**

Implications of climate change for the occurrence and  
predictability of tipping points

**Bregje van der Bolt**

## **Thesis committee**

### **Promotor**

Prof. Dr M. Scheffer

Distinguished Professor of Aquatic Ecology and Water Quality Management  
Wageningen University & Research

### **Co-promotor**

Dr. Egbert H. van Nes

Associate Professor, Aquatic Ecology and Water Quality Management Group  
Wageningen University & Research

### **Other members**

Dr Elisa Benincà, Rijkinstituut voor Volksgezondheid en Milieu, Bilthoven

Prof. Dr Fulco Ludwig, Wageningen University & Research

Prof. Dr Max G. Rietkerk, Utrecht University

Prof. Dr Appy Sluijs, Utrecht University

This research was conducted under the auspices of the Graduate School of Socio-Economic and Natural Sciences of the Environment (SENSE).



# **Times are changing**

Implications of climate change for the occurrence and  
predictability of tipping points

**Bregje van der Bolt**

## **Thesis**

submitted in fulfilment of the requirements for the degree of doctor  
at Wageningen University

by the authority of the Rector Magnificus

Prof. Dr A.P.J. Mol,

in the presence of the

Thesis Committee appointed by the Academic Board

to be defended in public

on Friday 10 January 2020

at 13.30 p.m. in the Aula.

Bregje van der Bolt

Times are changing. Implications of climate change for the occurrence and predictability of tipping points

146 pages

PhD thesis, Wageningen University, Wageningen, the Netherlands (2020)

With references, with summary in English

ISBN: 978-94-6395-180-7

DOI: <https://doi.org/10.18174/504573>

Voor Henk

*Had je dit nog maar kunnen zien.*



# CONTENTS

## **Chapter 1**

Introduction	1
--------------	---

## **Chapter 2**

Early-warning signals for marine anoxic events	7
------------------------------------------------	---

## **Chapter 3**

Early warning of tipping points in slow systems	33
-------------------------------------------------	----

## **Chapter 4**

Rate-induced tipping in a population of cyanobacteria	59
-------------------------------------------------------	----

## **Chapter 5**

Climate reddening promotes the chance of critical transitions	85
---------------------------------------------------------------	----

## **Chapter 6**

Afterthoughts	109
---------------	-----

References	125
------------	-----

Summary	136
---------	-----

Acknowledgements	138
------------------	-----

A few words about the author	142
------------------------------	-----

List of publications	143
----------------------	-----

SENSE certificate	144
-------------------	-----





# CHAPTER 1

## INTRODUCTION

Bregje van der Bolt

*“Time changes everything  
except something within us  
which is always surprised by change.”*

– Thomas Hardy

### TIPPING POINTS

As recent as 6,000 years ago, the Sahara looked like modern South Africa. Large rivers crossed the region, vegetation was abundant, and numerous wetlands were scattered over the area. But around 5,000 years ago, everything changed. The rivers dried up, trees died, and the soil disappeared. The Sahara shifted from a fertile and green state to the desert state we know today (deMenocal, Ortiz, Guilderson, & Sarnthein, 2000).

This change was most likely an example of a critical transition that happened at a tipping point: a point where the system shifts to another state. On an abstract level, the Sahara behaved as a capsizing canoe. Imagine that you are sitting in a canoe. If you lean over to one side, there is a point where you capsize; Suddenly, you are in another stable state. Also, returning to the previous state is difficult: once you capsized, getting back requires more than leaning a bit less to the side. It is hard to see the tipping point coming, because the position of the system changes relatively little up to the tipping point.

### FORESEEING TIPPING POINTS: SLOWING DOWN AS A SYMPTOM

A concept that is closely linked to tipping points is resilience. Ecological resilience is defined as the ability of the system to recover to the original state - or equilibrium - upon a disturbance (Holling, 1973). Close to the tipping point, a system has very low resilience. This can also be experienced while sitting in the canoe; When you are sitting in the middle of the canoe, a small wave will not tip you over. If you lean sideways, however, the same small wave could be just enough to bring you past the tipping point. In reality, the environment is never constant, and systems are permanently affected by a regime of disturbances. While these disturbances have the potential to cause a shift to an alternative stable state, we can also use these disturbances to determine the resilience of the system. When a system is close to a tipping point, it recovers more slowly from disturbances than when it is far from a tipping point. This phenomenon is called critical slowing down (Wissel, 1984). If a systems moves gradually towards the tipping point, the recovery from the disturbances becomes slower and slower (van Nes & Scheffer, 2007). The implication of critical slowing down is that the recovery rate of the system after a small experimental perturbation can be used as an indicator of how close the system is to the tipping point (van Nes & Scheffer, 2007).

Critical slowing down is expected to lead to an increase in autocorrelation of the system state (Ives, 1995). The overall rates of change in the system decrease, and as a result,



the state of the system at any given moment becomes more and more like its previous state. Imagine that you take a picture of a dancing person every second. If the person is dancing wildly, every picture will be completely different from the previous picture, but when the person is slowly dancing, subsequent pictures will look very similar. Over a whole night out, the pictures of the dancing person might be very different, but as the person gets more tired and starts dancing slower, successive pictures become more and more similar. The same occurs in the system state that is nearing a tipping point. The increase in ‘memory’ of the system can be measured in various ways, but the simplest method is to look at the lag-1 autocorrelation (Dakos et al., 2008; Held & Kleinen, 2004).

An additional effect of becoming tired may be that the dancer gets a larger swing. Such increase in the variance of the system state is another possible consequence of critical slowing down (S. R. Carpenter & Brock, 2006). As the return rates decrease when approaching the tipping point, the impact of the perturbations do not decay as fast. Before the system is back in its equilibrium, the next perturbation brings the system away from the equilibrium again. The accumulating effect of these perturbations results in an increase of the variance (Marten Scheffer et al., 2009).

## IMPLICATIONS OF RAPID CLIMATE CHANGE FOR TIPPING POINTS

The idea that we may sense the proximity of tipping points from the phenomenon of critical slowing down is based on the assumption that the state of a system is typically some kind of equilibrium state (Marten Scheffer, Carpenter, Dakos, & van Nes, 2015). This requires among other things that environmental drivers change slowly compared to the speed of the system. Otherwise the system cannot track the changing conditions fast enough and may wander far away from its equilibrium. Clearly, this assumption does not always hold. Some ecosystems respond relatively slowly to changes in the environment (Hughes, Linares, Dakos, van de Leemput, & van Nes, 2013; Karssenberg, Bierkens, & Rietkerk, 2017). Consequently, their state lags behind the equilibrium (or more precisely the dynamical ‘regime’) to which they would converge if conditions were constant. Critical slowing down may be difficult to observe in such systems before they reach a tipping point because the internal response rate of the system is slow to begin with. Current environmental changes occur at unprecedented rates (Joos & Spahni, 2008; Zeebe, Ridgwell, & Zachos, 2016). These changes include increases in atmospheric CO<sub>2</sub> and other greenhouse gasses (Joos & Spahni, 2008; Zeebe et al., 2016), loss of ice mass on land (Bevis et al., 2019), biodiversity loss (Rockström et al., 2009), and land-use change (Klein Goldewijk, Beusen, Van Drecht, & De Vos, 2011). These fast

## CHAPTER 1

rates of environmental change make the intrinsic response rates of the system relatively slow.

Another assumption of most theoretical studies of critical slowing down is that the system is forced with white noise, i.e. noise that is uncorrelated in time. The climate system, however, involves slow processes causing the power spectrum to have pronounced low frequencies. As a result, climatic dynamics that are forcing ecosystems and societies are often autocorrelated on time scales that are also characteristic of the systems they affect (Trenberth, 1984). In addition, in some parts of the climate, the stochastic regime of the climate is becoming more time-correlated. For example, the Pacific Decadal Oscillation and North Pacific sea surface temperatures have become more time-correlated in the period from 1900 to 2015 (Boulton & Lenton, 2015; Huntingford, Jones, Livina, Lenton, & Cox, 2013).

This thesis is concerned with tipping points in the context of climate change. The aim of this thesis is to help bridging the gap between theory and reality along two lines:

- *To assess how changes in the relative time scales of environmental change and the speed of the system affect the occurrence and predictability of tipping points.*
- *To assess how changes in the stochastic regime of the climate affect the probability of tipping.*

In other words, I analyze how changes in the relative timescales as a result of climate change may affect the chance of critical transitions, and how it may affect our ability to predict these transitions.

## THESIS OUTLINE

I start with a relatively straightforward case where the assumptions of the theory of critical slowing down appear to be met. In **Chapter 2**, I analyse repeated widespread marine anoxic events that occurred in the eastern Mediterranean Sea, using high resolution and almost evenly spaced records, and test whether an increase in the resilience indicators occurred prior to these events. The time series I used differ from most other climate reconstructions which often have a low resolution and irregularly spaced observations. The result is a relatively clean case where indicators of slowing down are clearly detectable, indicating that those anoxic events correspond to critical transitions of a system approaching a tipping point.


An obvious possibility when it comes to current climate change is the use of indicators of critical slowing down as warning flags suggesting a loss of resilience. However, this may be problematic in practise. One problem is that not all shifts to another stable state unfold rapidly. Slowly responding systems may show little change at all even if the tipping point has been passed already (Hughes et al., 2013). The resulting gradual change may go unnoticed. Certainly, such transitions do not fit the simple view that once the tipping point is exceeded, the system will quickly ‘collapse’ to the alternative stable state. In **Chapter 3** I ask under which conditions a change in trend in resilience indicators prior to shifts may become unnoticeable in such slow-responding systems.

If the system’s response is slow compared to the rate of change of the conditions, also another interesting phenomenon can occur. In some models a relatively fast change in the conditions may trigger a shift to an alternative stable state, whereas a change of the same magnitude but at slower rates would not. This phenomenon of rate-induced tipping has only been described recently (Ashwin, Wieczorek, Vitolo, & Cox, 2012; Marten Scheffer, Van Nes, Holmgren, & Hughes, 2008) and is especially relevant in the context of the ongoing rapid global change and its impact on ecosystems. Only two studies investigate the possibility of rate-induced tipping in ecology (Marten Scheffer et al., 2008; Siteur, Eppinga, Doelman, Siero, & Rietkerk, 2016). In **Chapter 4**, I demonstrate rate-induced tipping in a model of cyanobacteria with realistic parameter settings (Faassen et al., 2015).

Lastly, in **Chapter 5** I address the effect of the slowness of climate fluctuations on the probability that they will cause a critical transition in nature or society. Such slowness (or ‘memory’) is measured as temporal autocorrelation. The state of the atmosphere is autocorrelated on a daily timescale, while surface ocean temperatures can persist for several months (Frankignoul & Hasselmann, 1977; Hasselmann, 1976) and modes of decadal variability in surface ocean temperatures exist (Mantua et al., 1997; Schlesinger & Ramankutty, 1994). In addition, the autocorrelation in the environmental time series may change over time (Lenton, Dakos, Bathiany, & Scheffer, 2017).

The main findings are brought together in a broader context in **Chapter 6**. In this chapter, I question the applicability of the resilience indicators in a changing climate, address the problems with determining the underlying system dynamics from observations, and give an outlook on how future research might address such issues.

## CHAPTER 1



# CHAPTER 2

## EARLY-WARNING SIGNALS FOR MARINE ANOXIC EVENTS

Rick Hennekam\*,  
Bregje van der Bolt\*,  
Egbert H. van Nes,  
Gert J. de Lange,  
Marten Scheffer,  
and Gert-Jan Reichart

\* Joint lead authors

*“The consequences of our actions  
are so complicated, so diverse,  
that predicting the future  
is a very difficult business indeed.”*

- Albus Dumbledore

### ABSTRACT

In deep time, massive marine anoxic events have occasionally triggered mass extinction events. Today's oceans and seas are again losing oxygen due to rising temperatures and coastal eutrophication, leading to increasing worries about anoxic dead zones. Here, we present high-resolution reconstructions of past oxygen dynamics in the Mediterranean Sea using deep-sea sediments, revealing that the repeated shifts into marine anoxic events in this basin had the character of critical transitions. Such transitions happen when a system reaches a tipping point where change becomes self-propelling. Long before the onset of most anoxic events there was a gradual rise in temporal autocorrelation and variance in deoxygenation in the deep sediment cores (>1600 meter depth). These statistical indicators are hallmarks of critical slowing down, signalling a steady loss of resilience of the oxygenated state as the system approached a tipping point. Our results imply that, even without precise knowledge of the mechanisms involved, early-warning signals for widespread anoxia in marine systems are recognizable using an appropriate statistical approach.

*Submitted in revised form to PNAS*

## INTRODUCTION

Deoxygenation of our oceans and seas is one of the most profound consequences of global environmental and climatological change (Breitburg et al., 2018; Keeling, Körtzinger, & Gruber, 2010; Levin, 2018). Increasing water temperatures result in lower gas solubility, enhanced respiration processes, and stratification of the water column, while eutrophication increases primary productivity and related aerobic respiration of organic matter that settles to the seafloor (Keeling et al., 2010; Kemp, Testa, Conley, Gilbert, & Hagy, 2009). As a result, parts of the ocean become anoxic (zero oxygen). Oxygen is fundamental for aerobic life and biodiversity, and plays an essential role in the biogeochemical cycling of carbon, nitrogen and other important elements (Diaz & Rosenberg, 2008; Middelburg & Levin, 2009). Deoxygenation of our oceans will, therefore, have large consequences for marine organisms and biogeochemical cycling. Yet, mechanisms involved in the commonly rapid transition into anoxia are still poorly understood (Kemp et al., 2009; Levin, 2018), hampering prediction of these potential large-scale deoxygenation events in marine systems. Once shifted into an anoxic state, such systems may remain locked in an oxygen-depleted status quo – presumably through several feedback mechanisms – making restoration virtually impossible. Hence, it would be useful to have diagnostic indicators of the resilience of the oxygenated state, to probe if a transition into the anoxic state is likely. Here, we analyze past widespread anoxic events and associated organic-rich sediments ('sapropels') of the eastern Mediterranean Sea (Figure 2.1a), in search for such early-warning signals.

Anoxic events occurred regularly within this basin as a consequence of enhanced stratification and increased organic matter production (Rohling, Marino, & Grant, 2015). Episodes of deep-sea oxygen depletion are mainly related to changes in the hydrography, principally excessive monsoonal flooding from North Africa inhibiting intermediate- and deep-water formation and stimulating nutrient input (Rohling et al., 2015; Rossignol-Strick, 1985). These regular hydrological changes are strongly associated with changes in solar insolation (Figure 2.1b), being driven by variability in the Earth's axis and orbit shape relative to the Sun (i.e., orbital forcing) (Lourens, Wehausen, & Brumsack, 2001). Importantly, monsoonal changes are relatively gradual in comparison to the associated sudden transitions from oxic to anoxic conditions (and back), which occur within decades to centuries (Marino et al., 2007). This suggests that the abrupt transitions into anoxia correspond to critical transitions that happen as the system reaches a tipping point where change becomes self-propagating due to positive feedback mechanisms (Lenton, 2013).

## CHAPTER 2

As a system gradually approaches such a tipping point, recovery rates from small perturbations become increasingly sluggish (Marten Scheffer et al., 2009). In natural time-series where systems are subject to stochastic perturbations, such critical slowing down is often reflected in a rising variance and temporal autocorrelation (S R Carpenter & Brock, 2006; Ives, 1995; Marten Scheffer et al., 2009). This implies that in systems that gradually approach a tipping point such changes in the pattern of fluctuations may be interpreted as early-warning signals for critical transitions (Marten Scheffer et al., 2009).

To see if indicators of critical slowing down are detectable in the periods leading up to marine anoxic events, we reconstruct past oxygen conditions in the Mediterranean Sea using redox-sensitive trace element molybdenum (Tribovillard, Algeo, Lyons, & Riboulleau, 2006). Molybdenum (Mo) has been found to be an excellent indicator of oxygen depletion. It mimics changes in bottom-water oxygen and free-sulfide concentrations (Jilbert & Slomp, 2013), as Mo is largely unreactive in dissolved form under oxic conditions and locked in the sediment under conditions without oxygen and with free sulfide (called euxinia) (Algeo & Lyons, 2006). Recent technological advances in XRF-core-scanning (Hennekam, Sweere, de Lange, & Reichart, 2019), combined with the multivariate log-ratio calibration (MLC) (Weltje et al., 2015), allows to accurately measure Mo concentrations at resolutions necessary to observe potential early-warning signals. These novel tools are used here to produce high-resolution time series of two deep cores (>1600 m depth; MS66 and 64PE4o6E1) and one shallower core (1022 m depth; MS21), which in total contain eight past anoxic events. The obtained sampling rate (1-mm) relates to ~10-50 years, which allows to evaluate whether increased variability and autocorrelation are reliable early-warning indicators for tipping points in marine anoxia.

## RESULTS AND DISCUSSION

Repetitive episodes of eastern Mediterranean anoxia (sapropels numbered S<sub>1</sub> to S<sub>9</sub>; see Methods) related to insolation-driven monsoon intensifications (identified by titanium to aluminum ratios; Ti/Al) are clearly indicated by proxies for organic matter exported to the seafloor (barium; Ba) and anoxic conditions (Mo) (Figure 2.1b-d). In this area, Ti is mainly of aeolian origin, while Al originates mainly from Nile-derived clay (Lourens et al., 2001). Hence, Ti/Al indicates dry/wet phases related to North African monsoon intensity, largely following insolation (Lourens et al., 2001) (Figure 2.1b). Ba is here used as export-productivity proxy, as biogenic Ba (barite) is enriched in decaying organic matter settling to the seafloor (De Lange et al., 2008; Dymond, Suess, & Lyle, 1992).



Productivity likely increased because of additional nutrients by Nile River discharge, nutricline shoaling, and/or recycling of nutrients from the seafloor (Rohling et al., 2015). The signals truly reflect regional changes as the export-productivity patterns for the three cores look strikingly similar for the overlapping intervals (Figure 2.1c). The concurrent Ba variability within these and neighboring cores forms the foundation for the age models, which are tuned to excellently dated cave records (Grant et al., 2016; Ziegler, Tuenter, & Lourens, 2010) (see Methods). The high-resolution anoxia records, based on Mo (for ratios to Al see Extended Data Figure 2.1 and 4, showing that closed-sum effects are negligible), indicate a rapid oxidic-to-anoxic transition at the start of each sapropel (Figure 2.1d).

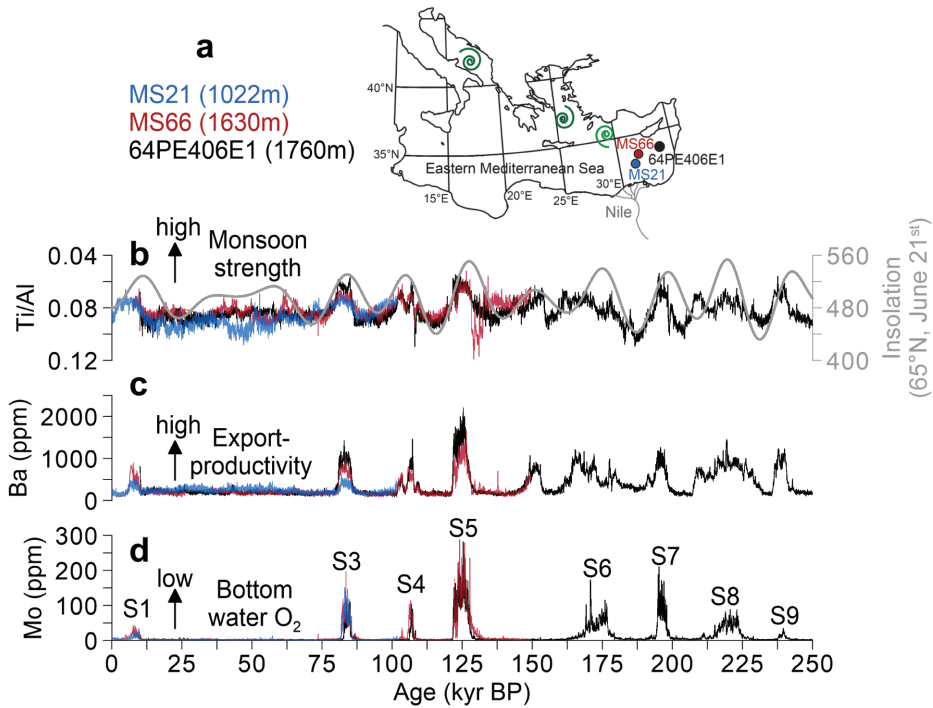


**Figure 2.1. Mediterranean Sea anoxic intervals (sapropels S1 to S9).** **a)** Map of the Eastern Mediterranean with core locations of the three studied cores: MS21 (blue), MS66 (red), and 64PE406E1 (black). Spirals indicate locations where modern-day intermediate-water (light green) and deep-water (dark green) formation occurs. **b)** Ti/Al ratio derived from MLC-calibrated XRF core scanning for the three cores. The June 21<sup>st</sup> 65°N insolation curve (W/m<sup>2</sup>) is shown in grey. **c)** Ba concentrations (ppm) derived from MLC-calibrated XRF core scanning for the three cores. **d)** Mo concentrations (ppm) derived from MLC-calibrated XRF core scanning for the three cores

## CHAPTER 2

Rising temporal autocorrelation and variance occur prior to most of the analyzed anoxic events in the relatively deep cores (MS66 and 64PE406E1) (Figure 2.2 and Table S2.1). These indicators of critical slowing down are calculated after detrending (see Methods and Extended Data Figure 2.5). There is no need to interpolate the data as the spacing between the data points is almost regular. Interpolating in this case led to unwanted aliasing effects that strongly affected autocorrelation and variance (Supplementary Information S2.1). Sensitivity analyses to probe the influence of bandwidth and window size confirm that the increases in variance and autocorrelation are robust against such choices of parametrization (Supplementary Information S2.2).

Our results suggest that the onsets of deep anoxic events were indeed associated to critical transitions at tipping points. Moreover, these results indicate that a gradual loss of resilience, as the system approached such tipping points, resulted in slowing down of the dynamics long (i.e., centuries to millennia) before the actual transitions (Fig. 2.2). Episodes of some oxygen depletion, hence, must have occurred well before the ultimate sudden shift to sapropel formation, potentially as anoxic ‘blankets’ (Casford et al., 2003).

Early-warning features for widespread anoxia are best captured at greatest depth, as suggested by the lack of increased autocorrelation and variance for shallow core MS21 for sapropel events S1 and S3 (Extended Data Figure 2.6). This concurs with reconstructions showing the strongest anoxia at greatest depths during sapropels (De Lange et al., 2008), and, by inference, intermittent anoxia seem to also develop earlier at larger depths. Similarly, the lack of increase in autocorrelation at ~1600–1800 meter during the relatively weak anoxic sapropels S1 and S9 suggests that signals for slowing down were absent at these depths.

Bistability between oxic versus anoxic states with rapid transitions in marine systems, such as the eastern Mediterranean Sea, must be driven by strong positive feedback mechanisms. A potential mechanism is the self-enforcing feedback between anoxic conditions and productivity. Increased productivity leads to anoxic conditions due to increased organic carbon burial and remineralization. In turn, anoxic conditions causes an increase of sedimentary phosphorus (P) efflux back to the water column (Kemp et al., 2009; Slomp, Thomson, & de Lange, 2002). Models that include these feedbacks are bistable and show critical slowing down in model simulations (Wang et al., 2012). Another possible mechanism is the Stommel’s salt-advection feedback (Stommel, 1961). Increased fresh-water input in the surface of the ocean decreases the salinity and the density of the water, decreasing the deep-water formation, leading to a slowing down of the overturning circulation. A decrease in the deep-water formation, in turn, reduces

the inflow of saltier and denser water from the western Mediterranean basin, which decreases deep-water ventilation even further (Rahmstorf et al., 2005; Stommel, 1961). Models of the thermohaline circulation are bistable due to the salt-advection feedback and show critical slowing down in model simulations (Dakos et al., 2008; Rahmstorf et al., 2005). Both these positive feedback mechanisms may be simultaneously at play, as reduced ventilation and increased productivity are both important to develop Mediterranean Sea anoxia (Rohling et al., 2015). The critical slowing down that we observe prior to the anoxic events does not allow unraveling which positive feedback mechanisms are relevant. Still, our results indicate the importance of these feedback processes involved in shifting an ocean basin into widespread anoxia.

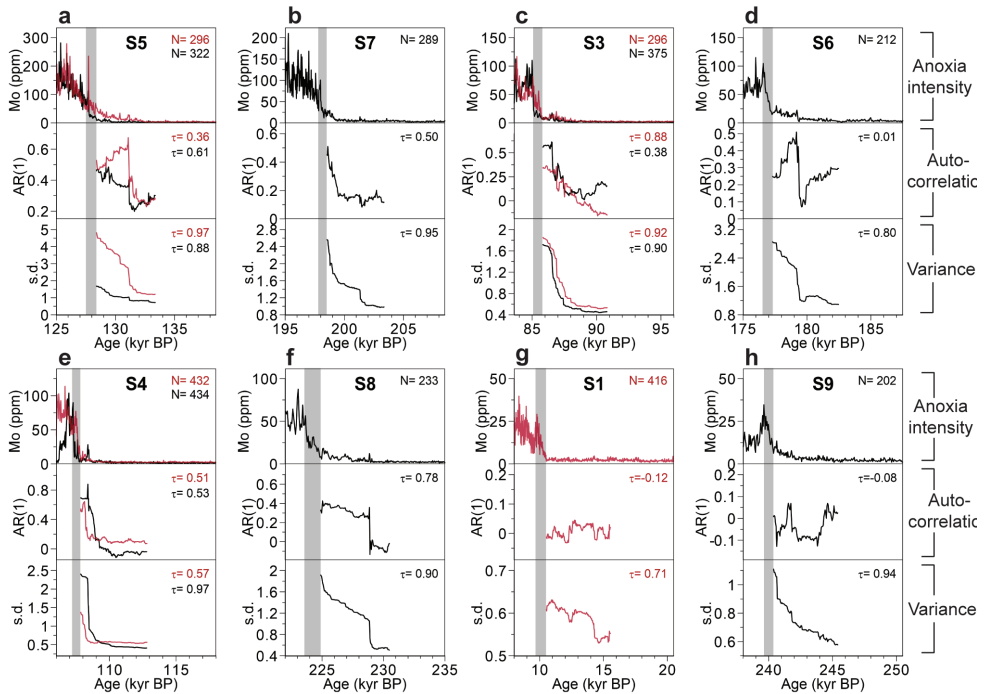
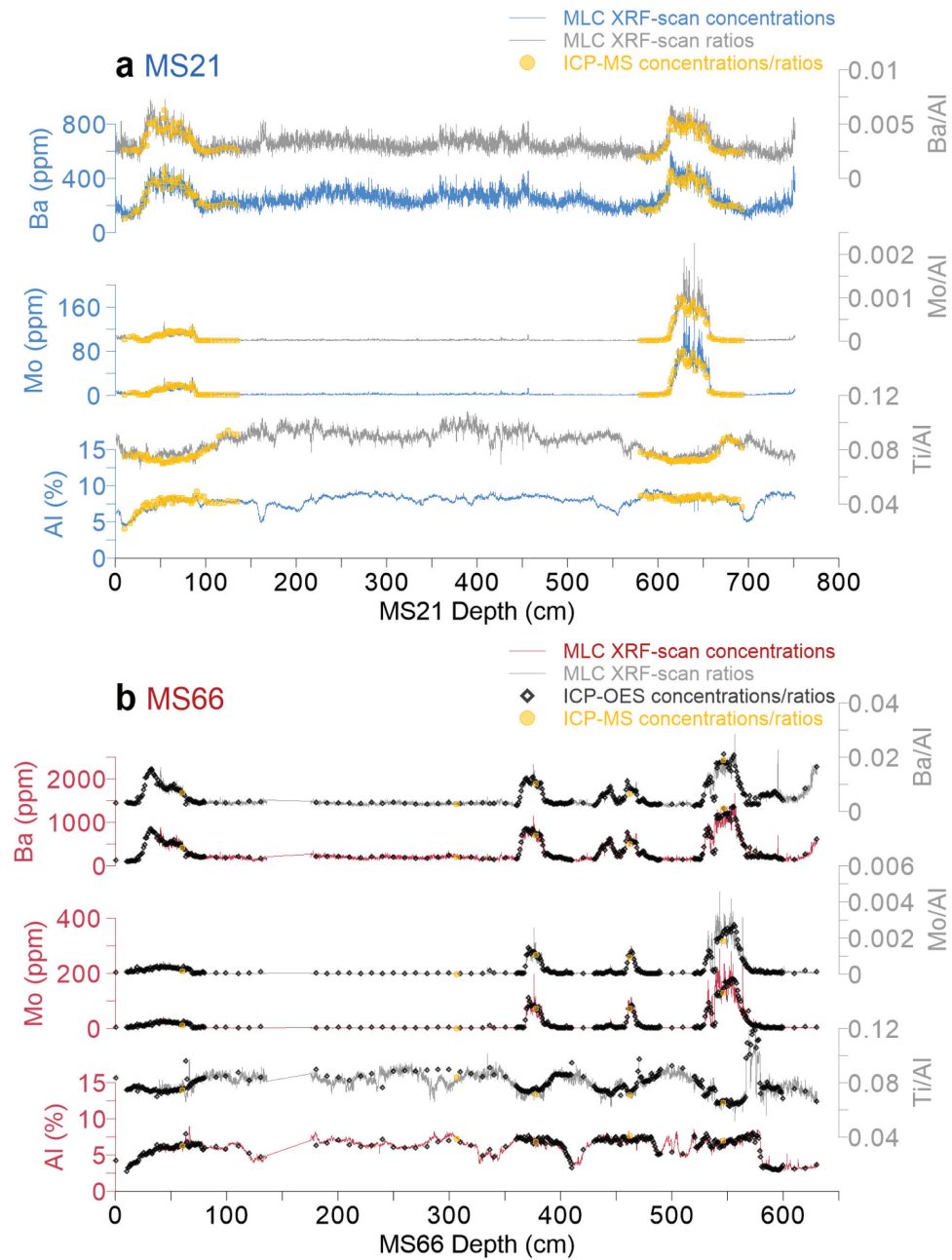
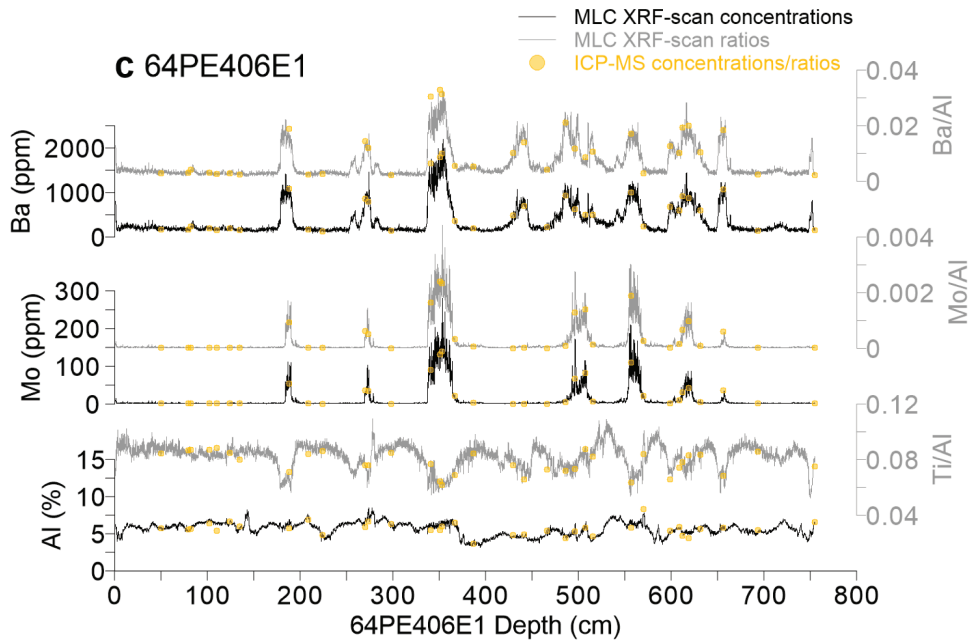


**Figure 2.2. Early-warning signals for eight past eastern Mediterranean anoxic events.** The anoxic events are ranked (a-h), based on their recorded Mo concentrations, from the strongest anoxic event at the top left (S5; a) and the weakest at the bottom right (S9; h). Each panel shows: an overview of the onset of the event (top), the pre-event autocorrelation as an indicator of slowing down (middle), and pre-event variance (bottom). The grey bands mark the transition intervals. Results for the two deepest cores are indicated: MS66 (red), and 64PE406E1 (black).

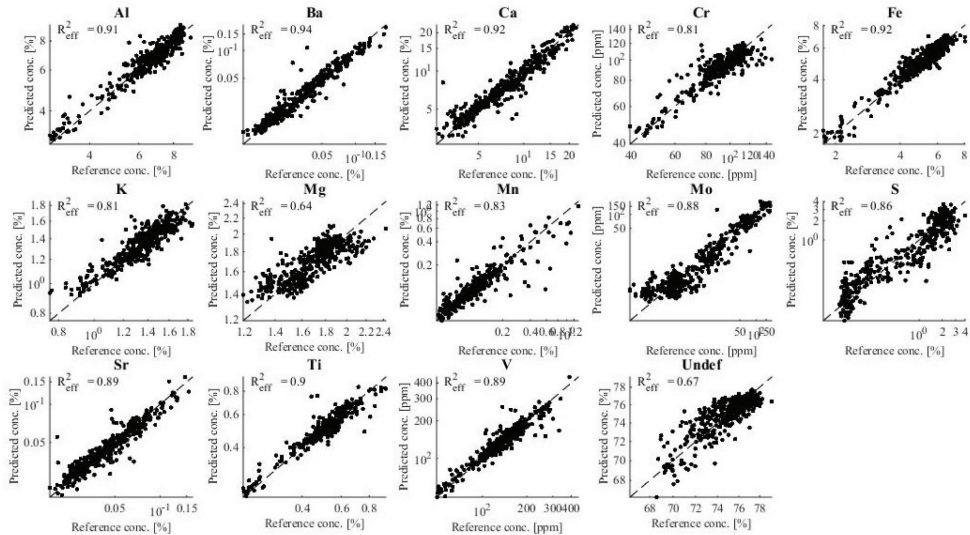
EXTENDED FIGURES



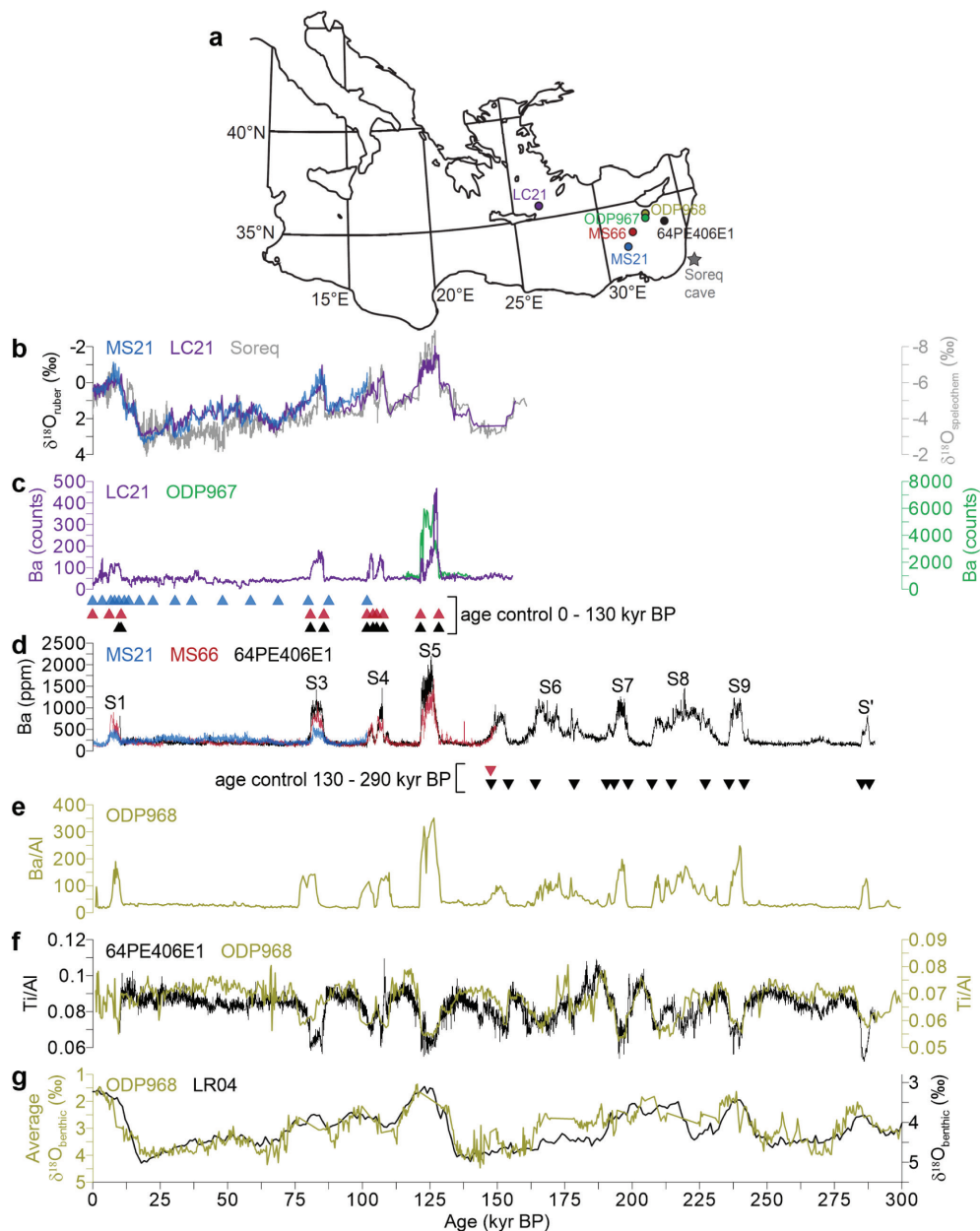
**Extended Data Figure 2.1.** The geochemical depth profiles of the cores. MS21 (blue; a), MS66 (red; b), and 64PE406E1 (black; c; see next page). Shown are Ba/Al, Ba (ppm), Mo/Al, Mo (ppm), Ti/Al, and Al (%), obtained through MLC XRF-core-scanning and the more conventional approaches of ICP-OES (black open diamonds) and ICP-MS (yellow circles). The conventional analyses were used for calibration of the XRF-core-scan results.



Extended Data Figure 1. (continued)



Extended Data Figure 2.2. Cross comparison of XRF-core-scanning and conventional geochemical analyses. Shown are the measured (ICP-MS and ICP-OES) and predicted (multivariate log-ratio calibrated XRF-core-scanning (Weltje et al., 2015)) concentrations for the three Mediterranean Sea cores combined, generated using the AvaaXelerate software (Bloemsmas, 2015).

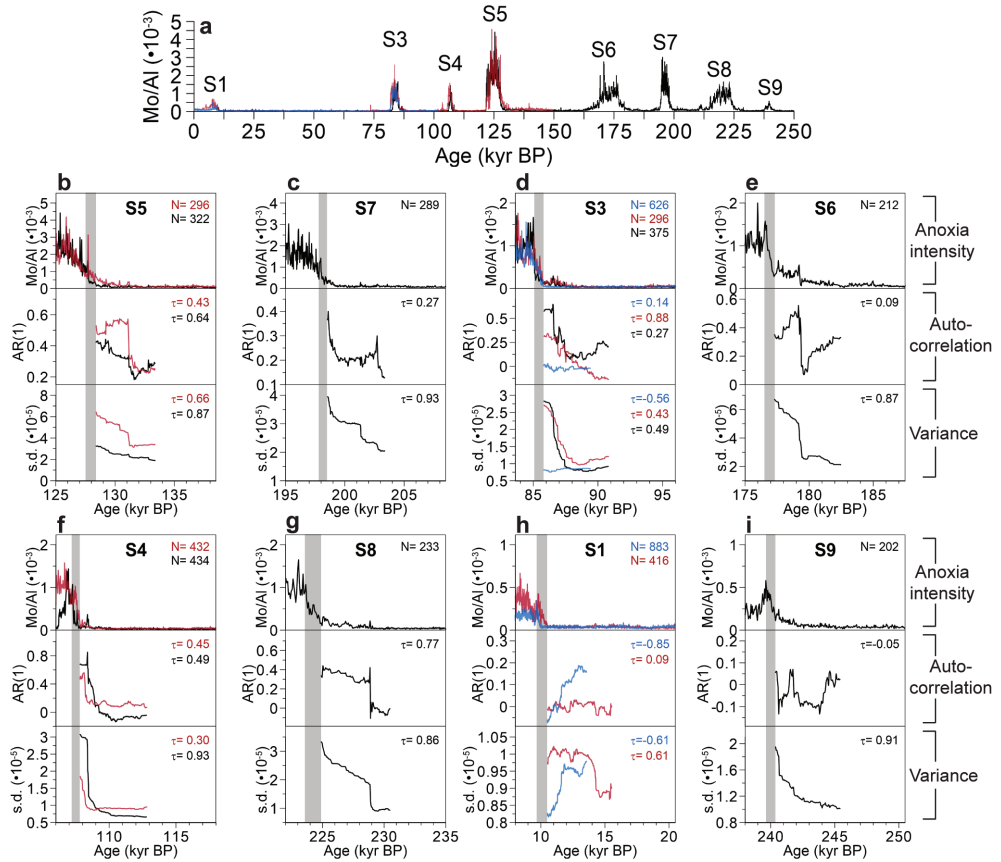


**Extended Data Figure 2.3. Age model construction.** **a**, Map of the cores used in this study (MS21, MS66, and 64PE406E1) and the companion records used for age model building (LC21, ODP967, ODP968, and Soreq cave). **b**, Soreq cave  $\delta^{18}\text{O}_{\text{speleothem}}$  versus LC21 (Grant et al., 2012) and MS21  $\delta^{18}\text{O}_{\text{ruber}}$  (Zwief et al., 2018). **c**, Ba intensities from XRF core scanning for LC21 (41-point moving average, following Grant et al. (2016)) and ODP967. **d**, Ba concentrations for MS21, MS66, and 64PE406E1 (this study). **e**, Ba/Al from ODP968 (Bloemsa, 2015). **f**, Ti/Al for 64PE406E1 (this study) and ODP968 (Ziegler et al., 2010). **g**, Comparison of average  $\delta^{18}\text{O}_{\text{benthic}}$  values, derived from different benthic foraminiferal species, for ODP968 (Ziegler et al., 2010) versus the LR04 benthic isotope stack (Lisiecki & Raymo, 2005). The age control points are shown for the

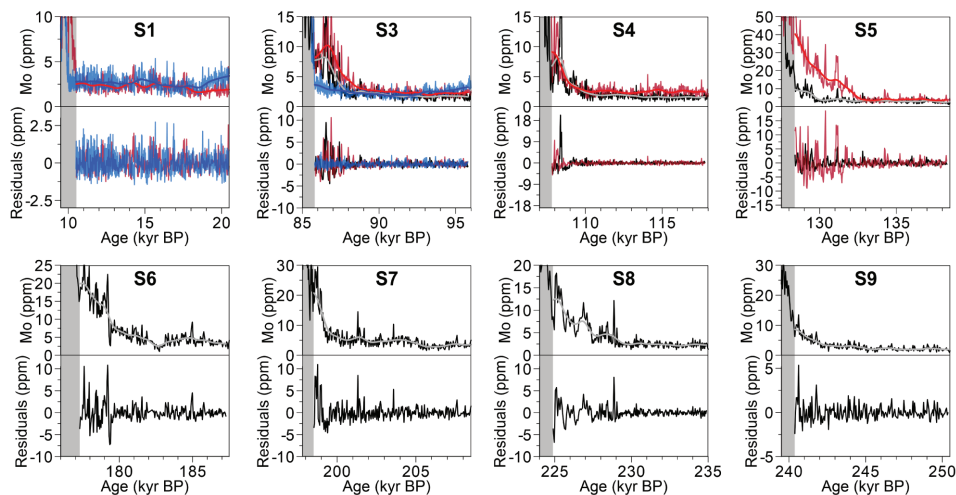


## EARLY-WARNING SIGNALS FOR MARINE ANOXIC EVENTS

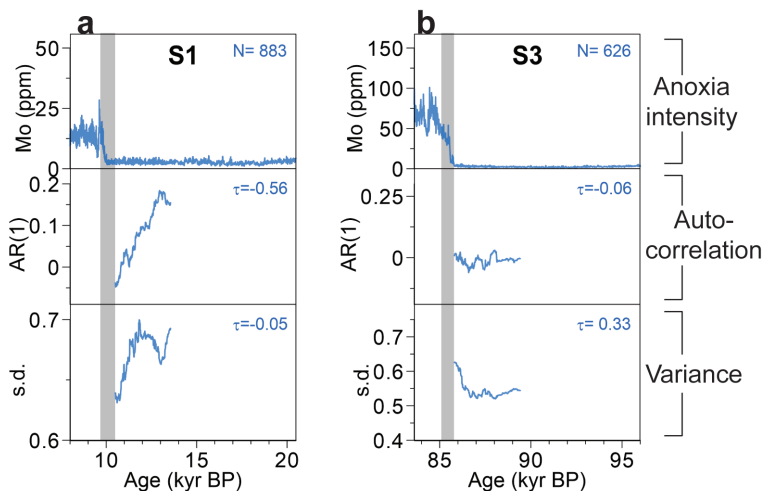
interval from 0-130 kyr BP ( $^{14}\text{C}$ -derived and through tuned to Soreq cave, LC21, and ODP967 records) and 130-290 kyr BP (tuned to ODP968) are indicated with triangles pointing upward and downward, respectively, and color coding following the colors of the cores in the map (a).



**Extended Data Figure 2.4. Early-warning signals for eight past eastern Mediterranean anoxic events with Mo to Al ratios.** a, Mo to Al ratio derived from MLC-calibrated XRF core scanning for the three cores. Note that elemental ratios to Al may be preferred to avoid closed-sum effects related to carbonate and organic matter concentration variability. However, results are quite similar as the concentration values as used in Figure 1 and 2 of the main text. b-i, Same as Figure 2 of the main text but than for Mo/Al instead of Mo concentrations.



**Extended Data Figure 2.5. Trend removal of the precursor phase of the eight eastern Mediterranean anoxic events S1 to S9.** The panels for the anoxic event show the Mo concentrations (ppm) for the three cores (MS21 in blue, MS66 in red, and 64PE406E1 in black) with the trends indicated by the thick lines (MS21 in blue, MS66 in red, and 64PE406E1 in grey) at the top. The panels show the residuals after removal of the trends (see Detrending in Methods) of the Mo records at the bottom. The grey bands mark the transition intervals for sapropels S1 to S9.



**Extended Data Figure 2.6. Early-warning signals for two past eastern Mediterranean anoxic events in shallow core MS21.** Shown are sapropel event S1 (a) and S3 (b) for relatively shallow core MS21 (blue). Each panel shows: an overview of the onset of the event (top), the pre-event autocorrelation (middle), and pre-event variance (bottom). The grey bands mark the transition intervals.



## SUPPLEMENTARY INFORMATION

### S2.1. METHODS

#### Sites, sediments, and sampling

Piston cores MS21 (30°20.7'N, 31°39.0'E; 1022 m water depth; 751.5 cm in length) and MS66 (33°1.9'N, 31°47.9'E; 1630 m water depth; 630 cm in length) were recovered during the MIMES cruise with the R/V Pelagia in 2004. Piston core 64PE406E1 (33°18.1'N, 33°23.7'E; 1760 m water depth; 920.5 cm in length) was recovered during the Eastern Mediterranean part of the 64PE406 (NESSC) cruise with the R/V Pelagia in 2016. The sediments consist primarily of grey-brown clays. All cores contain darker colored, organic-rich sediment intervals (i.e., sapropels), with MS21 containing sapropels S<sub>1</sub> and S<sub>3</sub>, MS66 containing sapropels S<sub>1</sub> to S<sub>5</sub>, and 64PE406E1 containing sapropels S<sub>1</sub> to S<sub>10</sub>. Note that the existence of sapropel S<sub>2</sub> (~55 kyr BP) is still controversial, and in any case, this sapropel interval is mostly missing or very weakly expressed in Eastern Mediterranean sediments<sup>32</sup> and thus not included in our analyses.

The working halves of the cores were sampled in order to calibrate the XRF-core-scan results. Core MS21 was discretely sampled with a 0.5-cm resolution, while cores MS66 and 64PE406E1 were sampled with a 1-cm resolution, for their entire core lengths.

#### Geochemical analyses

The three Mediterranean cores were analyzed for their inorganic geochemistry using X-Ray Fluorescence (XRF) core scanning with an Avaatech core scanner at the Royal Netherlands Institute of Sea Research (NIOZ). This core scanner contains a new generation Rayspec cubed SiriusSD silicon drift detector with a 40 mm<sup>2</sup> active area (30 mm<sup>2</sup> collimated) and a preamplifier integrated on the detector crystal, which is capable of accurate trace-element analyses (Hennekam et al., 2019). The wet core material was, before analyses, carefully flattened and then covered with a 4-μm SPEXCerti Ultralene foil to avoid sediment dehydration and contamination of the measurement prism during XRF-core-scanning. Measurements were performed on the reference halves of the core material with a 1 mm (down-core) by 12 mm (cross-core) slit size and with a 1-mm step size (i.e., 1-mm resolution results). We measured a range of elements, necessary for an effective calibration (see below), following the energy settings tested in Hennekam et al. (2019): Mg at 10 kV (no primary beam filter), Al to Fe at 20 kV (with an Al primary beam filter), Sr at 30 kV (with a Pd-thick primary beam filter),

## CHAPTER 2

and Mo and Ba at 50 kV (with a Cu primary beam filter). The currents for the 10 kV, 20 kV, 30 kV, and 50 kV measurements were set at 1.0 mA, 1.25 mA, 1.3 mA, and 0.5 mA, respectively, and measurement times were set at 30 s, 45 s, 60 s, 60 s, respectively. Eight reference materials (GSR-4, GSR-6, GSD-10, JSd-1, JSd-3, MESS 3, SARM 2, and SARM 3), loosely pressed in polyethylene containers, were measured before and after a core section. These standards indicated a relative standard deviation (i.e., precision) <10% for all measured elements, and showed that the XRF-core-scanner performance was constant for the entire duration of the experiment.

To calibrate the XRF-core-scanner data, a subset of the discrete samples were used and prepared for measured by inductively coupled plasma mass spectrometry (ICP-MS) and ICP-optical emission spectroscopy (ICP-OES). Samples were selected to ascertain a balanced representation of sapropel and non-sapropel geochemistry (see Extended Data Fig. 2.1). Aliquots of the discrete samples were freeze dried and ground to powder. Subsequently, ~100-125 mg of sample material was digested with an  $\text{HClO}_4$ - $\text{HNO}_3$ -HF acid mixture using the method described in Reitz et al. (Reitz, Thomson, de Lange, & Hensen, 2006). The ICP-MS measurements of core MS21 and ICP-OES measurements of core MS66 were performed at Utrecht University, while ICP-MS measurements of cores MS66 and 64PE406E1 were done at NIOZ. Repeated analyses of the ISE-921 (Utrecht University), MESS-3 and JSd-3 (NIOZ) standards showed an accuracy and precision (deviation from reference value and relative standard deviation) of: <5% and  $\pm 1\%$  for Al, <7% and  $\pm 2\%$  for Ti, <10% and  $\pm 2\%$  for Mo, and <6% and  $\pm 1\%$  for Ba.

The calibration of the XRF-core-scan data was executed within the AvaaXelerate software package (Bloemsma, 2015; Weltje et al., 2015) using the multivariate log-ratio calibration (MLC) approach. The samples measured by ICP-OES and ICP-MS of cores MS21, MS66, and 64PE406E1 were combined to form an extensive set calibration samples (N=443; Extended Data Figure 2.1). The “sample tolerance” option (set at  $\pm 0.5$  cm) in AvaaXelerate was used to effectively calibrate the 1-mm resolution XRF-core-scan data with the 0.5-1 cm resolution ICP-MS and ICP-OES data. A selection of major, minor, and trace elements were included (see Extended Data Figure 2.2) to obtain an optimal calibration, as a closed-sum to 100% is assumed. Silicon is lost during total digestion of sediment samples, and was therefore not measured through ICP-OES and ICP-MS, and thus also not used in the calibration. However, the MLC approach does incorporate elements not included in the calibration as the ‘undefined’ fraction to close the sum to 100% (see Extended Data Figure 2.2). The high  $R^2$  values obtained for our target elements Al, Ti, Mo, and Ba when cross-plotted to ICP-OES and ICP-MS reference values ( $R^2$  of 0.88-0.94; Extended Data Figure 2.2) exemplifies the accuracy

of the MLC approach to convert to XRF-core-scanning intensities into concentrations.

## Chronology

The age model of core MS21 was published in Zwiep et al. (Zwiep et al., 2018). In short, 9 radiocarbon dates were combined with tie-points between surface water planktic foraminifer *Globigerinoides ruber* oxygen isotopes ( $\delta^{18}\text{O}_{\text{ruber}}$ ) of core MS21 to the Soreq cave speleothem  $\delta^{18}\text{O}$  ( $\delta^{18}\text{O}_{\text{speleothem}}$ ) record. Moisture that arrives at the Soreq cave is mainly derived from the Eastern Mediterranean Sea surface waters, and, therefore, the  $\delta^{18}\text{O}_{\text{speleothem}}$  and  $\delta^{18}\text{O}_{\text{ruber}}$  largely co-vary. Hence, the excellent age model derived by U-Th dating ( $N=523$ ) of the Soreq cave speleothems can be transferred to Eastern Mediterranean Sea sediments (following (Grant et al., 2012)). Moreover, one tie-point was placed between the MS21 and LC21  $\delta^{18}\text{O}_{\text{ruber}}$  records, as its position at  $\sim 36.5$  kyr BP is relatively near the robust dating point of the LC21 Campanian-Ignimbrite tephra ( $\sim 39$  kyr BP) layer. Finally, the age model for MS21 was constructed with a Bayesian deposition model, executed within the ‘Bacon’ software in R (Blaauw & Christen, 2011), including all  $^{14}\text{C}$  dates and tie-points. The large coherency of the MS21 record and the LC21 and Soreq cave records shows the robustness of the age model (Extended Data Figure 2.3b).

The age models of cores MS66 and 64PE406E1 were constructed using the well-defined sapropel boundaries based on the Ba excursions (i.e., an export productivity proxy (Dymond et al., 1992)). Generally, sapropel boundaries are thought to be synchronous across the Ionian and Levantine basins, at least during sapropel S1 (De Lange et al., 2008). It seems that large Ba excursions during sapropels have similar timing, even though it is uncertain if anoxic conditions developed simultaneously at all sapropel times (e.g., for sapropel S5 (Marino et al., 2007)). The concurrent Ba excursions of LC21 (Aegean Sea) and ODP967 (Levantine Sea) (Data Fig. 2.3c), which age models were verified using common  $\delta^{18}\text{O}$  variability (Rodríguez-Sanz et al., 2017), shows that Ba excursions are also synchronous for this sapropel. As such, assuming that similar timing of Ba excursions apply to all sapropels, we used tie-points of Ba excursions in cores MS66 and 64PE406E1 to those same excursions in the best dated records available.

Sapropels S1, S3, S4, and S5 are currently best dated by linking the LC21  $\delta^{18}\text{O}_{\text{ruber}}$  variability to the same variability in the Soreq cave  $\delta^{18}\text{O}_{\text{speleothem}}$  (Grant et al., 2016). Hence, for the sapropels S1 to S5 we use the ages derived by Grant et al. (2016), and we transferred those ages to the same boundaries in cores MS66 and 64PE406E1 (Extended Data Figure 2.3d). For ages  $>130$  kyr (sapropels S6 to S9) we correlated our Ba excursions

## CHAPTER 2

to those observed in ODP968 (Ziegler et al., 2010). Assuming similar timing of the African and Asian monsoon, Ziegler et al. (2010) linked their ODP968 sapropel record to (well-dated) speleothem records from China. The excellent fit between the benthic foraminifer  $\delta^{18}\text{O}$  record from ODP968 and the global benthic isotope stack LR04 (Lisiecki & Raymo, 2005) exemplifies the strength of their age model (Extended Data Figure 2.3g). As such, for sapropels S6 to S' (including the 'ghost' sapropel between S5 and S6) we carefully matched the Ba records to transfer their age model to the end of MS66 (~150 kyr BP) and to ~290 kyr BP for core 64PE406E1 (Extended Data Figure 2.3e). The large coherency of 64PE406E1 Ti/Al and ODP968 Ti/Al from ~130 - 290 kyr BP shows the robustness of the 64PE406E1 chronology (Extended Data Figure 2.3f), as Ti/Al is an indicator of monsoon variability (Lourens et al., 2001) and not uniquely linked to sapropel formation.

We focus on the last 250 kyr BP in the main text, as this interval holds eight well-preserved sapropels. The top of core 64PE406E1 contains less than 1 cm of sapropel S1, which seems disturbed due to piston coring, and therefore 64PE406E1 sapropel S1 was excluded from the early-warning-signal statistics.

### Data selection

We selected the part of the time series that preceded the fast transition to an anoxic state (i.e., before the abrupt increase in the anoxia-proxy Mo to high values). The exact position of transitions were sometimes placed slightly before the published ages for sapropel S1 to S9 formation, to avoid including data points that were part of the transition itself, because inclusion of points that are part of the transition would bias the estimate of the autocorrelation at lag-1 (Dakos et al., 2008). Sapropels and related anoxia are thought to be mainly driven by precessional forced monsoon variability (Rohling et al., 2015; Rossignol-Strick, 1985) and therefore we focus on 10 kyr (~0.5 a precession cycle) before each transition.

### Detrending

To filter out the slow trends in the original records, we subtracted a Gaussian kernel smoothing function from the data (Extended Data Figure 2.5). The remaining residuals (Extended Data Figure 2.5) were used for the estimation of the resilience indicators. We chose a bandwidth in such a way that we did not overfit, while still removing the long term trend. We used the same bandwidths for all the different records (bandwidth = 900).

## The dynamic indicators of resilience

We estimated the autocorrelation and variance within rolling windows of half the size of the records. An increase in the autocorrelation at lag-1 indicates that the system has become increasingly similar between the consecutive data points (Held & Kleinen, 2004), and is therefore, a simple way of measuring slowing down. We calculated the autocorrelation at lag-1 by fitting an autoregressive model of order 1 within each sliding window up to the transition point. The autoregressive model of order 1 is a linear AR(1) process of the form:  $x_{t+1} = \alpha_1 x_t + \varepsilon_t$ , where  $\alpha_1$  is the autoregressive coefficient (Box, Jenkins, Reinsel, & Ljung, 2015) and  $\varepsilon_t$  is a Gaussian white noise process. Slowing down will also cause the variance to increase prior to a complete transition (Marten Scheffer et al., 2009). We measured the variance as standard deviation ( $SD = \frac{1}{n-1} \sum_{i=1}^n (z_i - \mu)^2$ ). We tested for evidence of an increase in the estimates of the leading indicators by estimating the nonparametric Kendal  $\tau$  rank-correlation coefficient (Mann, 1945).

## Code and data availability

All analyses were implemented in Rv3.4.3. (R project for Statistical Computing). The leading indicators were calculated using scripts that are based on the ‘earlywarnings’ package in R (Dakos et al., 2012). The geochemical data supporting the findings of this study are archived in the PANGAEA data repository (<https://www.pangaea.de/>).

## S2.2 PRE-PROCESSING OF THE DATA

In general, the time intervals between the data points were very similar over all records, except for a few missing data points (Figure S2.1). As the early warning signals require that the data is evenly spaced (Dakos et al., 2012), we checked whether our results were robust to interpolation. We used linear interpolation to generate a dataset that is evenly spaced with the same number of data points as the original data and compared the early warning signals of the interpolated data (Figure S2.2) with the signals of the original records (Figure 2.2).

In most cases the trend in autocorrelation was of the same order of magnitude, but there were some remarkable differences. In three cases (S3-MS21, S6, and S9) the interpolated records showed a stronger trend in autocorrelation than the original records, and four other cases where the opposite occurred (S1-MS21, S3- 64PE4o6E1, S4- 64PE4o6E1, and S7). In the case of record S6 and S9, only the interpolated data showed

## CHAPTER 2

a significant trend in autocorrelation. The trends in variance were also mostly in the same order of magnitude, except for record S<sub>3</sub>-MS<sub>21</sub>, where a negative trend in variance was observed in the interpolated record, but a positive trend in the original record. There was one case (S<sub>8</sub>) in which interpolation yielded a stronger increase in variance than the original record. In the other cases the opposite (S<sub>1</sub>-MS<sub>21</sub>, S<sub>3</sub>- 64PE<sub>406E1</sub>, S<sub>6</sub>, S<sub>7</sub>, and S<sub>9</sub>) or no changes were observed.

On a closer inspection, the trends that occurred in the interpolated data sets only, seemed to be an artefact of a systematic change in the spacing of the original data points towards the transition (Figure S2.3c). Due to this effect we observe that in parts of the data set the points were actually computed by averaging subsequent data points of the original data while in other parts effectively the original data were used (Figure S2.3d).

Therefore we think interpolation introduced some spurious trends, when the original records were already almost equally spaced (Figure S2.3). We conclude that we cannot use interpolation in these cases, while the mistake due to the unequal spacing of the original records seems negligible. Using the original data was also more conservative, as we see fewer significant trends.

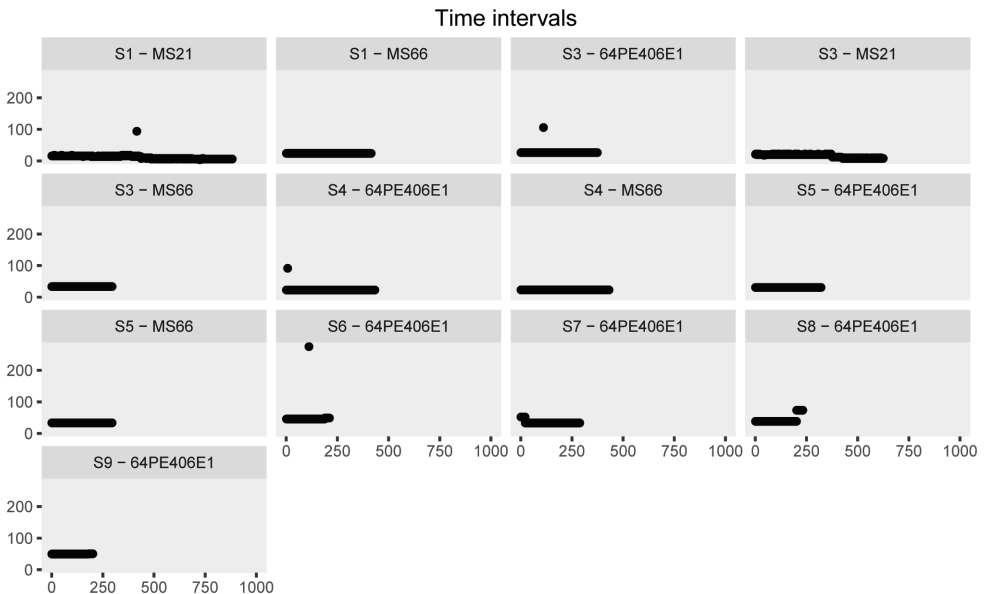


**Figure S2.1.** Plots of the time intervals between consecutive points in the original records. Smaller time intervals indicate a higher density of data points. In all cases, except for events S<sub>8</sub> and S<sub>9</sub>, the time intervals in the original record do not increase close to the transitions.

## EARLY-WARNING SIGNALS FOR MARINE ANOXIC EVENTS

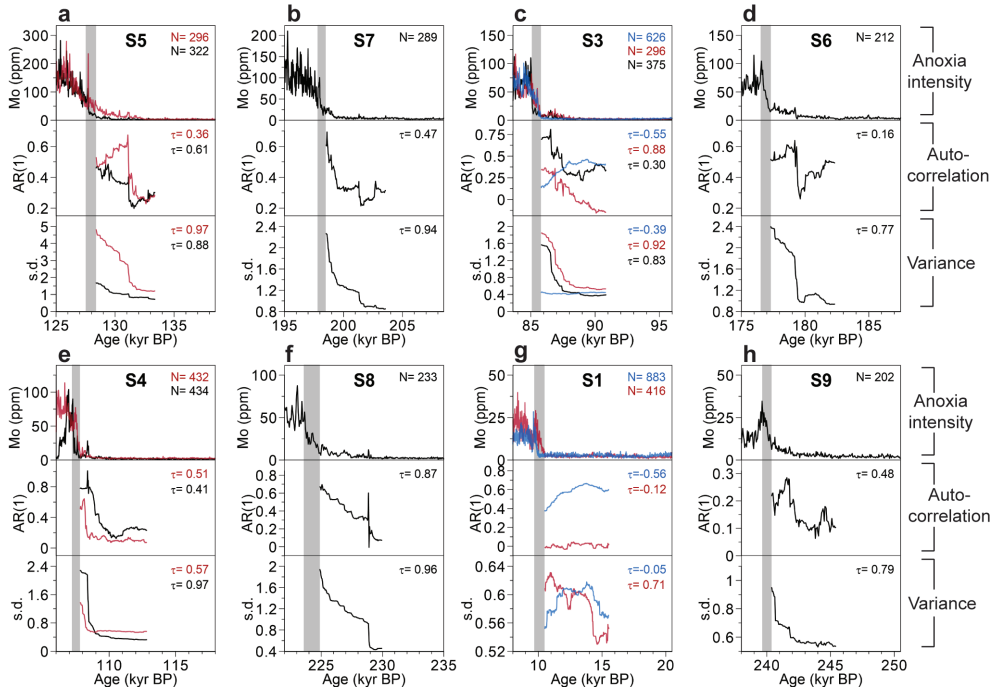


**Figure S2.2. Early warning signals for the interpolated records of the eight past eastern Mediterranean anoxic events.** As in the figure in the main text (Fig. 2.2), the anoxic events are ranked (a-h), based on their recorded Mo concentrations, from the strongest anoxic event at the top left (S5; a) and the weakest at the bottom right (S9; h). Each panel shows: an overview of the event (top), autocorrelation (middle), and variance (bottom). The grey bands mark the transition intervals, while the arrows show the moving window used to calculate the early warning signals. Results for the three studied cores are indicated: MS21 (blue), MS66 (red), and 64PE406E1 (black).

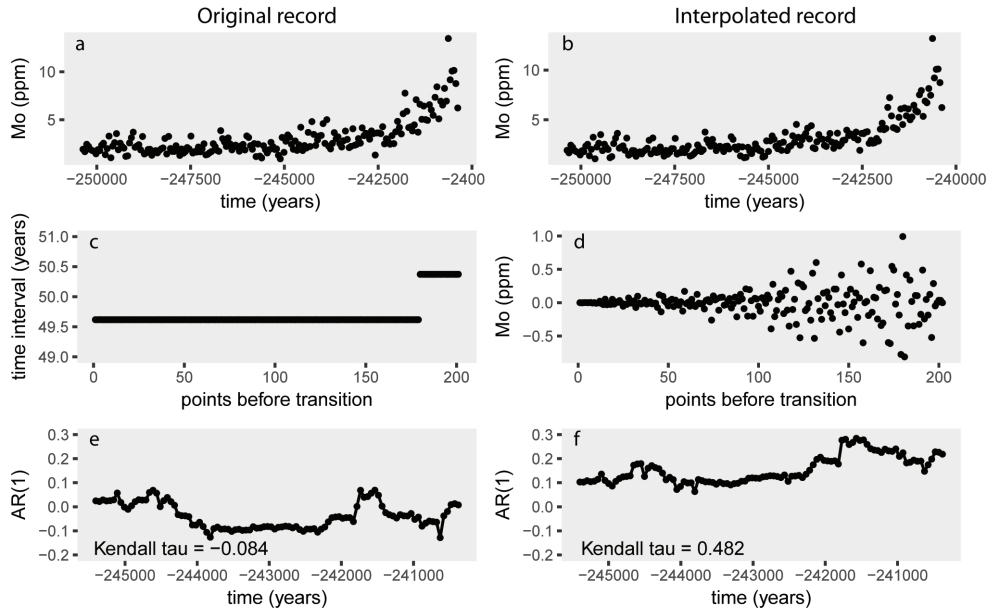


**Figure S2.3.** The effect of interpolation on the trend in  $AR(1)$  for event S9. Panels a and b show the time series, while panel c shows the time interval between consecutive points. Panel d shows the difference between the original and the interpolated record for each point before the transition, and panels e and f show the trend in autocorrelation, expressed in Kendall's tau.



### **S2.3 SENSITIVITY TO WINDOW SIZE AND BANDWIDTH**

We removed the slow trends in the original and interpolated records by applying a Gaussian kernel smoothing function and subtracted it from the records to obtain the residuals. The choice of standard deviation used in the kernel function (defined by the bandwidth size) for filtering is important. Using a too-wide bandwidth does not remove slow trends, but a too-narrow bandwidth removed the short-term fluctuations that we use to determine signs of slowing down. We picked a bandwidth that was the same for all records, but did not result in overfitting in any of the records. In addition, we used a sliding window of half the record to determine the early warning indicators. The choice for sliding window size is a trade-off between time resolution, and the reliability of the estimate in that window. Using a smaller window size allows one to track short-term changes, but the small amount of data points in the window makes the estimate less reliable. The results of our analyses are influenced by the choices we made for bandwidth and sliding window size. A systematic sensitivity analysis for bandwidth and window size choice, indicate that our results are robust, and that more significant trends could have been obtained by choosing another bandwidth and window size for each specific record (Figure S2.4 and Figure S2.5).

### **S2.4 SIGNIFICANCE OF TRENDS**

To test whether the observed trends could be the result of randomness, we created surrogate time series with the same power spectra and length as the records, but with random phases in the Fourier modes<sup>2</sup>. We estimated the probability that our trends in the resilience indicators would be observed by chance as the number of cases in which the Kendall tau was equal to or higher than the estimate of the original record. The probability estimates for each record are shown in Table S2.2 and Table S2.3. The probability for observing a trend in the resilience indicators differs per indicator and per record. Low probabilities of finding the observed trends in autocorrelation by chance, were estimated in the records of events S3-MS66, S4-64PE4o6E1, S8 and in all records for standard deviation, except for S1-MS21, S3-MS21, and S4-MS66.

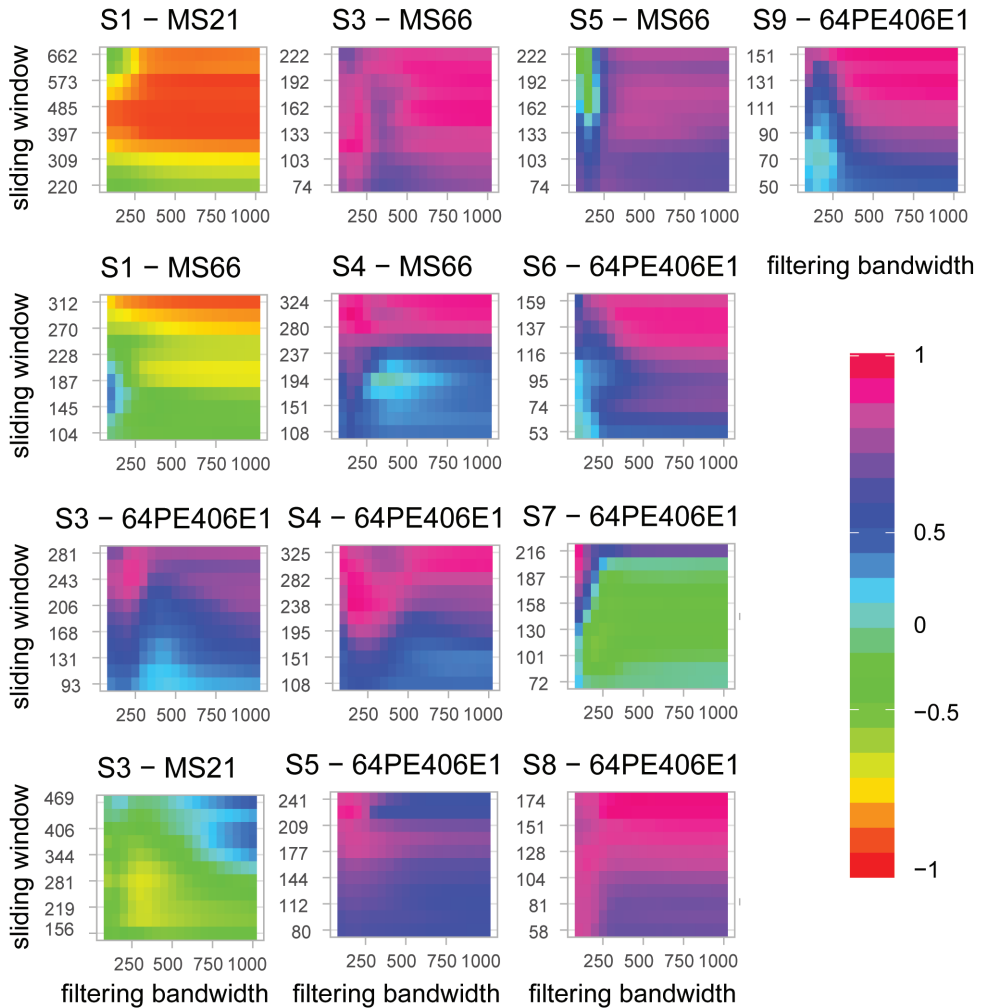


**Figure S2.4.** The effect of the bandwidth and sliding window size on the observed trend in the autocorrelation for the paleorecords as measured by the Kendall's tau.

# EARLY-WARNING SIGNALS FOR MARINE ANOXIC EVENTS

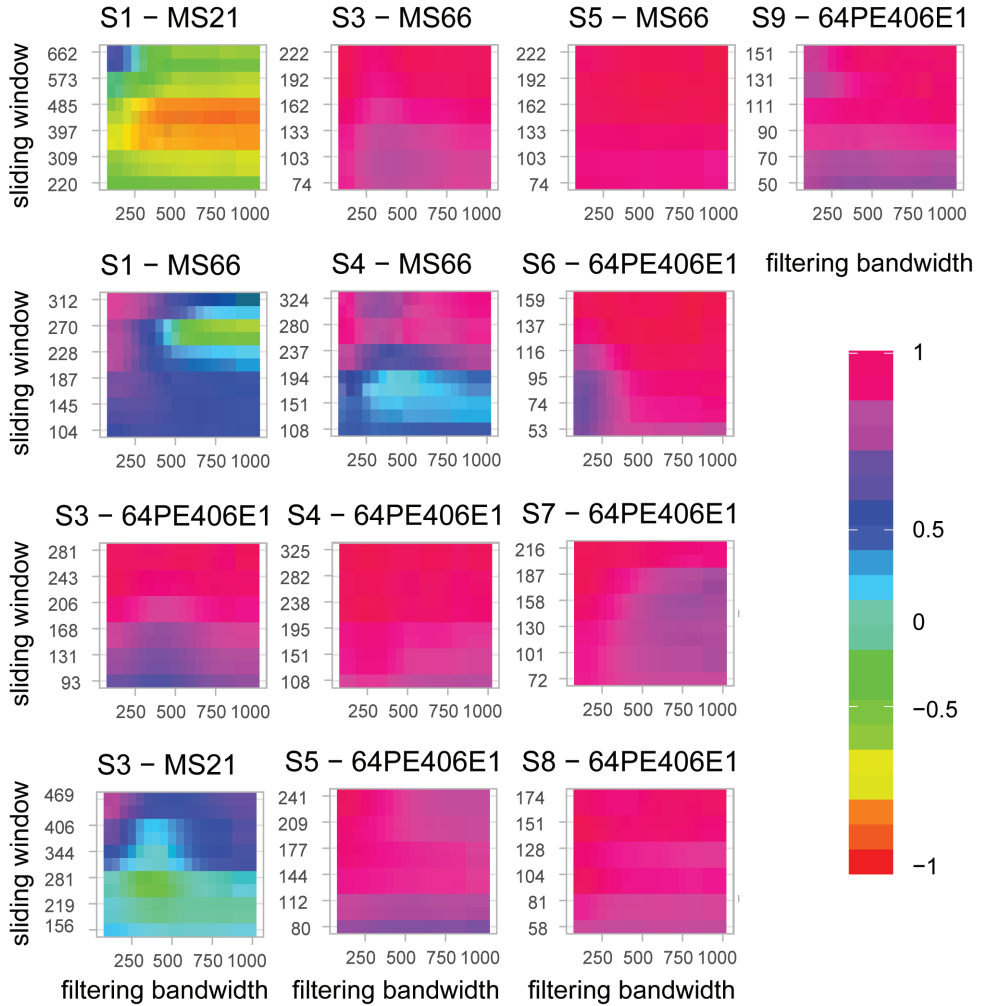


**Figure S2.5.** The effect of the bandwidth and sliding window size on the observed trend in variance for the paleo records as measured by Kendall's tau.

## CHAPTER 2

**Table S2.1.** Summary of the trend statistic for the original and the interpolated record and their probabilities

RECORD	AR1 KENDALL T ORIGINAL	AR1 KENDALL T INTERPOLATED	SD KENDALL T ORIGINAL	SD KENDALL T INTERPOLATED
S1 - MS21	-0.856	-0.555	-0.396	-0.051
S1 - MS66	-0.12	-0.12	0.71	0.71
S3 - 64PE406E1	0.376	0.304	0.901	0.828
S3 - MS21	-0.064	-0.552	0.331	-0.391
S3 - MS66	0.879	0.879	0.92	0.92
S4 - 64PE406E1	0.532	0.413	0.965	0.97
S4 - MS66	0.51	0.51	0.569	0.569
S5 - 64PE406E1	0.606	0.606	0.878	0.878
S5 - MS66	0.359	0.359	0.971	0.971
S6 - 64PE406E1	0.009	0.157	0.799	0.77
S7 - 64PE406E1	0.499	0.468	0.953	0.942
S8 - 64PE406E1	0.783	0.866	0.897	0.958
S9 - 64PE406E1	-0.084	0.482	0.944	0.794

**Table S2.2.** The probability of observing the estimated values for the Kendall's tau of the original records for a set of 1,000 surrogate time series

RECORD	P-VALUE AR1	P-VALUE SD
S1 - MS21	Inf	0.995
S1 - MS66	0.556	0.087
S3 - 64PE406E1	0.176	0.001
S3 - MS21	0.668	0.425
S3 - MS66	0.012	0.001
S4 - 64PE406E1	0.001	0.001
S4 - MS66	0.136	0.108
S5 - 64PE406E1	0.114	0.002
S5 - MS66	0.252	0.001
S6 - 64PE406E1	0.5	0.011
S7 - 64PE406E1	0.182	0.001
S8 - 64PE406E1	0.069	0.001
S9 - 64PE406E1	0.507	0.001

## EARLY-WARNING SIGNALS FOR MARINE ANOXIC EVENTS

**Table S2.3.** *The probability of observing the estimated values for the Kendall's tau of the interpolated records for a set of 1,000 surrogate time series.*

RECORD	P-VALUE AR1	P-VALUE SD
S1 - MS21	0.935	0.887
S1 - MS66	0.578	0.083
S3 - 64PE406E1	0.198	0.012
S3 - MS21	0.969	0.716
S3 - MS66	0.009	0.001
S4 - 64PE406E1	0.002	0.001
S4 - MS66	0.125	0.106
S5 - 64PE406E1	0.103	0.001
S5 - MS66	0.256	0.001
S6 - 64PE406E1	0.368	0.026
S7 - 64PE406E1	0.155	0.001
S8 - 64PE406E1	0.002	0.001
S9 - 64PE406E1	0.15	0.014





# CHAPTER 3

## EARLY WARNING OF TIPPING POINTS IN SLOW SYSTEMS

Bregje van der Bolt,

Marten Scheffer,

and Egbert H. van Nes

*“Meep, Meep”*  
- Road Runner

### ABSTRACT

The resilience of a system can be estimated using dynamical indicators of resilience (DIORs). An increase in the DIORs could be interpreted as an early warning signal for an upcoming critical transition. However, in order to be able to estimate the DIORs, observational records need to be long enough to capture the slowest response rate of the system. As the current rate of anthropogenic forcing is faster than in previous times, and the intrinsic response rate of some parts of the climate are slow, we may expect difficulties estimating the resilience from modern time series. So far, there have been no systematic studies of the effects of the intrinsic response rates of the dynamical systems and the rates of forcing on the detectability trends in the DIORs prior to critical transitions. Here, we quantify the performance of the resilience indicators variance and temporal autocorrelation, in systems with different intrinsic response rates and for different rates of forcing. Our results show that the rapid rise of anthropogenic forcing to the Earth may make it difficult to detect changes in the resilience of ecosystems and climate elements from time series.



## INTRODUCTION

Resilience is the capacity of a system to absorb perturbations without shifting to an alternative state (Holling, 1973). A way to quantify the resilience of a system is to estimate the intrinsic return rate to equilibrium, which has been shown to decrease with the resilience (van Nes & Scheffer, 2007; Wissel, 1984). The return rate can be determined using perturbation experiments, but this is often not possible for complex systems. Instead, every system is permanently subject to natural perturbations from the environment. When one monitors the system and its relevant parameters, the system's dynamic responses to these perturbation can be captured and used to estimate the resilience of the system. This is reflected by an increase in the dynamical indicators of resilience (DIORs), variance (S. R. Carpenter & Brock, 2006) and temporal autocorrelation (Ives, 1995), of the system state.

In order to be able to estimate the DIORs, you need observational records that are long enough to capture the slowest response timescale of the system (Lenton, 2011). The sampling frequency - the interval between values in the time series - is also important. Systems need to be sampled at intervals shorter than the characteristic time scales of the slowest return rate (Held & Kleinen, 2004; Thompson, 2011). At one point, however, it does not help to sample at shorter intervals. For instance, sampling the temperature of the ocean every millisecond does not give more information, because the system does not respond on such short timescales.

These considerations about the length of the time series and the sampling interval, however, are about relative rather than absolute time scales. For instance, the resilience of the postural balance of a person can be determined from a time series with a total length of just 30 seconds. The typical response rate for physiological meaningful postural control processes is in the order of 3 Hz (0.333 s) (Kanekar, Lee, & Aruin, 2014). This implies that a time series of 30 seconds covers many 'micro-recoveries' of the system. On the other hand, the sampling frequency of 1000 Hz (1 ms) of the equipment is an overkill, as it does not carry meaningful information on the systems response (Gijzel et al., 2018).

While such limitations are straightforward, the problem of estimating return times as an indicator of resilience, becomes more complicated if the resilience of the system is a moving target, i.e. changing in time. A particular important example is the situation in which a change in the conditions is slowly moving the system towards a tipping point or more precisely a zero-eigenvalue bifurcation, where the systems shifts to the alternative stable state. The typical way to monitor such changing resilience is to calculate the

## CHAPTER 3

DIORs within a sliding moving window. This method is based on the idea that the DIORs should be estimated as the data are becoming available (Dakos et al., 2012).

A decrease in the resilience of the system could be interpreted as an early warning signal for an upcoming critical transition at the bifurcation point (Scheffer et al., 2009). This is, however, only possible under a limited set of conditions (Boettiger, Ross, & Hastings, 2013; Dakos, Carpenter, van Nes, & Scheffer, 2015). Otherwise, the probability of false negatives and false positives tends to become very high. In addition, strong environmental perturbations may obscure the trends in the DIORs (Perretti & Munch, 2012) and can force a system to another state far from the tipping point. These limitations, have led to the suggestion to abandon the term ‘early warning signal’ in this context altogether (Scheffer, Carpenter, Dakos, & van Nes, 2015).

Nonetheless, there is an obvious demand for early warning signals for critical transitions. For instance, early warning for climate tipping points could have considerable social and economic value for societies (Lenton, 2011). The DIORs have been shown to increase before abrupt climate transitions in the past (Dakos et al., 2008). However, how abrupt were those transitions really? And how much time would be needed to detect a loss of resilience? The rates of change in the current anthropogenic forcing are much faster than in the times for which we studied the ‘early warning signals’ for past transitions (Joos & Spahni, 2008; Zeebe, Ridgwell, & Zachos, 2016). As the intrinsic response rates of the oceans and ice caps are rather slow (in contrast to atmospheric systems) we may expect difficulties when it comes to assessing return rates from modern time series.

So far, there have been no systematic studies of the intertwined effects of slowness of the dynamical system and the rates of ‘forcing’ on our chances to detect trends in the resilience from time series. Therefore, we use model-generated data of systems that gradually move towards a tipping point, to quantify how the response rate of the system affects the strength of the resilience indicators prior to a critical transition.

## METHODS

### MODEL DESCRIPTIONS

We used four well-studied minimal model with alternative stable states to generate data with different assumptions about the system's response rate (see Table S3.1 for model equations). The first model describes the logistic growth of a resource  $N$  that is harvested following a sigmoidal functional response (May, 1977). It describes the transition from an underexploited to an overexploited state as the harvesting pressure crosses a threshold. The second model describes the nutrient dynamics of a lake (Stephen R. Carpenter, Ludwig, & Brock, 1999). At low nutrient input rates, the lake loses nutrients to the sediment or hypolimnion. Once a threshold in the nutrient input rates is passed, there is a high recycling from the sediment or hypolimnion as a result of lower oxygen levels and the lake becomes eutrophic. The third model describes a population with an Allee effect (Courchamp, Clutton-Brock, & Grenfell, 1999; Scheffer, 2009). It describes the extinction of a population as the harvest, or loss rate increases. The fourth model describes the dynamics of tree cover as a function of precipitation (van Nes, Hirota, Holmgren, & Scheffer, 2014). For a range of precipitation levels, this model can be in a high, intermediate or low tree cover state.

In all models, we introduced a parameter,  $\varepsilon$ , to control the speed of the system's response. We also assume that each model is subject to random additive independent disturbances, so the general form of each model is:

$$dX = \varepsilon(f(X, c)dt + \sigma dW)$$

where  $f$  is the deterministic equation that governs the dynamics of the state variable  $X$  as a function of  $c$ , the control parameter which causes the system to switch between stable states.  $dW$  is a white noise process with a scaling factor  $\sigma$ .

### GENERATION OF THE TIME SERIES

In order to test whether resilience indicators signal an upcoming transition in slow systems, we ran the model for different values of  $\varepsilon$ : ranging from 0.1 to 1 with a step of 0.1. We started from equilibrium and slowly increased the control parameter to make sure that the system crosses the tipping point. We ran the model for an additional 2000 time steps with a constant value of the driver to make sure that the system has enough time to reach the new equilibrium. For each value of  $\varepsilon$ , we simulated 100 replicates.

## CHAPTER 3

In the main text we focus on the results from the overharvesting model, but we analysed the effect of the time scale  $\varepsilon$  also for three other minimal models with alternative stable states (see Table S3.1 and the Supplementary Information for details). We only used the points in the simulated time series that correspond to the period before the transition. It is important to exclude points that are part of the transition, because due to increased serial correlation and increased variance, including these points would bias the estimate of the resilience indicators (Dakos et al., 2012). In systems with a low intrinsic response rate, however, it is difficult to determine the exact onset of the transition, because the decline in the system state is more gradual than in a fast-responding system (see Fig. 3.1). We defined the transition arbitrarily as the first point where the state variable was smaller than a specific threshold (see Table S3.1) for ten consecutive time points.

The intrinsic response rate of the system alters not only the detectability of the resilience indicators but in practice usually also the length of the time series prior to the regime shift. Both effects can be important, but we first focus on the slowness of the system. Therefore we standardized the generated time series and selected the 2500 data points prior to the transition. Standardizing the time series removed the differences in time series length of the different response rates of the system.

In addition, we compared the performance of the resilience indicators for different levels of time-correlation in the noise process for the overharvesting model (see Supplementary Information for details)

In these scenarios, the system becomes slow to respond to changes in the forcing and the noise process, because  $\varepsilon$  scales both the deterministic equation and the noise process. When only the rate of change increases, however, this does not necessarily mean that the system also responds more slow to perturbations. Therefore, we also tested for the Overharvesting model how the resilience indicators perform when only the rate of change increases (see Supplementary Information for details).

To show that a decrease of the intrinsic response rate of the system is similar as an increase in the rate of change of the driver, we performed simulations with the overharvesting model in which we kept  $\varepsilon$  constant ( $\varepsilon = 1$ ), but changed the rate at which we changed the control parameter. In each of these simulations, we increased value of the control parameter linearly from 1.6 to 2.8 by a fixed rate (0.0024, 0.0012, 0.0006, 0.003) per time step. We include the statistical effect that the time series will likely be shorter when the driver changes rapidly. We take a fixed sampling interval, so if the environmental change is rapid, we have less observations.

All the simulated time series were produced with the software package GRIND for MATLAB (accessed at <http://spars-center.org/grind>), which used a Euler-Maruyama method to solve the stochastic equation. The estimation of the resilience indicators was performed in R v.3.4.3 (<http://www.r-project.org/>) using an adapted version of the R package earlywarnings (Dakos et al., 2012).

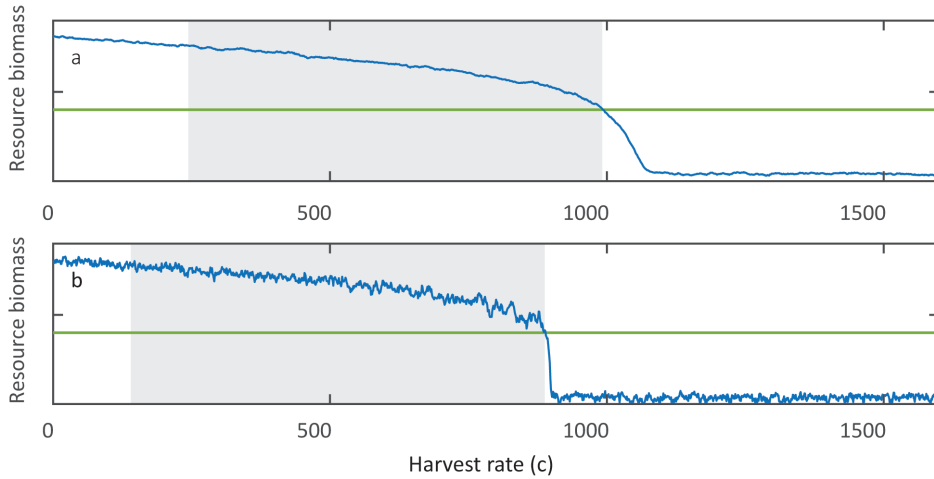


**Figure 3.1.** Example time series for a system that responds slow ( $\epsilon=0.1$ , panel a) and fast ( $\epsilon=1$ , panel b). The red lines indicate the threshold value, and the grey area indicates the part of the time series that is selected for standardizing.

## RESILIENCE INDICATORS

We calculated two different dynamical indicators of resilience (DIORs): the autocorrelation at the first lag, and the standard deviation of the data. To filter out long trends that may cause autocorrelation, we subtracted a Gaussian kernel smoothing function with a predefined bandwidth from the data (Dakos et al., 2012). The remaining residuals were used for the estimation of the resilience indicators. We estimated the DIORs on the data points within a sliding window of half the size of the time series. We tested for evidence of a trend in the indicators by estimating the nonparametric Kendall rank-correlation tau statistic of the estimates of the DIORs. A strong positive correlation between time and the DIORs indicates a strong trend, which we would expect to occur when approaching a tipping point (Dakos et al., 2012).

### SIGNIFICANCE TESTING

To test whether the trends in the indicators are significant, we calculated the chance that the estimates of the indicators are due to chance alone. We produced surrogate time series with the same power spectrum and variance as the original time series, but with random phases (Ebisuzaki, 1997). For each parameter setting, we generated 100 surrogate time series based on the first replicate of the generated data sets. For each of these surrogate records, we estimated the trend of the resilience indicators (as Kendall's tau) in the same way as the original records. The 97.5<sup>th</sup> percentiles of the distributions of tau values of each set of surrogate records were considered the lower bound of the confidence interval ( $p=0.025$ , single-tailed).

### RESULTS

In all models, we find consistent patterns in the trend of the resilience indicators (DIORs) for the different time scales of the system's response ( $\epsilon$ ). Higher  $\epsilon$ 's produce stronger positive trends for both autocorrelation and standard deviation (Figure 3.2 and Figure S3.1-2). As the speed of the system's response becomes slower, the number of time series that do not show a significant increase in the resilience indicators increases (Table S3.2). Note that we keep the lengths of the data sets fixed. These results indicate that critical transitions are indeed harder to detect when the intrinsic response rate of the is low.

When the noise process is not scaled with the system's response ( $\epsilon$ ), the timing of the shift becomes less predictable, but on average the system shifts earlier (Figure S3.3). An earlier transition decreases the predictability of the transition, because the time series before the transition is shorter, and the system shifts further away from the tipping point, where the resilience of the system is higher. When the noise is weaker, the perturbations bring the system less far away from the equilibrium, and the system shifts on average closer to the tipping point, and the variation in the moment if shifting is smaller. In addition, the pattern in the DIORs is similar to time series in which the noise process is scaled with  $\epsilon$  (Figure S3.4).

When the noise process is time-correlated, the pattern in DIORs is similar for systems with noise processes that are and are not time correlated (Figure S3.5). When the standard deviation of the noise process is higher, however, the system shifts earlier in a time-correlated environment than in an environment without time-correlation (Figure S3.6), decreasing the predictability of the transition.

The intrinsic response rate of the system should be measured relative to the rate of change in the environmental driver. Therefore, we expect a similar effect of an increase in the rate of change in the environment as a decrease in the response rate of the system. To show this, we generated data sets in which the intrinsic response rate of the system is the same ( $\varepsilon=1$ ), but the rate of change of the driver changes. We included here the statistical effect of a faster change on the length of the data sets, assuming that a manager samples at a fixed rate. It is clear that in this scenario the indicators are indeed much harder to detect when the rate of change of the driver increases (Figure 3.3). Also if this statistical effect is excluded by fixing the number of points in the period where the resilience decreases, we still find that DIORS are harder to detect when the rate of the driver is high (Figure S3.7).

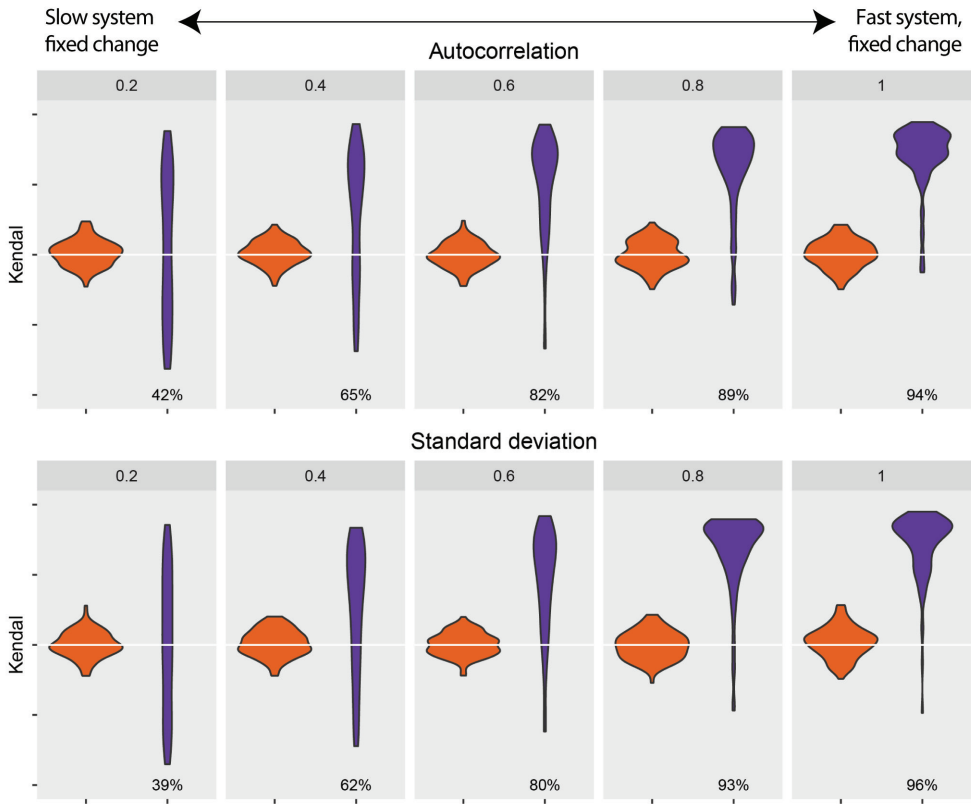


**Figure 3.2.** Strength of the trends in autocorrelation for the Overharvesting model in the original time series (purple) and null models (orange). The violin plots indicate the distribution of Kendall tau values for the 100 replicates for each level of  $\varepsilon$ . The size of the generated data sets is standardized to 2500 points (See Methods). The percentages represent the fraction of trends in the original time series that are significantly higher than the null models ( $p=0.025$ , single-tailed).

### DISCUSSION

Our analysis confirms the suspicion that the rapid rise of anthropogenic forcing to the Earth system may make it difficult to detect changes in resilience of ecosystems and climate elements from natural time series. Relatively slow systems will not only lag behind their equilibria, but the period to monitor the system might be too short to detect critical slowing down (Lenton, 2011). The intrinsic response rate of a system is relative rather than absolute. Therefore, the effect of the slowness of the system on the DIORs is system and situation specific. In order to assess the specific limitations in more detail it would be important to use realistic models that incorporate the key processes in any system with the appropriate time constants.

Although the slowness of ecosystems and climate elements may be a problem when it comes to assessing their resilience when limited time is available, there is potentially a bright side to slowness when it comes to our options for managing such change. When the response is slow enough, it may be that even though the theoretical tipping point is already passed, the systems responds sufficiently slowly to allow ‘catching it in free fall’ and reversing the change (Hughes, Linares, Dakos, van de Leemput, & van Nes, 2013). Again, all considerations of time scales are relative. Even extremely rapid quantum jumps in atoms can be caught using real-time monitoring and reversed during their completion (Mineev et al., 2019).

The difference between this example of quantum jumps and the challenge for societies to respond to critical transitions in climate elements or ecosystems is two-fold. On the one hand, change unfolds much more slowly, giving us more time. On the other hand, social response may be slowed down by a complex set of mechanisms (Biggs, Carpenter, & Brock, 2009; Scheffer, Westley, & Brock, 2003). Most importantly, it requires time to reach consensus on action, especially if evidence is weak (Scheffer et al., 2003). The latter point is relevant for our line of enquiry. Can we detect if a system is entering ‘free fall’ in the sense that the system has passed a tipping point and is now propagated by self-reinforcing processes towards a contrasting state? As we have shown, indicators of critical slowing down are unlikely to be of much help in such situations. Instead other approaches will need to be developed to detect such situations as early as possible.



## EARLY-WARNING OF TIPPING POINTS IN SLOW SYSTEMS

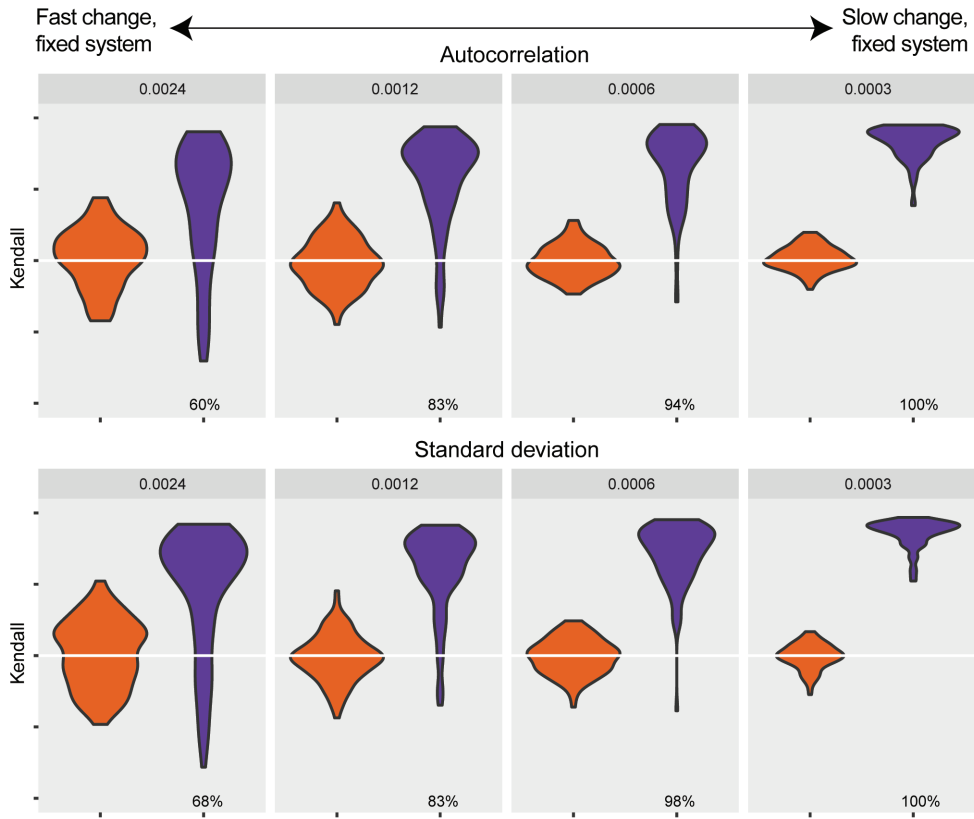


**Figure 3.3.** Strength of the trends for the resilience indicators for different rates of change. The violin plots indicate the distribution of Kendall tau values of the indicators determined with the hundred time series (purple) compared to the ones determined with the null model (orange). We fixed the sampling interval so with fast change there are less sampling points.

## SUPPLEMENTARY INFORMATION

### S3.1 WITHOUT SCALING OF THE NOISE

In the main text we analyzed the scenario in which the system becomes slow to respond to both changes in the forcing, and to the noise process. When only the rate of change increases, however, this does not necessarily mean that the system also responds more slow to perturbations. In order to test how the resilience indicators perform in this situation, we adapted the Overharvesting model in such a way, that the noise process is not scaled by  $\varepsilon$ :

$$dN = \varepsilon(N - \alpha N^2 - c \frac{N^2}{N^2 + 1})dt + \sigma dW$$

Where all parameters have the same value, except for  $\sigma$ , which was 0.025. We performed the same analysis as mentioned in the main text. We compared the trends to the trends from runs from the model of the main text, but with a  $\sigma$  of 0.025. Results can be found in Figure S3.4.

### S3.2 DIFFERENT NOISE TYPES

To test how the resilience indicators perform in an environment with correlated noise, we introduced a noise term with time-correlation to the overharvesting model, and compared the performance of the resilience indicators for different levels of time-correlation in the noise process. We used the following stochastic differential equation, called an Ornstein-Uhlenbeck process, to generate the time-correlated noise with an average of 0:

$$dT_\alpha = (-\gamma T_\alpha)dt + \sigma dW$$

Where  $\gamma (\geq 0)$  corresponds to negative feedbacks that act to restore any anomaly to the mean,  $T_\alpha=0$ . The smaller the negative feedback, the larger the autocorrelation of  $T_\alpha$ :  $\gamma=0$  corresponds to an unbounded random walk. We solved the equation using an Euler-Maruyama scheme. With this scheme and a sampling time step of 1, the relation between  $\gamma$  and the autocorrelation  $\alpha$  of the discrete time series that are generated can be described as:

$$\alpha(1) = 1 - \gamma$$

We used the created time series of  $T_\alpha$  to stochastically force the (over)harvesting model as follows:

$$\frac{dX}{dt} = \varepsilon(f(X, c) + T_\alpha)$$

We ran the model with three different data sets of  $T_\alpha$  with different values for the autocorrelation  $\alpha$ : a)  $\alpha=0$  and  $\beta=0.1$ , b)  $\alpha=0.35$  and  $\beta=0.1$ , c)  $\alpha=0.7$  and  $\beta=0.1$ . The first scenario has a white noise process, and the last two scenarios have noise processes that are time-correlated.

### S3.3 FAST RATES OF CHANGE

In the main text we showed that the intrinsic response rate of the system is similar as an increase of the rate of change of the driver. We included the statistical effect that the time series are shorter when the driver changes rapidly.

To analyze what would happen in the time series are standardized but capture a similar range of the system dynamics for all rates, we generated time series that have 2500 data points. This means that if the rate of change is 0.00048, the control parameter changes at every data point, but that the time series in which the control parameter is changed with a faster rate are oversampled. The 1800 data points before the transition are selected. By doing so, you both lose the statistical effect of the length of the time series and the effect of only selecting the a small part of the system dynamics.

In this scenario, the trend in the resilience indicators is similar to the scenario in which the whole time series is used (see Figure 3.3). Both indicators are much harder to detect when the rate of change of the driver increases (Figure S3.7). This scenario represents the situation in which a manager would increase the sampling frequency for a system in a fast changing environment compared to a system in a slowly changing environment. So even if a manager would increase the sampling frequency in order to increase the time series length, the change occurs too fast to detect critical slowing down.

### S3.4 SENSITIVITY ANALYSIS

The utility of each of the resilience indicators also depends on the choices made when performing the analyses. Therefore, it is necessary to check the robustness of our results to choices made, such as the bandwidth used for Gaussian kernel smoothing, and the size of the rolling window in which we estimated the indicators. Therefore, we estimated the trends for the resilience indicators for a combination of sliding window sizes ranging from 25% to 75% of the time series in increments of 10 points and eight different filter bandwidths (bandwidth = 1, 2, 4, 6, 8, 10, 12, 14, 16, 18, 20, 22, 24, 26, 28, 30, 32, 34, 36, 38, 40) (Dakos et al., 2008). The result show that we could have chosen a combination that would have given us stronger trends in the resilience indicators (Figure S3.8 and S3.9). In the text and Supplementary Information, the bandwidths used are: 10, 25, 20, 250, for the overharvesting model, the population model, the eutrophication model and the tree cover model respectively.

### S3.5 SUPPLEMENTARY FIGURES

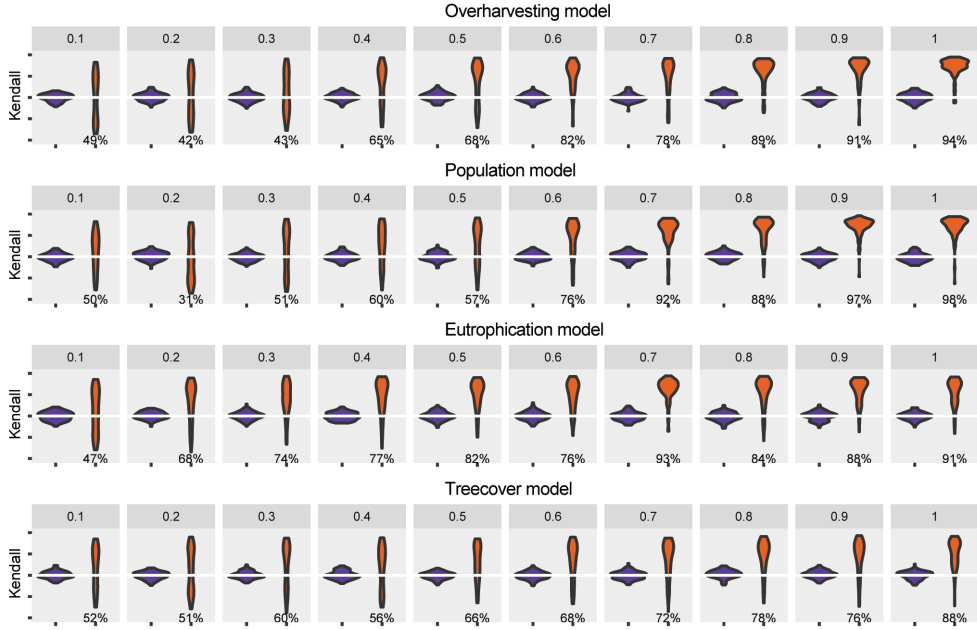


**Figure S3.1.** Strength of the trends in autocorrelation for the four different models in the original time series (orange) and null models (purple). The violin plots indicate the distribution of Kendall tau values for the 100 replicates for each level of  $\epsilon$ . The size of the generated data sets is standardized to 2500 points (See Methods). The percentages represent the fraction of trends in the original time series that are significantly higher than the null models ( $p=0.025$ , single-tailed).

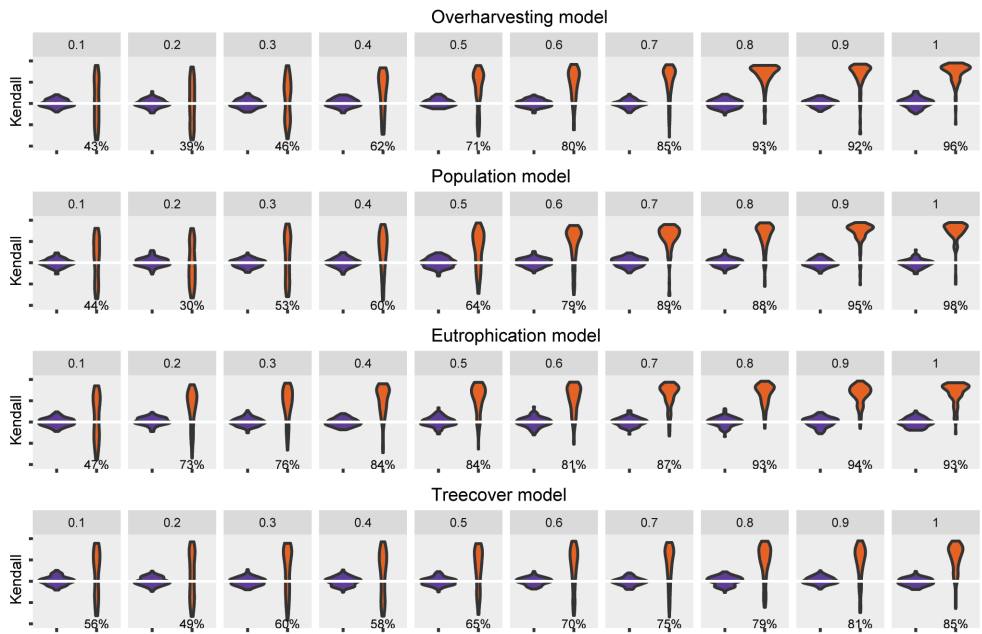


**Figure S3.2.** Strength of the trends in variance for the four different models in the original time series (orange) and null models (purple). The violin plots indicate the distribution of Kendall tau values for the 100 replicates for each level of  $\epsilon$ . The size of the generated data sets is standardized to 2500 points (See Methods). The percentages represent the fraction of trends in the original time series that are significantly higher than the null models ( $p=0.025$ , single-tailed).

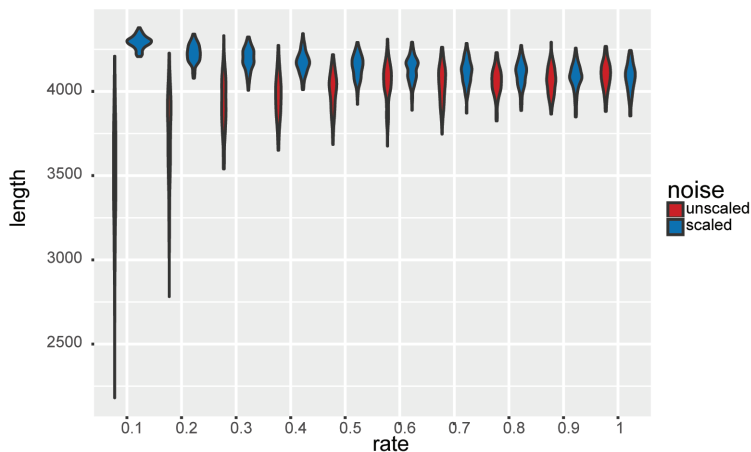


**Figure S3.3.** Length of the time period before the crash in the Overharvesting model, when the driver is changed within 5,000 time steps for the model without scaling of the noise (red) and scaling of the noise (blue) for different rates. When the noise is not scaled, the length of the period before the transition increases as the speed of the system increases. For scaled noise, an opposite trend is observed.

## EARLY-WARNING OF TIPPING POINTS IN SLOW SYSTEMS

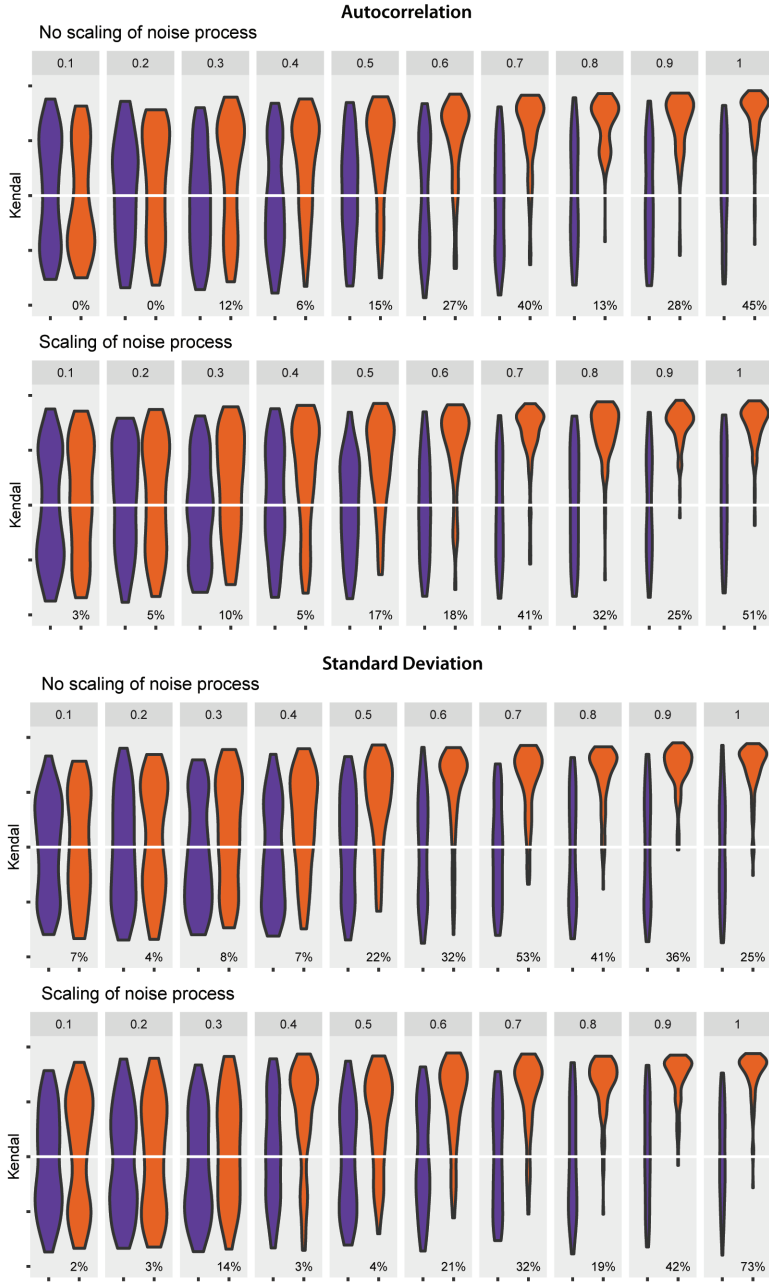


**Figure S3.4.** Strength of the trends in autocorrelation and standard deviation for the overharvesting model where the parameter  $\epsilon$  scales only the system's response (upper panel), or both the noise and the system's response (lower panel). The violin plots indicate the distribution of Kendall tau values for the 100 replicates for each level of  $\epsilon$  (purple) and the null model (orange) (See Methods). The percentages represent the fraction of trends in the original time series that are significantly higher than the null models ( $p=0.025$ , single-tailed).

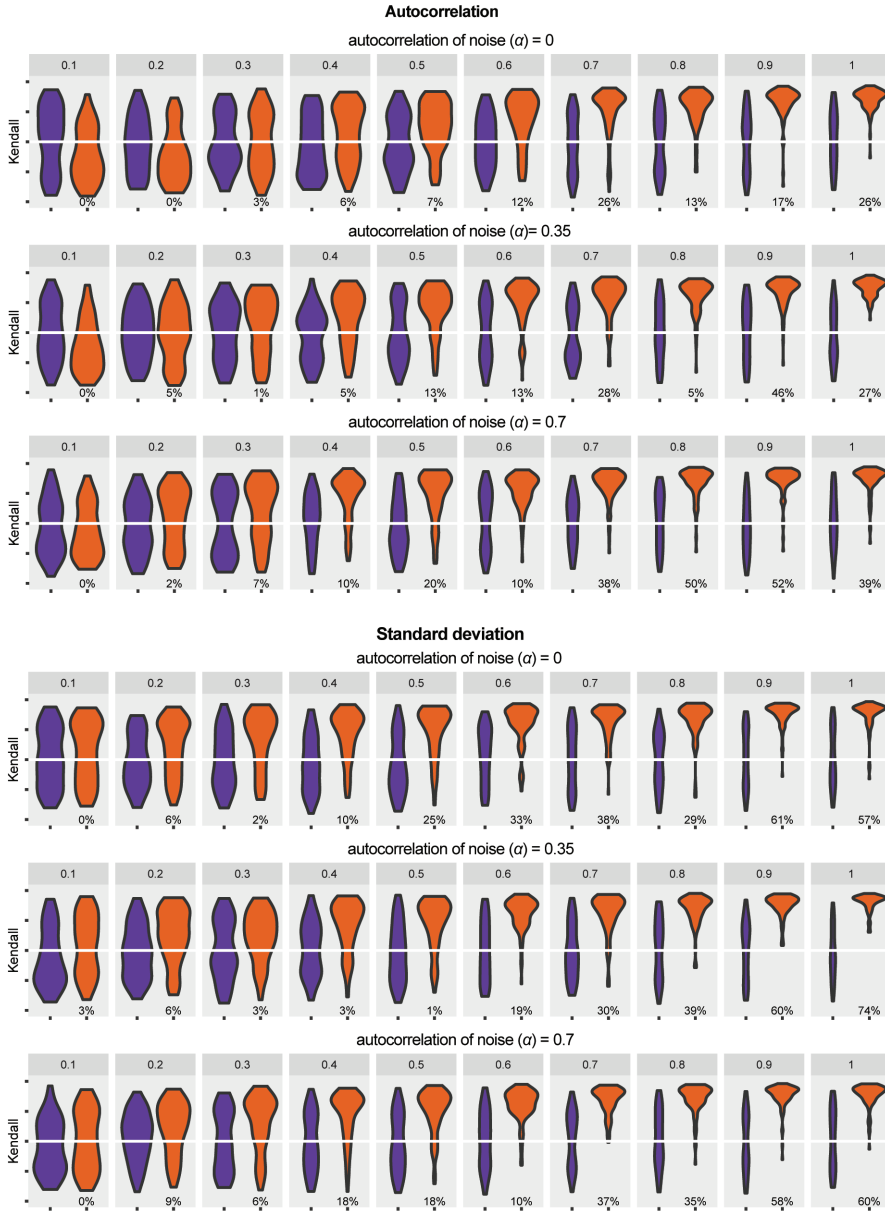


**Figure S3.5.** Trends in autocorrelation and variance of the simulations of the overharvesting model with different levels of temporal autocorrelation in the noise process ( $\alpha$ ). The violin plots indicate the distribution of Kendall tau values for the 100 replicates for each level of  $\epsilon$  (purple) and the null model (orange) (See Methods). The percentages represent the fraction of trends in the original time series that are significantly higher than the null models ( $p=0.025$ , single-tailed).



## EARLY-WARNING OF TIPPING POINTS IN SLOW SYSTEMS

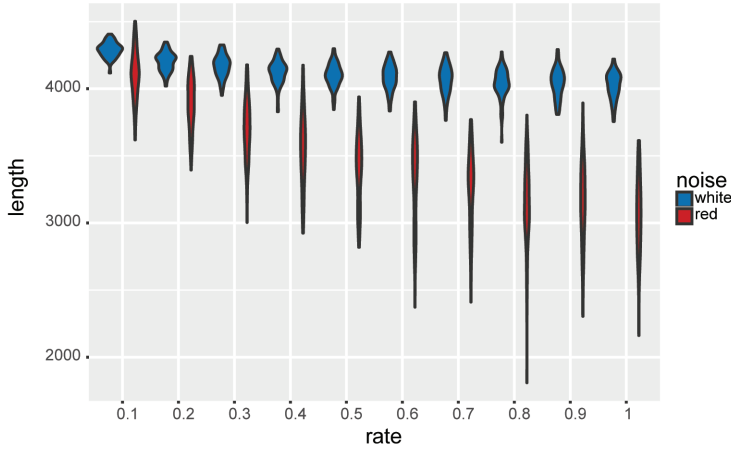


Figure S3.6. Length of the time period before the crash in the Overharvesting model, when the driver is changed within 5,000 time steps for the model with a noise process that is not time-correlated (white noise, blue violin plots) and is time-correlated (red noise with  $\alpha=0.7$ , red violin plots) for different rates. When the noise is time-correlated, there is a greater variation in the moment of shifting, regardless of the internal speed of the system. On average, the system shifts earlier than when the noise process is not time-correlated. In addition, the faster the system, the shorter the period before the transitions in a red environment.

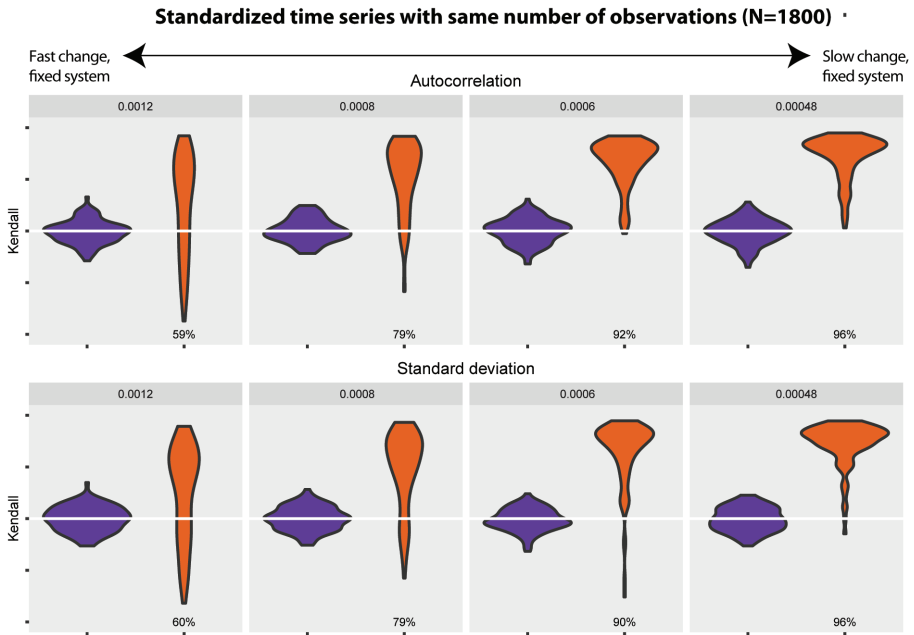
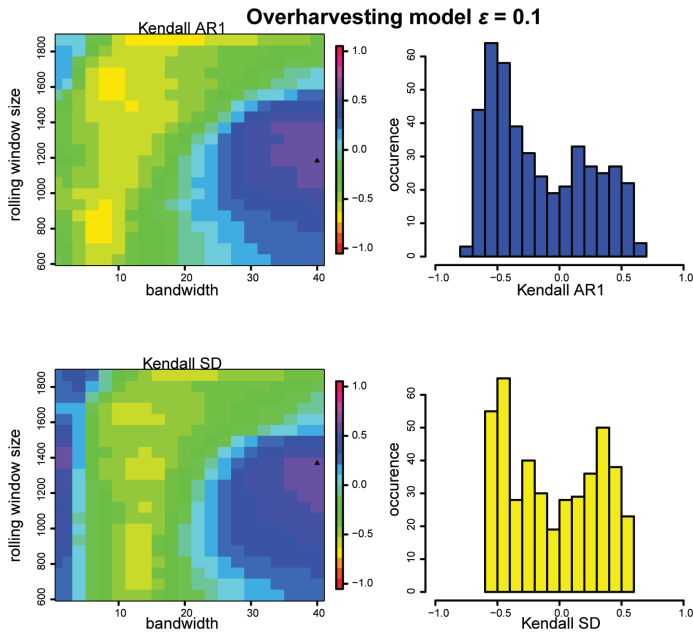
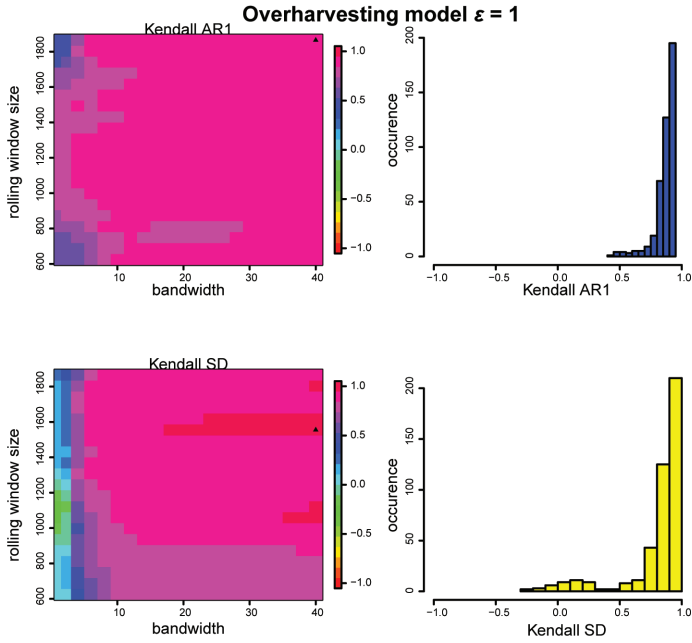


Figure S3.7. Strength of the trends for the resilience indicators for different rates of change when the time series are standardized by increasing the sampling frequency for higher rates of change (time series length = 1800 data points). The violin plots indicate the distribution of Kendall tau values of the indicators determined with the time series (orange) compared to the ones determined with the null model (purple).



**Figure S3.8.** Contour plots show the effect of the size of the sliding window and the width of the kernel filter on the observed trend in the resilience indicators as measured by the Kendall's tau for a time series with  $\varepsilon = 0.1$ . Arrows indicate the combination that gives the highest trend. In the main text, we used a sliding window of 1250 (50% of the time series), and a bandwidth of 10.



**Figure S3.9.** Contour plots show the effect of the size of the sliding window and the width of the kernel filter on the observed trend in the resilience indicators as measured by the Kendall's tau for a time series with  $\varepsilon = 1$ . Arrows indicate the combination that gives the highest trend. In the main text, we used a sliding window of 1250 (50% of the time series), and a bandwidth of 10.

## S3.6 SUPPLEMENTARY TABLES

Table S3.1. Model equations and parameter settings used in this study

MODELS	STATE VARIABLES AND PARAMETERS		VALUE
<b>OVERHARVESTING MODEL (MAY 1977)</b>  $\frac{dN}{dt} = \varepsilon (N - \alpha N^2 - c \frac{N^2}{N^2 + 1} + \sigma \frac{dW}{dt})$	N	Resource biomass (state)	
	$\varepsilon$	Speed of the system's response	0.1-1
	a	Competition term	0.1
	c	Maximum harvest rate (control)	1.6-2.8
	$\sigma$	SD of white noise	0.15
	dW	Wiener process with white Gaussian noise	
<b>EUTROPHICATION MODEL (CARPENTER ET AL. 1999, EQ. 1)</b>  $\frac{dN}{dt} = \varepsilon (a - b N + c \frac{N^p}{N^p + m^p} + \sigma \frac{dW}{dt})$	N	Nutrient concentration (state)	$\text{g m}^{-3}$
	$\varepsilon$	Speed of the system's response	0.1-1
	a	Nutrient loading rate (control)	$0.1\text{-}0.9 \text{ g m}^{-3} \text{ day}^{-1}$
	b	Nutrient loss rate	$0.9 \text{ day}^{-1}$
	c	Maximum recycling rate from sediment or hypolimnion	$1 \text{ g m}^{-3} \text{ day}^{-1}$
	m	Nutrient concentration at which recycling reaches half the maximum rate	$1 \text{ g m}^{-3}$
	p	power of Hill function	8
	$\sigma$	SD of white noise	0.02
	dW	Wiener process with white Gaussian noise	
<b>ALLEE EFFECT MODEL OF POPULATION (COURCHAMP ET AL., 1999)</b>  $\frac{dN}{dt} = \varepsilon (r N (1 - \frac{N}{K}) (\frac{N}{K} - \frac{C}{K}) - h N + \sigma \frac{dW}{dt})$	N	Biomass of population	$\text{g m}^{-2}$
	$\varepsilon$	Speed of the system's response	0.1-1
	C	Critical population biomass for positive growth	$10 \text{ g m}^{-2}$
	h	Harvest rate (control)	$0.0\text{-}0.1 \text{ day}^{-1}$
	K	Carrying capacity of population	$100 \text{ g m}^{-2}$
	r	Growth rate of population	$0.3 \text{ yr}^{-1}$
	$\sigma$	SD of white noise	0.5
	dW	Wiener process with white Gaussian noise	
<b>TREE COVER MODEL (VAN NES ET AL. 2014, EQ. 2)</b>  $\frac{dC}{dt} = \varepsilon ((\frac{P}{h_p + P r_m}) C (1 - \frac{C}{k}) - m_a C (\frac{h_a}{c + h_a}) - m_f C (\frac{h_f^p}{h_f^p + c^p}) + \sigma \frac{dW}{dt})$	C	Tree cover	75 %
	$\varepsilon$	Speed of the system's response	0.1-1
	$h_a$	Tree cover below which there is an increased mortality due to an Allee effect	10 %
	$h_f$	Tree cover below which the fire mortality increases steeply	64 %

## EARLY-WARNING OF TIPPING POINTS IN SLOW SYSTEMS

	$h_p$	The precipitation where the expansion rate is reduced by a half of its maximum	$0.5 \text{ mm day}^{-1}$
	$k$	Maximum tree cover	90 %
	$m_a$	Maximum loss rate for increased mortality at low tree cover densities	$0.15 \text{ yr}^{-1}$
	$m_f$	Maximum loss rate due to fire	$0.11 \text{ yr}^{-1}$
	$p$	Exponent in Hill function for fire effect	7
	$P$	Mean annual precipitation (control)	$5\text{-}1 \text{ mm day}^{-1}$
	$r_m$	Maximum expansion rate of tree cover	$0.3 \text{ yr}^{-1}$
	$\sigma$	SD of white noise	0.2
	$dW$	Wiener process with white Gaussian noise	

## CHAPTER 3

**Table S3.2.** Trends in autocorrelation and variance for all the model simulations for different levels of  $\epsilon$ . The trends are expressed as Kendall tau values, and the median and the 5 and 95 percentiles from the distributions are reported.

INDEX	OVERHARVESTING MODEL			POPULATION MODEL			EUTROPHICATION MODEL			TREECOVER MODEL		
$\epsilon$	AR1 median	(5,95)		AR1 median	(5,95)		AR1 median	(5,95)		AR1 median	(5,95)	
<b>0.1</b>	0.145	-0.787	0.714	0.174	-0.649	0.732	0.157	-0.658	0.798	0.252	-0.609	0.785
<b>0.2</b>	0.109	-0.762	0.794	-0.095	-0.714	0.729	0.489	-0.534	0.815	0.169	-0.564	0.780
<b>0.3</b>	0.058	-0.602	0.820	0.189	-0.688	0.789	0.429	-0.371	0.862	0.447	-0.601	0.813
<b>0.4</b>	0.428	-0.513	0.801	0.314	-0.507	0.844	0.575	-0.248	0.884	0.348	-0.621	0.822
<b>0.5</b>	0.580	-0.450	0.843	0.332	-0.528	0.802	0.618	-0.158	0.864	0.320	-0.496	0.807
<b>0.6</b>	0.620	-0.149	0.842	0.609	-0.405	0.859	0.580	-0.137	0.862	0.455	-0.503	0.830
<b>0.7</b>	0.652	-0.425	0.881	0.684	-0.131	0.877	0.684	0.067	0.886	0.530	-0.440	0.837
<b>0.8</b>	0.706	0.003	0.888	0.741	-0.048	0.915	0.682	-0.136	0.898	0.572	-0.370	0.867
<b>0.9</b>	0.749	0.101	0.914	0.756	0.307	0.880	0.697	0.111	0.879	0.533	-0.379	0.884
<b>1</b>	0.752	0.174	0.902	0.772	0.358	0.917	0.662	0.003	0.884	0.609	-0.002	0.860
$\epsilon$	SD median	(5,95)		SD median	(5,95)		SD median	(5,95)		SD median	(5,95)	
<b>0.1</b>	0.052	-0.744	0.800	0.166	-0.720	0.732	0.154	-0.686	0.780	0.352	-0.719	0.869
<b>0.2</b>	0.030	-0.772	0.708	-0.050	-0.702	0.656	0.462	-0.452	0.778	0.135	-0.672	0.836
<b>0.3</b>	0.192	-0.611	0.771	0.196	-0.670	0.805	0.501	-0.374	0.861	0.381	-0.632	0.844
<b>0.4</b>	0.397	-0.637	0.777	0.382	-0.575	0.832	0.607	-0.042	0.871	0.339	-0.666	0.862
<b>0.5</b>	0.533	-0.505	0.819	0.428	-0.426	0.787	0.643	-0.065	0.903	0.402	-0.474	0.835
<b>0.6</b>	0.573	-0.210	0.847	0.597	-0.452	0.835	0.612	-0.046	0.884	0.484	-0.550	0.871
<b>0.7</b>	0.666	-0.240	0.870	0.667	0.039	0.861	0.727	0.047	0.882	0.562	-0.486	0.873
<b>0.8</b>	0.766	0.030	0.888	0.710	-0.042	0.904	0.728	0.177	0.902	0.562	-0.396	0.880
<b>0.9</b>	0.758	0.016	0.896	0.789	0.190	0.911	0.703	0.164	0.886	0.574	-0.305	0.902
<b>1</b>	0.799	0.347	0.912	0.787	0.351	0.917	0.769	0.107	0.900	0.654	-0.063	0.878

## EARLY-WARNING OF TIPPING POINTS IN SLOW SYSTEMS

**Table S3.3.** Percentages of the 100 runs that had a significant positive trend (Kendall's test with a confidence level of 0.95, two-tailed, and  $p < 0.025$ ) or that were significantly different than the null model (Null, single-tailed,  $p < 0.025$ ) for both resilience indicators.

INDEX	OVERHARVESTING MODEL				POPULATION MODEL			
$\varepsilon$	AR1		SD		AR1		SD	
	Kendall	Null	Kendall	Null	Kendall	Null	Kendall	Null
0.1	52%	49%	50%	43%	59%	50%	59%	44%
0.2	52%	42%	49%	39%	41%	31%	44%	30%
0.3	51%	43%	55%	46%	62%	51%	58%	53%
0.4	68%	65%	71%	62%	70%	60%	73%	60%
0.5	74%	68%	81%	71%	67%	57%	73%	64%
0.6	91%	82%	87%	80%	85%	76%	86%	79%
0.7	87%	78%	87%	85%	93%	92%	95%	89%
0.8	91%	89%	94%	93%	93%	88%	92%	88%
0.9	96%	91%	93%	92%	98%	97%	95%	95%
1	96%	94%	98%	96%	98%	98%	98%	98%
INDEX	EUTROPHICATION MODEL				TREECOVER MODEL			
$\varepsilon$	AR1		SD		AR1		SD	
	Kendall	Null	Kendall	Null	Kendall	Null	Kendall	Null
0.1	55%	47%	53%	47%	62%	52%	62%	56%
0.2	77%	68%	78%	73%	56%	51%	58%	49%
0.3	85%	74%	85%	76%	65%	60%	66%	60%
0.4	88%	77%	90%	84%	65%	56%	63%	58%
0.5	90%	82%	87%	84%	70%	66%	73%	65%
0.6	87%	76%	92%	81%	76%	68%	76%	70%
0.7	95%	93%	95%	87%	80%	72%	82%	75%
0.8	90%	84%	98%	93%	86%	78%	84%	79%
0.9	96%	88%	97%	94%	84%	76%	84%	81%
1	94%	91%	98%	93%	94%	88%	91%	85%

## CHAPTER 3





# CHAPTER 4

## RATE-INDUCED TIPPING IN A POPULATION OF CYANOBACTERIA

Bregje van der Bolt,  
and Egbert H. van Nes

*“Time may change me  
But I can’t trace time  
I said that time may change me  
But I can’t trace time”*

- David Bowie

### ABSTRACT

Ecosystems can have tipping points at which a critical transition to another dynamical regime may occur. Recent studies show that in some situations fast rates of change may trigger a critical transition, whereas change of the same magnitude but at slower rates would not. Even though considering rate-induced tipping is important for understanding and predicting ecosystem response to the ongoing rapid environmental change, few studies describe rate-induced tipping in ecology. Here, we demonstrate rate-induced tipping in a model of cyanobacteria with realistic parameter settings. We show that there is a range of initial conditions at which a gradual increase in environmental conditions can potentially cause a collapse, depending on the rate. In our model a pulse in the environmental conditions can also cause a temporary collapse, but that is dependent on both the rate and the duration of the pulse. Furthermore, the kind of stochastic environmental regime can influence the probability of inducing rate-tipping. Our results imply that, even though the identification of rate sensitive ecosystems will be challenging, we should incorporate critical rates of change in our ecosystem assessments and management.

## INTRODUCTION

In the recent years the notion that ecosystems can have tipping points has received considerable attention. The term ‘tipping point’ is loosely defined as a threshold point in conditions after which runaway change brings a system to a new state. Under current levels of climate change the likelihood of such transitions in ecological systems is increasing (Bestelmeyer et al., 2011; Klein Goldewijk et al., 2011). These critical transitions are of great concern because recovery is difficult due to hysteresis. Several mechanisms can lead to critical transitions, but all mechanisms have in common that self-enforcing feedbacks (van Nes et al., 2016) cause the critical transitions. In the mathematical literature three classes of transitions between states are distinguished: bifurcation-induced, noise-induced and rate-induced tipping (Ashwin et al., 2012).

Bifurcation-induced tipping is due to a gradual change in external condition (Figure 4.4a, b). As a result of the change in conditions, the resilience of the current state erodes until the system reaches a bifurcation point at which the state becomes unstable and the system shifts to an alternative state. Because the resilience of the system changes as the system approaches the tipping point, this type of tipping can be detected using resilience indicators (Marten Scheffer et al., 2009).

In the case of noise-induced tipping, not a change in external conditions, but a perturbation in the system state, results in a shift from one state to another. When the perturbation is large enough to bring the system across the unstable equilibrium (top of the hill between two valleys, Figure 4.4c), the system shifts to the other equilibrium. Because this type of tipping does not involve a change in the stability of the system, the tipping point cannot be anticipated using resilience indicators (Gsell et al., 2016).

Rate induced tipping is caused by a high speed of change in external conditions rather than the absolute level. It has been described recently (Ashwin et al., 2012) and can occur only in susceptible systems, i.e., systems that are ‘forward basin unstable’ (Ashwin, Perryman, & Wieczorek, 2017). Rate-tipping can only be understood if we consider that a system is not always in a steady state and that the equilibrium can change if conditions change. If the external conditions change fast compared to the response rate of the system, the actual system state can deviate from the stable state if the system cannot track the changing equilibrium. If the change in external changes is below the critical rate, the system state lags behind the steady state but stays in the same basin of attraction (Figure 4.4f, purple ball). If the external changes are above a critical rate, the system is unable to cope with the rapid changes and is brought out of the basin of attraction (Figure 4.4f, orange ball). Subsequently, the system shifts to

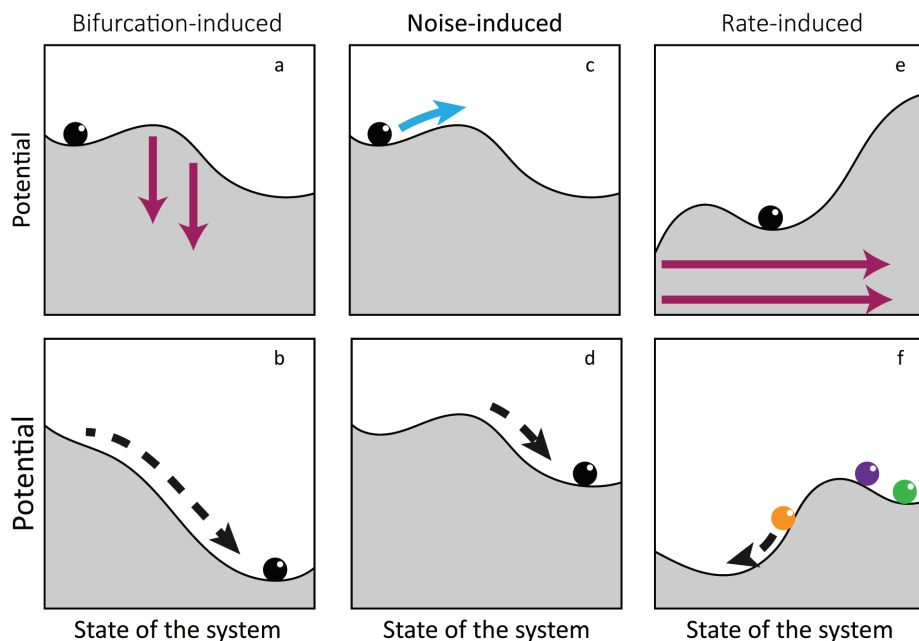


**Figure 4.4.** Three types of tipping in a system with alternative stable states: bifurcation-induced (a,b), noise-induced (c,d) and rate-induced (e,f). The upper panels show the initial stability landscapes. Pink arrows show the change in the stability landscape, and the blue arrow shows a change in the state of the system. The lower panels show the stability landscapes at the tipping point, and the dotted arrows indicate the self-enforced change of the system. In the case of bifurcation-induced tipping the potential landscape changes because environmental conditions change, and as a result the initial basin of attraction vanishes and the system moves towards another equilibrium (depicted by the ball). With noise-induced tipping, the potential landscape does not change, but the system is brought past the unstable equilibrium (top of the hill between two valleys) by a perturbation in the state of the system (blue arrow). With rate-tipping the potential landscape moves sideways due to rapid change of conditions. Only if the change happens too fast, the system does not follow the change in equilibrium and can lag behind the stable state (purple ball) or be pulled out of the basin of attraction (orange ball). If the system can respond fast enough, however, the system is able to track the changing equilibrium and is approximately in stable state (green ball).

another stable state. If the system can respond fast to the changing equilibrium, the system will approximately remain in steady state (Figure 4.4f, green ball). Rate-induced tipping, can also occur in excitable systems where a fast change in conditions cause the system to cycle once (Wieczorek, Ashwin, Luke, & Cox, 2011). While there is a vast amount of literature on bifurcation-induced and noise-induced tipping, there are only few studies that describe rate-induced tipping in ecology (Marten Scheffer et al., 2008; Siteur et al., 2016).

A candidate system for rate-induced tipping seems to be a population of cyanobacteria. Experiments have shown that in chemostats, phytoplankton communities can have

tipping points and show critical slowing down before the transition (Faassen et al., 2015; Veraart et al., 2012). It has been proposed that a self-enforcing feedback that involves photoinhibition can cause these alternative stable states (Faassen et al., 2015; Veraart et al., 2012). Photoinhibition is a decrease in the rate of photosynthesis as a result of high light. High light levels cause damage to the photosynthetic machinery of the cells, which lowers the photosynthetic rates, or protective mechanisms to avoid damage can lower the rate of photosynthesis (Long, Humphries, & Falkowski, 1994; Takahashi & Murata, 2008). This means that although phytoplankton need light for photosynthesis, too much light lowers their productivity. High concentrations of phytoplankton may reduce photoinhibition under high light conditions by self-shading, which implies that there is a self-enforcing feedback (Holmgren, Scheffer, & Huston, 1997; Veraart et al., 2012). As a result of this feedback, phytoplankton communities can maintain a high biomass under light levels that would prohibit growth in a low biomass system. When the light intensity reaches a certain threshold, the shading becomes insufficient to prevent photoinhibition, and as a result, biomass decreases, the system becomes even more vulnerable to the high light, and the biomass decreases even further, resulting in a shift to a collapsed state (Veraart et al., 2012).

In this paper we study a model of phytoplankton growth in a chemostat, and show that for realistic parameter settings (Faassen et al., 2015) there can be rate-induced tipping if light levels increase rapidly in this system. We focus on three different types of changes in environmental conditions: a gradual increase to a new level, a pulse perturbation, and a regime of perturbations. After we have explored the conditions for which the model shows rate-induced tipping, we discuss the implications of these results for other ecosystems and ecosystem management under current rates of climate change.

## METHODS

### MODEL

To explore if phytoplankton communities are sensitive to the rate of change in light intensity, we use a simple model that describes the photoinhibition of phytoplankton in a chemostat (Gerla, Mooij, & Huisman, 2011). The changes in the phytoplankton concentration of the chemostat can be described as follows:

$$\frac{dA}{dt} = P_{av}(I_z(z, A))A - lA \quad (4.1)$$

Where  $A$  is the algae concentration ( $\text{g m}^{-3}$ ),  $l$  the loss rate of phytoplankton ( $\text{d}^{-1}$ ) due

## CHAPTER 4

to flushing and  $P_{av}(I_z(z,A))$  is the average production rate in the water column ( $d^{-1}$ ) as function of the light availability. In the chemostat the light comes from the side and the light is attenuated in the water due to light absorption and scattering. The light intensity in the water column follows the Lambert-Beer law. According to this formula, the light intensity expressed as photon flux  $I_z$  ( $\mu\text{mol m}^{-2} \text{s}^{-1}$ ) decays exponentially with position  $z$  (m):

$$I_z = I_{in} e^{-K_d z} \quad (4.2)$$

Where  $K_d$  is the light attenuation coefficient of particles in the water ( $m^{-1}$ ). This light attenuation depends on particles and substances in the water. Therefore, also the phytoplankton biomass has an effect on the light attenuation coefficient. This effect is approximately linear with biomass, so in our model  $I_z$  is a function of both  $z$  and  $A$ :

$$I_z(z, A(t)) = I_{in} e^{-K_d z - k A(t) z} \quad (4.3)$$

Where  $k$  is the specific extinction of phytoplankton ( $m^2 g^{-1}$ ). The spatial averaged light limitation of phytoplankton in the chemostat can be calculated by integration over the total water column  $D$  (m):

$$P_{av}(I_z(z, A(t))) = \frac{1}{D} \int_0^D P_z(I_z(z, A(t))) dz \quad (4.4)$$

The relationship between light availability  $I_z$  and the relative phytoplankton production  $P_z$  can be described with the Peeters-Eilers equation, that includes the effect of photoinhibition (Peeters & Eilers, 1978):

$$P_z(I_z(z, A(t))) = P_{\max} \frac{I_z(z, A(t))}{a I_z(z, A(t))^2 + b I_z(z, A(t)) + c} \quad (4.5)$$

Where  $P_{\max}$  is the maximum growth rate of phytoplankton ( $d^{-1}$ ). The precise meaning of the parameters  $a$ ,  $b$ , and  $c$  are hard to interpret. Therefore, Peeters and Eilers introduced two new parameters:  $I_{opt}$ , the optimum light availability for production, and  $I_k$ , that defines the slope of the curve at  $I_z=0$ . Specifically,  $I_k$  is the light availability where the maximum production is reached if the initial slope was continued. The parameters  $a$ ,  $b$ , and  $c$  can be expressed as function of these two new parameters:

$$a = \frac{I_k}{I_{opt}}, \quad b = 1 - 2 \frac{I_k}{I_{opt}}, \quad \text{and} \quad c = I_k \quad (4.6)$$

The integral of the phytoplankton production (Eq. 4.5) can be solved analytically (Peeters & Eilers, 1978). The default values of the parameters of the model (Eq. 4.2 and 4.5) describe phytoplankton in a chemostat (Faassen et al., 2015) and can be found in Table 4.1. The model was analyzed using Grind for MATLAB (<http://www.sparcs-center.org/grind.html>) which uses a Runge-Kutta numerical solver (ode45). For continuation of bifurcations, GRIND uses MatCont version 6.10 (Dhooge, Govaerts, & Kuznetsov, 2003).

## SIMULATED INCOMING LIGHT INTENSITIES

We focus on three different kinds of change in the incoming light intensity: a gradual increase to a new level, a pulse perturbation, and a stochastic regime of perturbations. First, we increased the light intensity with different rates to check when the model can track the equilibrium. After that, we analysed how pulses in the light intensity affect the phytoplankton community in the chemostat. Lastly, we determined how the system is affected by a stochastic regime of perturbations. The analysis of phytoplankton dynamics under constant environmental conditions can be found in Supplementary Information S4.1.

In the first scenario, we increased the light intensity from a low value ( $I_{in} = 100 \mu\text{mol m}^{-2} \text{s}^{-1}$ ) to a high value ( $I_{in} = 800 \mu\text{mol m}^{-2} \text{s}^{-1}$ ) with a constant rate. This scenario is called ‘steady drift’ (Ashwin et al., 2012) and is implemented in the model as follows:

$$\frac{dI_{in}}{dt} = \begin{cases} r & \text{if } I_{in} < I_{in,max} \\ 0 & \text{otherwise} \end{cases} \quad (4.7)$$

Where  $r$  is the rate by which the light intensity is increased. The initial conditions are the equilibrium states ( $A^*$ ) for the low light conditions ( $I_{in}=100$ :  $A^*=6.1779$ ).

Next, we explored the potential effects of a pulse in a rate-sensitive system. We exposed the model to a brief pulse in the value of the parameter  $I_{in}$ . The effect of such a pulse is different than a gradual increase in light intensity, because not only the relative rate, but also the duration of the pulse determines whether the system tips or not. During the pulse we let  $I_{in}$  approach a maximum value exponentially (this is called ‘unsteady drift’ (Ashwin et al., 2012),  $I_{in}$  will remain at the maximum value for a specific duration, after which  $I_{in}$  decreases exponentially back to the start value (see Figure 4.7a). The formula for the unsteady drift is:

$$\frac{dI_{in}}{dt} = \begin{cases} r(I_{in,max} - I_{in}) & \text{if } t > t_{start} \text{ and } t > t_{end} \\ r(I_{in,min} - I_{in}) & \text{otherwise} \end{cases} \quad (4.8)$$

Where  $I_{in,max}$  is the maximum value of the pulse of  $800 \mu\text{mol m}^{-2} \text{s}^{-1}$ , and  $I_{in,min}$  the base light intensity.

The simulations started with the ecosystem in equilibrium with low light  $I_{in,min}$  and we applied the pulse after 100 time steps. We considered the biomass collapsed when it gets below a value of  $10^{-8} \text{ g m}^{-3}$ . If the incoming light intensity is brought back to the low light intensity, the system will eventually recover, as in this model there is only one stable state with low light, but the recovery will take very long compared to the systems' timescale.

To explore how this system with rate-induced tipping is affected by environmental variability with different power spectra, we created time series of hypothetical environmental fluctuations  $T_a$  using the following stochastic differential equation:

$$\frac{dT_a}{dt} = -\gamma T_a + \beta \frac{dW}{dt} \quad (4.9)$$

Where  $\beta$  is a parameter scaling the variance of the noise,  $dW/dt$  is a Wiener process where the increments are normally distributed.  $\gamma$  is  $\geq 0$  and corresponds to negative feedbacks that act to restore any anomaly to the mean,  $T_a=0$ . The smaller  $\gamma$ , the larger the autocorrelation of  $T_a$ ;  $\gamma=0$  corresponds to an unbounded random walk (Brownian motion). We solved the equation using an Euler-Maruyama scheme with time step 1. With this scheme and time step, the relation between  $\gamma$  and the autocorrelation  $\alpha$  of the discrete time series generated with this model can be described as  $\alpha(1) = 1-\gamma$  (sampling time step =1).

In reality, when the temporal autocorrelation of the environmental variability increases, the variance of the variability also changes (see Figure S4.12). To study the effect of the time-correlation in isolation, we scaled the parameter  $\beta$  in such a way to keep the expected variance of  $T_a$  at a constant value using the following equation:

$$\beta = \sigma \sqrt{\frac{(1-\alpha^2)}{\Delta t}} \quad (4.10)$$

We ran the model with time series of  $T_a$  with different levels of autocorrelation  $\alpha$  ( $\gamma$  of Eq. 4.9  $1-(1-\alpha)/dt$ ), ranging from 0 to 0.9 with an increment of 0.05, and different



levels of standard deviation ( $\sigma$ ), ranging from 0.02 to 0.3 with an increment of 0.01. We increased the incoming light intensity from 100 to 800 (Eq. S1), with a rate that is below the critical rate ( $r_{\text{crit}} = 0.1378$ ,  $r = 0.13$ ). For each level of autocorrelation and standard deviation  $\sigma$  we repeated the simulations 1,000 times to determine what percentage of the runs collapsed.

We assumed that the environmental variable  $T_a(t)$  can have different effects on the phytoplankton biomass. The first assumption was that the stochastic fluctuations directly act on the phytoplankton biomass in the following way:

$$\frac{dA}{dt} = (P_{av}(I_z(z, A(t)))A(t)) - l A(t) + T_a(t) \quad (4.11)$$

The second assumption was that the environmental fluctuations are added to the incoming light intensity in the following way:

$$\frac{dI_{in}}{dt} = r(I_{in, \max} - I_{in}) + T_a(t) \quad (4.12)$$

Where  $r$  is the rate by which the light intensity is increased ( $r_{\text{crit}} = 0.1378$ ,  $r = 0.13$ ) and  $I_{in, \max}$  the maximum value of the incoming light intensity of  $800 \mu\text{mol m}^{-2} \text{s}^{-1}$ . Similar to the previous analysis, we ran the model with generated time series of  $T_a$  with different levels of autocorrelation  $\alpha$  ( $\gamma$  of Eq. 4.9  $1=(1-\alpha)/dt$ ), ranging from 0 to 0.9 with an increment of 0.05, and different levels of standard deviation ( $\sigma$ ), ranging from 10 to 80 with an increment of 2.5. With each parameter setting we repeated 1,000 runs of the model. We determined for each ensemble of runs what percentage of the runs collapsed.

**Table 4.1.** Description of the parameters and state variables with their initial conditions and default values.

VARIABLE	VALUE	DESCRIPTION	UNITS
A	6.1779	Phytoplankton biomass	$\text{g m}^{-3}$
$I_{in}$	100	Light intensity	$\mu\text{mol m}^{-2} \text{s}^{-1}$
D	0.05	Size of the water column	m
$I_K$	40	Slope of the light curve at $I_z=0$	$\mu\text{mol m}^{-2} \text{s}^{-1}$
$I_{\text{OPT}}$	150	Optimum light intensity of phytoplankton	$\mu\text{mol m}^{-2} \text{s}^{-1}$
K	3	Specific light attenuation coefficient of phytoplankton	$\text{m}^2 \text{g}^{-1}$
$K_D$	$10^{-5}$	Background light attenuation coefficient	$\text{m}^{-1}$
L	0.4	Loss of phytoplankton due to flushing	$\text{day}^{-1}$
$P_{\text{MAX}}$	0.49	Maximum productivity	$\text{day}^{-1}$

**RESULTS****GRADUAL INCREASE OF LIGHT INTENSITY**

We started all simulations from a state in which the phytoplankton population size was adapted to the low light conditions, which implies that the biomass is relatively low. If the light intensity is increased slowly, the phytoplankton could grow fast enough for self-shading. When we increased the light intensity very rapidly, the system shifted to the other state because the growth-rate of the phytoplankton was too slow to keep up with the increased light intensity (blue line, Figure 4.5a).

The reason why this model has rate-induced tipping can also be understood from the  $(I_{in}, A)$ -phase plane of the model (Figure 4.5b). If  $I_{in}$  changes gradually, the system can follow the equilibrium and the phytoplankton biomass increases (green line, Figure 4.5b). If  $I_{in}$  changes too fast, however, the system is brought past the unstable equilibrium and as a consequence, the phytoplankton biomass collapses (blue line, Figure 4.5b). The critical rate for r-tipping depends on the initial conditions and the maximum light intensity. The conditions where rate tipping is potentially possible have “forward basin instability” (Ashwin et al., 2017). This is the case if an instantaneous change in environmental conditions can bring the system to an alternative basin of attraction while no bifurcation point is crossed (Ashwin et al., 2017). In a simple model with one state variable, this instability can be read from the phase plane (Figure 4.6), A change with infinite speed from an initial condition to a higher value for the incoming light intensity can be visualized as a horizontal line (like the orange arrow). If that straight line crosses the unstable equilibrium (Figure 4.6, green line), the system is forward basin instable, because the new equilibrium is in another basin of attraction than the initial equilibrium and the fold bifurcation  $F_1$  is not passed. Initial conditions for which rate-tipping could occur in this model, are indicated in Figure 4.6 (red dots).

**EFFECT OF LIGHT INTENSITY PULSES**

In the previous section we have explored the impact of a gradual increase of incoming light on tipping, showing that when the increase in light intensity goes too fast, the system cannot track the changing equilibrium. Next to gradual increase, drivers of environmental change can also increase for a brief period of time. For example, when environmental conditions are reversed as a result of an implemented policy. Furthermore, the increasing frequency and duration of extreme weather events (Coumou & Rahmstorf, 2012) like heat waves and droughts also act as pulses on ecosystems.

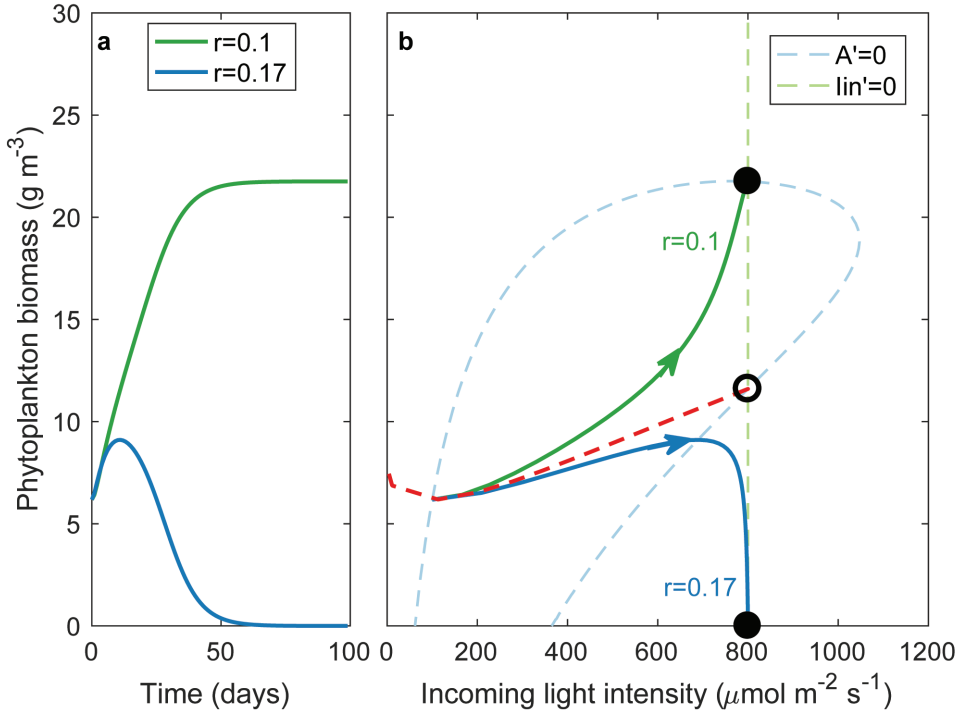


**Figure 4.5.** Simulated effects of the rate of change ( $r$ ) in light intensity ( $I_{in}$ ) on phytoplankton biomass. a) If the light intensity is increased slowly, the phytoplankton can grow fast enough to provide self-shading and the system will move towards a high-biomass equilibrium (green line). If the rate is too fast, the phytoplankton cannot grow fast enough to provide shade and the system collapses (blue line). b) The  $(I_{in}, A)$ -phase plane of the model. The blue dotted line is the nullcline of the phytoplankton biomass. The green dotted line is the nullcline for  $I_{in}$ , which is a vertical line at  $I_{in,max}$  ( $I_{in,max}=800$  for these settings). If  $I_{in}$  changes very fast, the system is brought past the separatrix (red dotted line) and moves to the collapsed state (blue line), while if  $I_{in}$  changes more gradually, the system can follow the equilibrium and the phytoplankton biomass increases (green line).

In this model, a pulse will always have a temporary effect, as the system is not bistable at the initial conditions. Reverting the change will eventually result in recovery. This recovery, however, can take long if the other stable state is reached. We define a temporary collapse as a biomass value below  $10^{-8} \text{ g m}^{-3}$ , and analyse when this happens.

As with the gradual increase in light intensity, if the rate of change is too fast, the system cannot track the changing equilibrium and the system is brought in the alternative basin of attraction and the phytoplankton starts collapsing. In contrast to gradual increase, the pulse should last long enough to cause a collapse. If the light intensity is lowered already before the phytoplankton biomass is collapsed, the biomass returns to the initial biomass state. For each specific rate there is a specific minimum duration that is needed for the system to collapse. For higher rates, shorter durations are needed

## CHAPTER 4

for the biomass to collapse (Figure 4.7b).

With our initial conditions, the critical rate for rate-tipping to occur is  $0.1378 \text{ day}^{-1}$ . With this rate, the duration of the pulse needs to be at least 382 days for the system to collapse (i.e. biomass  $< 10^{-8} \text{ g m}^{-3}$ ). If the rate is very high ( $r > 1000$ ), the critical duration of the pulse is still around 112 days, indicating that for a pulse to have an effect on the phytoplankton community, the duration of the pulse should be longer than 112–382 days, depending on the rate of change.

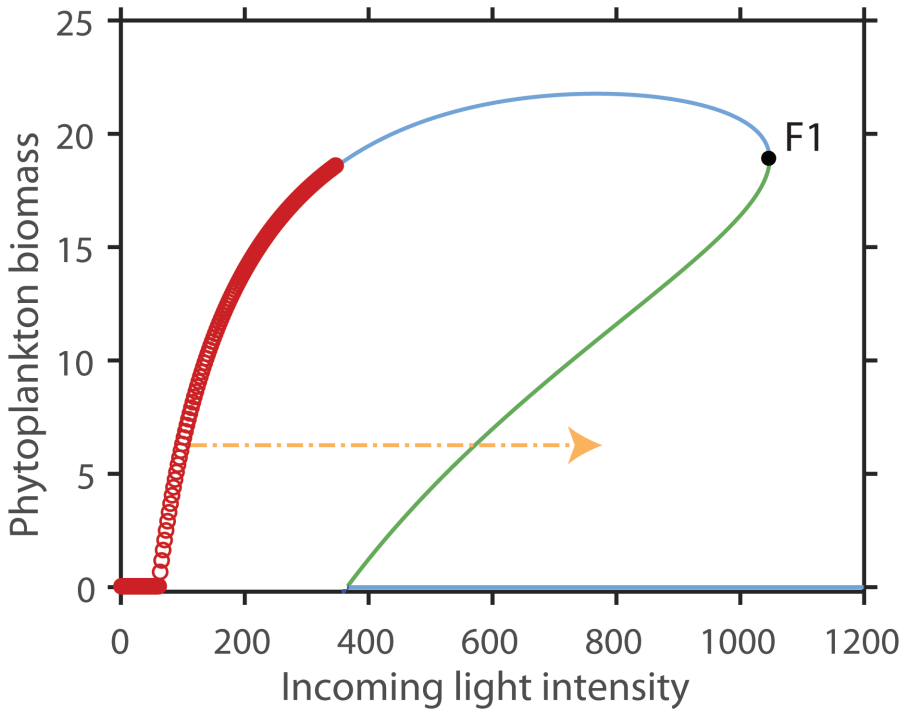


**Figure 4.6.** Initial conditions that are forward basin instable (red dots). The blue line indicates the stable equilibrium, the green line the unstable equilibrium and  $F_1$  is the fold bifurcation. When a change in the incoming light intensity occurs with infinite speed (horizontal line, as for example the orange arrow) and crosses the unstable equilibrium, the new equilibrium is in another basin of attraction than the initial equilibrium, while the fold bifurcation  $F_1$  is not passed. If this is the case, the system is forward basin instable.

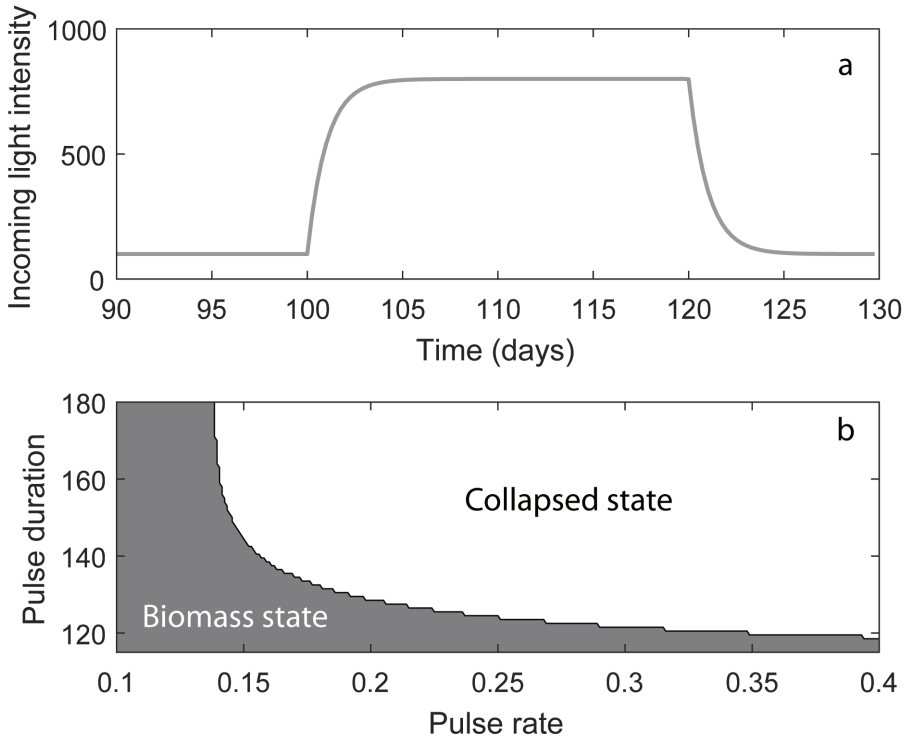


**Figure 4.7.** Simulation experiment altering pulse duration and intensity for an exponential increase of the light intensity. (a) Example time series of  $I_{in}$  with a pulse of 140 days. (b) The response of the phytoplankton biomass to pulses that increase and decrease exponentially with different rates of change (x-axis) and different durations of the pulse (y-axis).

## EFFECT OF STOCHASTIC PERTURBATION REGIMES IN LIGHT INTENSITY

In reality, ecosystems are subject to a regime of perturbations in the environmental conditions, this is also called environmental variability. In different environments, the variability can have different power spectra. Previous research indicates that systems with bifurcation-induced tipping are sensitive to the frequencies of the environmental variability. Longer periods of adverse conditions result in an higher probability of tipping in a more time-correlated environments (van der Bolt, van Nes, Bathiany, Vollebregt, & Scheffer, 2018). Because our previous analyses show that the phytoplankton biomass is sensitive to the duration of pulses, increased time-correlation in the environmental variability might also affect the probability of a collapse in biomass.

Our results (see Figure 4.8) indicate a higher probability of shifting in a system with more time-correlated stochasticity. The stochastic fluctuations in the phytoplankton

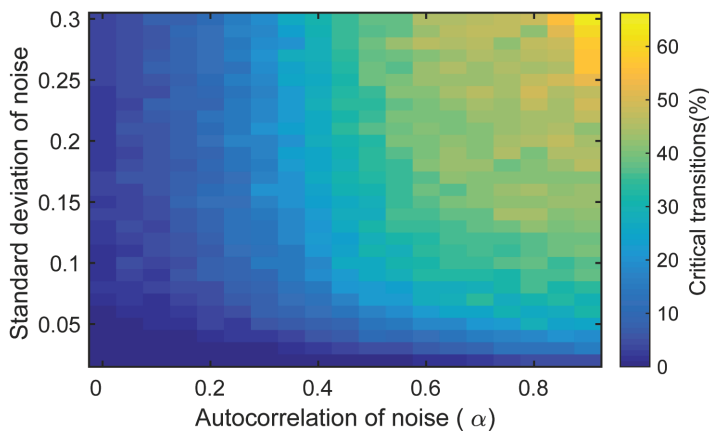


**Figure 4.8.** The response of the phytoplankton biomass to an increase in the light intensity in a stochastic environment. Combined effects of autocorrelation and the standard deviation of the fluctuations in the phytoplankton biomass on the percentage of runs in which the phytoplankton biomass collapses when the rate of change of the incoming light intensity is  $0.13 \text{ day}^{-1}$ .

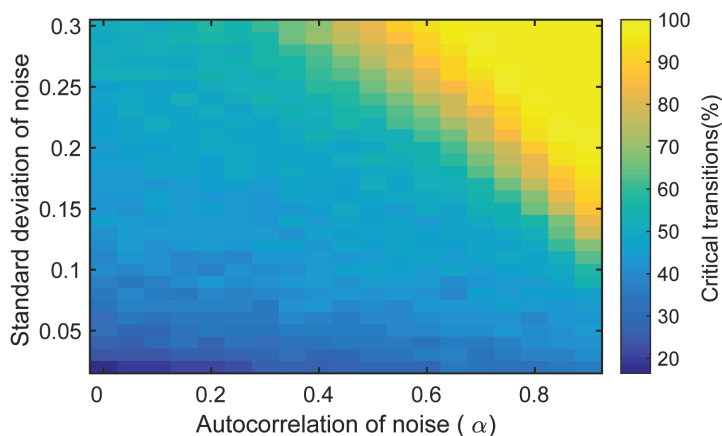


**Figure 4.9.** The response of the phytoplankton biomass to an increase in the light intensity with stochastic fluctuations on the light intensity. Combined effects of autocorrelation and the standard deviation of the fluctuations on the percentage of runs in which the phytoplankton biomass collapses when the rate of change is  $0.13$ .

biomass have an influence on whether the phytoplankton can provide enough shading for the biomass to withstand the incoming light intensity. If the phytoplankton biomass is lower, the critical rate is lower, meaning that the change in incoming light intensity should be more gradual in order for the phytoplankton to be able to grow enough to provide shading. In an uncorrelated environmental signal ( $\alpha=0$ , see Figure S4.11a) the fluctuations in the biomass are very rapid but do not last long enough to cause a collapse. In a more time-correlated environment (for example,  $\alpha=0.8$ , see Figure S4.11c), however, the fluctuations in the phytoplankton biomass have a longer duration and as a consequence, the biomass can collapse at lower rates.

When the environmental variability affects the incoming light intensity, increased time-correlation in the variability also causes a higher probability of shifting in the phytoplankton biomass (see Figure 4.9). In this case, the fluctuations are in the driver, and opposite to fluctuations in the state of the system, they do not affect the critical rate. When the fluctuations are uncorrelated, the fluctuations are very rapid but the phytoplankton biomass does not have time to respond to the short changes. When the fluctuations are correlated, however, the fluctuations are slower and can cause an temporary increase in light intensity on top of the gradual increase, that results in a collapse of the biomass (see Figure 4.9).

## DISCUSSION AND CONCLUSIONS

We have shown with this model with realistic parameter settings (Faassen et al., 2015) that speed of change can be critical for the effect that environmental conditions have on phytoplankton. Although our model of phytoplankton is not new, and the idea of rate induced tipping may seem intuitive in this case, rate tipping has not been described before for this system. We show that not only a gradual increase in environmental conditions can also cause a collapse, but also a pulse in the conditions can cause a temporary collapse. In addition, the kind of stochastic regime can influence the probability of shifting.

With the current rates of environmental change (Joos & Spahni, 2008; Klein Goldewijk et al., 2011), the questions arises what kind of systems are sensitive to rate-induced tipping. A way to see if a model potentially can have rate tipping is to test for forward basin instability (Ashwin et al., 2017). This can tested numerically by comparing the effects of a gradual change in conditions with an instantaneous change to the same level. In our model, there is a range of initial conditions where rate tipping can occur. As our model has one state variable, forward basin instability can easily been seen from

## CHAPTER 4

the bifurcation diagram. Due to the hump-shaped bifurcation diagram, there are initial conditions where an instantaneous change in conditions (here an increase in light) brings the state to the other basin of attraction (see orange arrow in Figure 4.6). When the conditions stay long enough at that level the system will tip to the alternative basin of attraction (rate tipping).

Although this feature may be useful to identify models with rate-tipping, the identification of rate sensitive species or ecosystems in the real world might be more difficult; rate-induced tipping has not yet been observed in real ecosystems. A number of experimental studies, however, do show rate-dependent outcomes (Bell & Gonzalez, 2009; Collins & de Meaux, 2009; Lindsey, Gallie, Taylor, & Kerr, 2013; Perron, Gonzalez, & Buckling, 2008). One of the factors that makes it difficult to predict the effect of rapid environmental change on ecosystems, is that species may respond differently to changes in the environment. Besides shifting in abundance, species may respond by shifting their spatial or temporal range, by phenotypic plasticity or by adaptive microevolution (Charmantier et al., 2008; Chen, Hill, Ohlemüller, Roy, & Thomas, 2011; Holt, 1990; Visser, 2008). Each of these mechanisms may have their own critical rate, but the rate will be species and event specific. Thus, further exploration of rate-sensitivity in ecosystems will require a better understanding of how different species within the ecosystem respond to environmental change. In addition, we need to explore whether more complicated ecosystem models also show rate-induced critical transitions, and if so, whether these systems have similar features.

Despite our limited understanding of their occurrence, the possibility of rate-induced tipping in ecosystems has profound implications for the way we assess the impact of global change on ecosystems, and the way we manage our ecosystems. Besides identifying and quantifying planetary boundaries in order to create a safe operating space for our ecosystems, we now also need to incorporate critical rates of change.



## SUPPLEMENTARY INFORMATION

### S4.1. BASIC MODEL DYNAMICS

#### Basic phytoplankton dynamics

The incoming light intensity ( $I_{in}$ ) affects the growth of phytoplankton, and for specific values of incoming light intensity, the system can have alternative stable states. Under such conditions, the per-capita productivity of phytoplankton first increases with plant biomass due to increased shading and then declines again as a result of competition for light (Fig. S4.1a). It is easy to see from this figure that phytoplankton biomass has only a positive growth rate at intermediate densities (between  $E_2$  and  $E_3$  in Figure S4.6a); at lower densities there is photoinhibition and at higher densities light limitation. The low biomass state ( $E_2$ ) is an unstable equilibrium, meaning that a small perturbation in the phytoplankton biomass will bring the system either to the high biomass equilibrium ( $E_3$ ), or to extinction ( $E_1$ , Figure S4.6b).

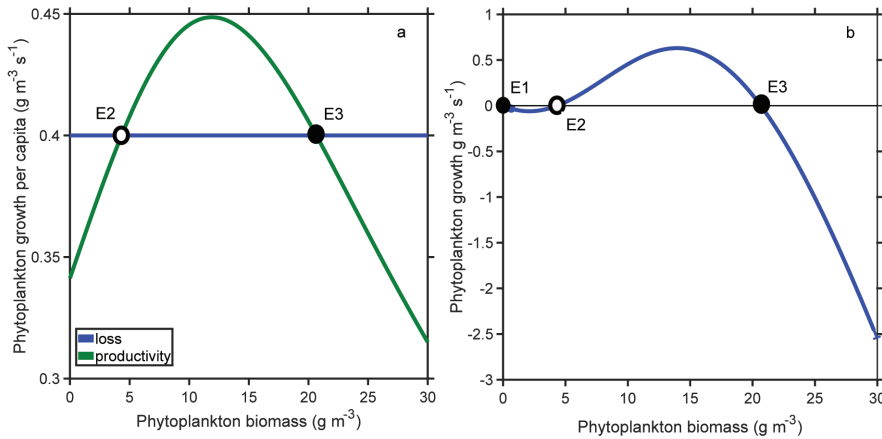


**Figure S4.6.** (a) The per capita rate of change in phytoplankton biomass depends on the difference between productivity and losses. At intermediate phytoplankton biomass the net growth is positive. At lower biomass the the phytoplankton cannot shade each other out, while at higher biomass the competition for light becomes too high. (b) The biomass growth rate as a function of biomass. At the biomass levels where the net growth is zero, the system is in equilibrium. The heavy dots ( $E_1$  and  $E_3$ ) are stable equilibria, while the light dot ( $E_2$ ) is an unstable equilibrium. Parameter settings for this figure can be found in Table 1.

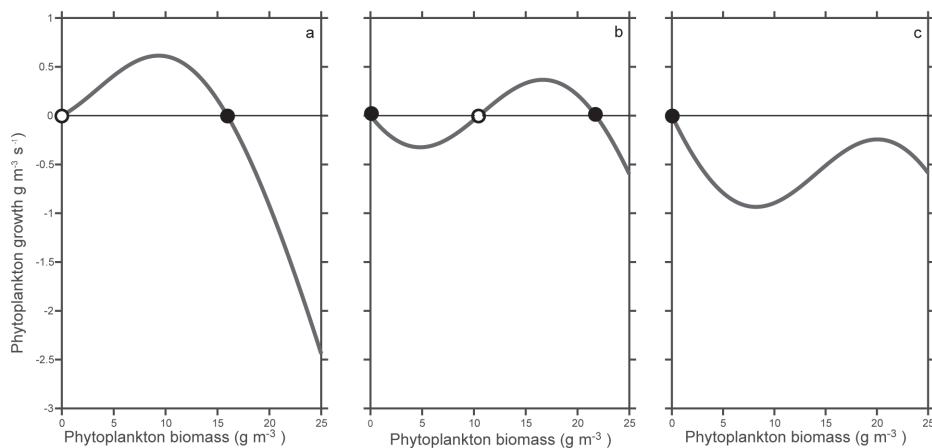


**Figure S4.7.** The relation between changes in phytoplankton growth and biomass for different levels of incoming light intensity ( $I_{in} = 250, 750$  and  $1250$ ). At the point where the change in phytoplankton biomass is zero, the system is in equilibrium. A black dot indicates a stable equilibrium, an open dot an unstable equilibrium.

If you change the parameter values of the model the rates of change and consequently, the equilibria change. For instance, when you decrease  $I_{in}$ , the productivity is always larger than the losses at low biomass, so the collapsed state becomes unstable and there is only one stable equilibrium (solid dot, Figure S4.7a). On the other hand, if  $I_{in}$  is increased,  $P_1$  and  $P_2$  collide, implying that for higher  $I_{in}$ , the loss rate exceeds the production rate irrespective of the population density (Figure S4.7c). In this case the only equilibrium left is the collapsed state ( $A=0$ ).

### Effects of the environmental conditions

To explore how the incoming light intensity affects the equilibria of the model, we did a bifurcation analysis with  $I_{in}$  ranging from 0 to  $1500 \mu\text{mol m}^{-2} \text{s}^{-1}$ . For the default parameter settings (see Table 1), the model has three biological relevant bifurcations within this range of  $I_{in}$  (Figure S4.8): two transcritical bifurcations and one fold bifurcation. A transcritical bifurcation is a point at which two equilibria cross and exchange stability, and a fold bifurcation is the point at which the stable and the unstable equilibrium merge. In this model, there is a transcritical bifurcation at low light ( $T_1$ , at  $I_{in} = 61.6604$ ) below which there is too little light for phytoplankton to grow, and a transcritical bifurcation at intermediate light ( $T_2$ , at  $I_{in} = 364.902$ ), above which the light intensity is too high for phytoplankton to colonize an empty system. The fold bifurcation occurs at high light ( $F_1$ , at  $I_{in} = 1047.27$ ) and high biomass, so there is high self-shading by phytoplankton (Figure S4.8).

To visualize how the incoming light intensity affects the outcome of the model, we construct a 2 dimensional bifurcation diagram with  $I_{in}$  and  $I$ , the loss of phytoplankton due to flushing, on the axes. In the diagram we can distinct three regions with different model predictions: no phytoplankton, only phytoplankton and alternative stable states (Figure S4.9). The specific flushing rate at which the transcritical bifurcation (blue line, T1 & T2) occurs is dependent on  $I_{in}$ . Likewise, the curve that represents the fold bifurcation (green line, F1 & F2), also shows the dependence of the fold bifurcation on  $I$  and  $I_{in}$ . If  $I_{in}$  becomes bigger than  $I_{opt}$  (default  $I_{opt}=150$ ), there exists a window of  $I$  for which the systems has alternative stable states (Figure S4.9). Of  $I_{in}$  is lower than  $I_{opt}$ , there is also a region with alternative stable states, but this region only exists for negative phytoplankton biomasses and is therefore not biological relevant (F2 part of the green line, Figure S4.9). If  $I$  becomes bigger than the maximum productivity ( $p_{max} = 0.49$ ), positive growth is never possible and phytoplankton cannot exist.

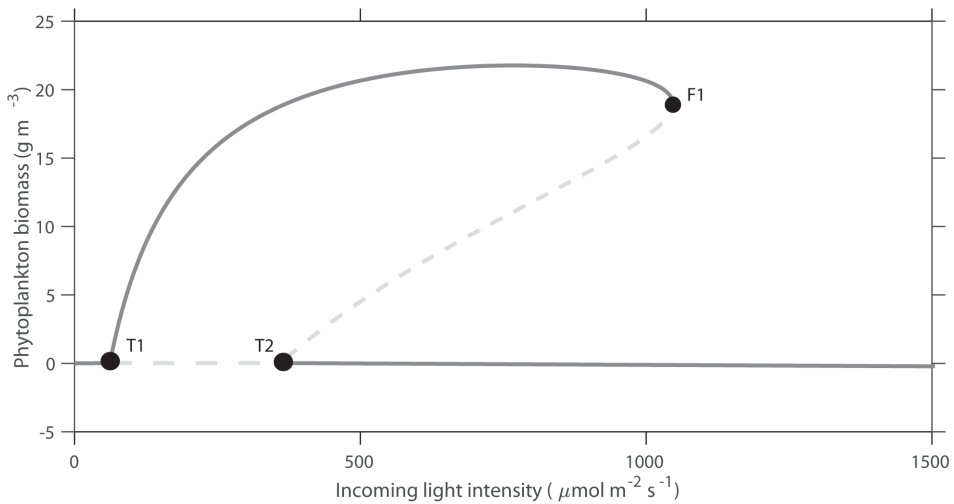


**Figure S4.8.** Bifurcations of the phytoplankton for different levels of light intensity ( $I_{in}$ ) and phytoplankton biomass ( $A$ ). There are three biological relevant ( $A \geq 0$ ) bifurcations: at T2 there is a transcritical bifurcation at low light, below which there is too little light for phytoplankton to grow. At F1 there is a fold bifurcation with high light and high self-shading by the phytoplankton, and at T1 there is another transcritical bifurcation, above this intermediate light intensity, there is no colonization of the collapsed state.

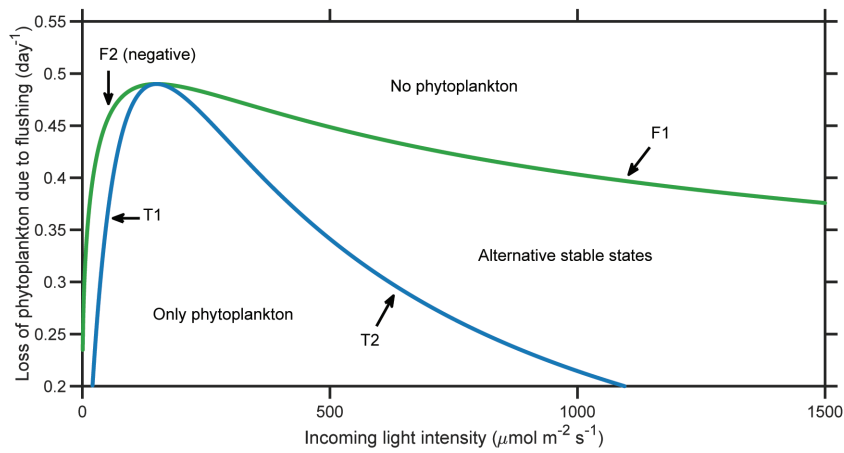


**Figure S4.9.** Two-dimensional bifurcation diagram for incoming light intensities between 0 and  $1500 \mu\text{mol m}^{-2} \text{s}^{-1}$  and loss of phytoplankton due to flushing between 0.2 and 0.55 per day. The green line shows the fold bifurcations, and the blue line the transcritical bifurcations. The part of the curve that represents the second fold bifurcation (F2) is biologically not relevant, as values for the phytoplankton are negative for this bifurcation. The bifurcations divide the diagram in three distinct regions: parameter combinations in which phytoplankton cannot exist, where there is only phytoplankton and a region in which alternative stable states can occur.

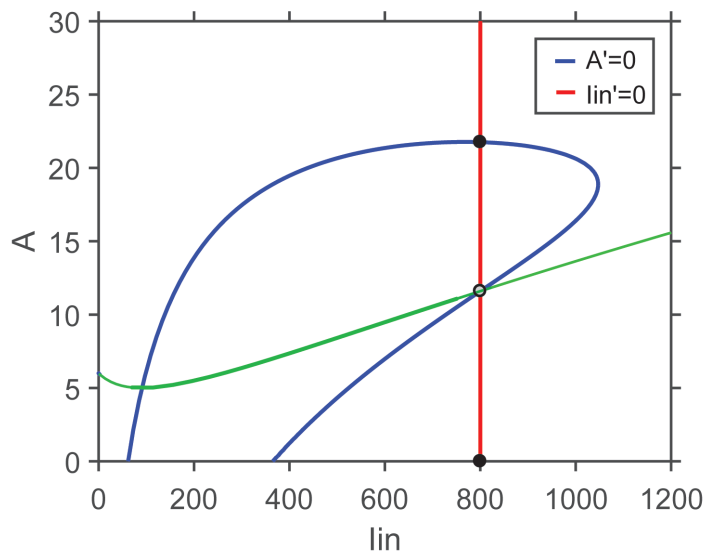


**Figure S4.10.** Phase plane analysis at the ( $I_{in}$ ,  $A$ ) plane. The blue, solid line is the separatrix, above which rate-induced tipping does not occur.

## S4.2. UNSTEADY DRIFT

Although steady drift is the simplest assumption for the change of the light conditions, there are also other options, like letting the light intensity exponentially approach a maximum value (called ‘unsteady drift’ (Ashwin et al., 2012)). An advantage is that this approach allows for a phase plane analysis in the  $(I_{in}, A)$  plane. The unsteady drift is implemented with the following equation:

$$\frac{dI_{in}}{dt} = r(I_{in,max} - I_{in}) \quad (S4.1)$$

With  $r = 0.1$ . In Figure S4.10 one can see the conditions for which rate-tipping is possible. The blue, solid line is the separatrix and above this line, the speed is either too slow to induce rate-induced tipping, or rate-induced tipping is never possible.

When the value for  $r$  is changed, the separatrix changes. With higher values for  $r$ , tipping becomes easier as the system diverges more from the initial state equilibrium and it becomes more difficult to follow the equilibrium state. For lower rates, the system is more likely to follow the equilibrium and rate-induced tipping does not occur. When  $r$  becomes larger than 1, the separatrix approaches the saddle almost in a horizontal line (Figure S4.11).

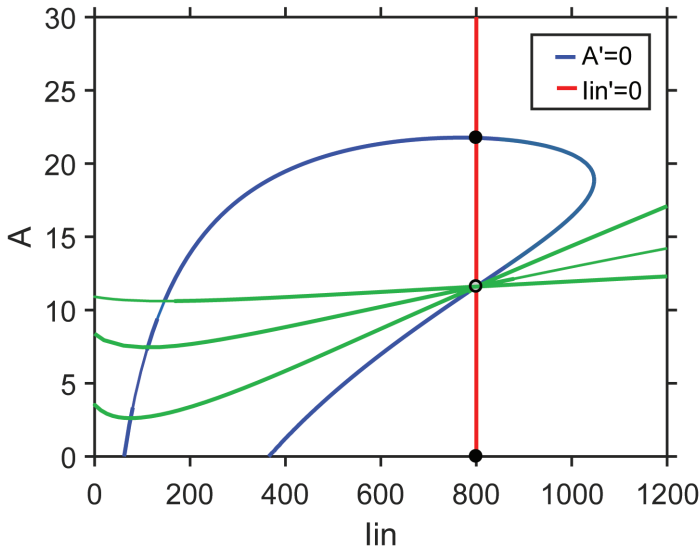


**Figure S4.11.** The separatrix in the phase plane analysis for different values of  $r$ . The higher the value for  $r$ , the larger the range of conditions for which there is rate-induced tipping.

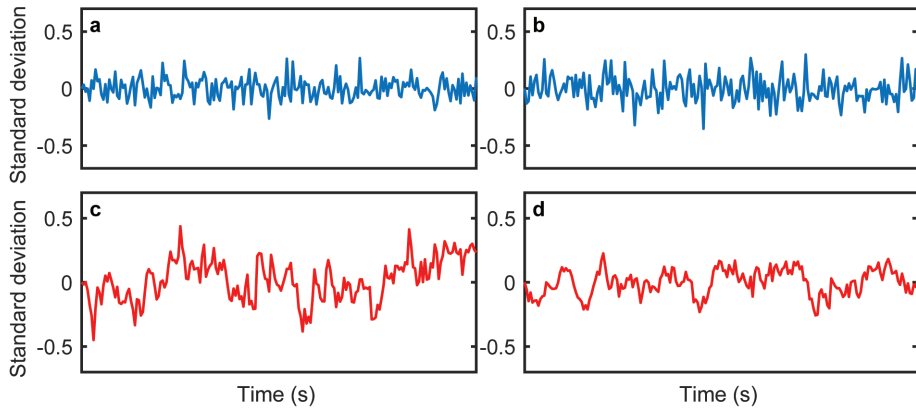


**Figure S4.12.** Example runs of environmental variability with and without scaling of the variance. The left-hand panels are without scaling (a, c), and the right-hand with scaling (b, d). The upper panels are time series without time-correlation (blue lines,  $\alpha=0$ ), and the lower panels (red lines,  $\alpha=0.8$ ) are time-correlated.

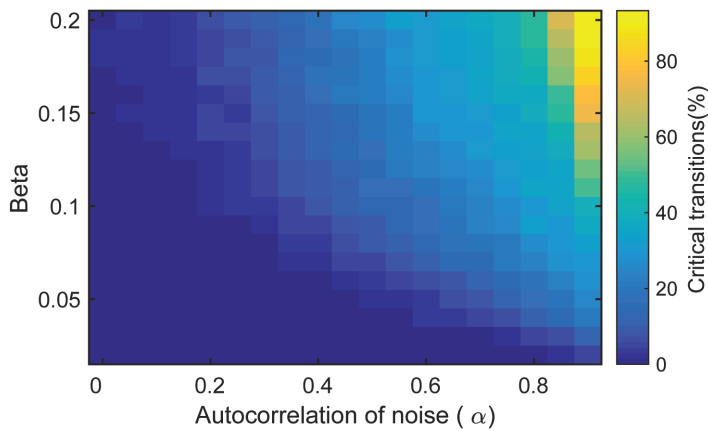


**Figure S4.13.** Combined effects of the autocorrelation and the scaling parameter ( $\beta$ ) of the fluctuations in the environment on the percentage of runs in which the phytoplankton biomass collapses. The rate of change in the incoming light intensity is  $0.12 \text{ day}^{-1}$ .

**S4.3. THE EFFECT OF SCALED ENVIRONMENTAL VARIABILITY**

In reality, when the time-correlation structure of environmental variability increases, the variance of the variability also changes (see Figure S4.12). In our equation for environmental variability without scaling, a decrease in  $\gamma$  results in an increase in the variance as a response to weakening feedbacks (reduced  $\gamma$ , while  $\beta$  stays constant). In the main text we scaled the variance, but as can be seen in Figure S4.13, the probability of a critical transition increases as the variance of the environmental variability increases. The same holds for an increase in temporal autocorrelation, so increased time-correlation in the environmental variability increases the chance of undergoing a critical transition both by the effect of increased variance and increased temporal autocorrelation.

## CHAPTER 4

### S4.5. MATLAB SCRIPT

Script to determine the critical value for rate and duration, using GRIND and a simple bisection method for optimizing.

```
function [aval,range]=find_crit_value(paname,crit,range,iterations)
%find a critical rate
%this function uses the intersection method to find the threshold
%the criterion should distinguish between the two values of the range
(one
%of both should be true the other false)
%After some point more iterations give no further increase in accuracy
(as
%grind does not distinguish between the initial conditions)
global g_Y
if nargin<2
    answer=inputdlg({'Parameter name','criterion','Range of the
parameter','iterations'},'find_crit_value',1',{' ',' ','30'});
    parname=answer{1};
    criterion=answer{2}';
    range=str2num(answer{3});
    iterations=str2num(answer{4});
end
origval=evalin('base',paname);
if nargin<2
    range=[origval*0.1 origval*10];
end
if nargin<4
    iterations=20;
end
if ischar(range)
    range=str2num(range);
end
assignin('base',paname,range(1))
time -s -r
disp(g_Y(end,:))
val1=i_initvar;
ke
crit1=evalin('base',crit);
i_keep(val1);
assignin('base',paname,range(2))
time -s -r
disp(g_Y(end,:))
ke
crit2=evalin('base',crit);
```



```

i_keep(val1);
if crit2==crit1
    error('grind:find_crit_val','range or criterion not correct')
end
if origval==0
    parval1=1;
else
    parval1=origval;
end
for i=1:iterations
    aval=(range(2)+range(1))/2;
    assignin('base',parname,aval)
    fprintf('%s=%g:  ',parname,aval)
    time -s -r
    ke
    crit2=evalin('base',crit);
    f=val();
    fprintf('%s ',f{:})
    fprintf('\n')
    i_keep(val1);
    if crit2==crit1
        range(1)=aval;
    else
        range(2)=aval;
    end
end
if crit1

    aval=range(1);

else

    aval=range(2);

end
assignin('base',parname,origval)

```

## CHAPTER 4



# CHAPTER 5

## CLIMATE REDDENING PROMOTES THE CHANCE OF CRITICAL TRANSITIONS

Bregje van der Bolt,

Egbert H. van Nes,

Sebastian Bathiany,

Marlies E. Vollebregt,

and Marten Scheffer

*“In life and in the Universe,  
may your signal be high,  
and your noise be low.”*

- Neil deGrasse Tyson

### ABSTRACT

Climate change research often focuses on trends in the mean and variance. However, analyses of paleoclimatic and contemporary dynamics reveal that climate memory – as measured for instance by temporal autocorrelation - may also change substantially over time. Here, we show that elevated temporal autocorrelation in climatic variables should be expected to increase the chance of critical transitions in climate-sensitive systems with tipping points. We demonstrate that this prediction is consistent with evidence from forests, coral reefs, poverty traps, violent conflict and ice sheet instability. In each example, the duration of anomalous dry or warm events elevates chances of invoking a critical transition. Understanding effects of climate variability thus requires research not only on variance, but also on climate memory.

*This chapter is based on the paper: Bregje van der Bolt, Egbert H. Van Nes, S. Bathiany, Marlies E. Vollebregt and Marten Scheffer (2018). Climate reddening increases the chance of critical transitions. Nature Climate Change, 8(6), 478.*

## INTRODUCTION

Although many systems respond gradually to climate change, some systems may have tipping points where a small change can trigger a large response that is not easily reversible (Groffman et al., 2006; Marten Scheffer, 2009). Such critical transitions have been studied mostly in simple models, e.g. refs (May, 1977; Marten Scheffer, Carpenter, Foley, Folke, & Walker, 2001), where climate variability is either left out or modelled as white noise (Stephen R. Carpenter et al., 1999; van de Leemput, van Nes, & Scheffer, 2015), i.e. noise that is uncorrelated in time. However, such uncorrelated noise is a mathematical idealisation. In reality, the climate system involves slow processes causing the power spectrum to have pronounced low frequencies (a red spectrum). As a result, climatic time series are often autocorrelated on time scales that correspond to the diurnal to decadal time scales of change that are also characteristic for key variables of ecosystems and society (Trenberth, 1984). For instance, the state of the atmosphere is highly correlated from one day to the next, anomalies in surface ocean temperatures can persist for several months (Frankignoul & Hasselmann, 1977; Hasselmann, 1976), and there are modes of decadal variability (Mantua et al., 1997; Schlesinger & Ramankutty, 1994). Importantly, the autocorrelation in climatic variables may change over time (Lenton et al., 2017). For instance, the Pacific Decadal Oscillation and North Pacific sea surface temperatures have become more autocorrelated in the period from 1900 to 2015 (Boulton & Lenton, 2015; Huntingford et al., 2013), and large changes in climate variability are to be expected in the Arctic where sea ice loss leads to larger persistence and smaller variance in temperature variability (Bathiany et al., 2016; Wagner & Eisenman, 2015).

Here we address the question of how such a change in the autocorrelation of climatic variables may affect the likelihood of climate-driven critical transitions in nature and society. Intuitively, this possibility is straightforward. For instance, one can imagine a single prolonged heatwave or drought to have different effects than a series of shorter ones when it comes to pushing ecosystems to a critical threshold. Noise-driven transitions have been studied in an abstract sense in physics (Hänggi & Jung, 1995; Hänggi, Mroczkowski, Moss, & McClintock, 1985; Horsthemke & Lefever, 1984), but this literature remains rather disconnected from the work on social and ecological transitions. In ecology, studies have addressed the effects of environmental variability on extinction risk (Greenman & Benton, 2003; Heino, Ripa, & Kaitala, 2000; Mustin, Dytham, Benton, & Travis, 2013; Petchey, 2000; Ripa & Lundberg, 1996; Rudnick & Davis, 2003; Schwager, Johst, & Jeltsch, 2006; Vasseur, 2007; Vasseur & Yodzis, 2004), the probability of critical transitions in marine ecosystems (Boulton & Lenton, 2015),

## CHAPTER 5

and the dynamical patterns that can be displayed by simple exploitation models (John H. Steele & Henderson, 1994). However, a general framework is lacking for the expected effects of the autocorrelation of climate fluctuations on critical transitions in nature and society.

To explore how changes in climate variability may affect systems with tipping points, we first ask how the size and duration of single environmental perturbations affect these systems. Next, we examine systematically how the autocorrelation and variance of climate variability separately affect the likelihood of a critical transition and how the autocorrelation of climate variability affects the duration of extreme events using an established ecological model as an example. Subsequently, we discuss evidence from five systems in which the duration of anomalously warm or dry events has been shown to elevate the chance of critical transitions: forests, coral reefs, the poverty trap, human conflict, and the West Antarctic ice-sheet. We then review changes in climate variability and call for a research focus on drivers of climate memory and how it affects climate-sensitive systems.

## THEORETICAL PREDICTIONS

### RESPONSE TO SINGLE PERTURBATIONS

As a first step to see how changes in the dynamic regime of climatic drivers may affect the likelihood of critical transitions, consider the effect of an idealized single perturbation such as a temporary change in environmental conditions (Figure 5.1, red arrow). Because it takes time for the system to respond to a change in conditions (Figure 5.1, black arrows), the moment at which the conditions are reversed to the original (Figure 5.1, green arrows) determines the fate of the system. If the conditions recover fast, the system reverts to the original state (Figure 5.1, trajectory  $1 \rightarrow 2 \rightarrow 3 \rightarrow 4 \rightarrow 1$ ). However, recovery of the conditions at a later moment can cause the system to settle in the alternative equilibrium (Figure 5.1, trajectory  $1 \rightarrow 2 \rightarrow 3' \rightarrow 4' \rightarrow 5$ ).

Obviously, the outcome depends not only on the magnitude but also on the duration of such a pulse perturbation of conditions. As an illustration of this, consider a simple deterministic overharvesting model (May, 1977) that has two fold bifurcations, giving a range of parameter values with two stable equilibrium solutions: underexploited and overexploited (for model details see Methods section). As a perturbation, we temporarily increase the maximum harvest value  $c$  in a stepwise fashion. A systematic analysis (Figure 2) shows how the critical perturbation size for a shift to an overexploited

state is inversely related to the duration of such simple pulse perturbations.

## EFFECTS OF STOCHASTIC PERTURBATION REGIMES

We now turn to the question of how a certain regime of stochastic fluctuations in the conditions affects the probability of invoking a critical transition. In a deterministic situation, this transition always happens approximately at the bifurcation point, but in the stochastic version, this is no longer true. We study at which harvest rate the transition takes place as a function of the frequency spectrum of the stochastic fluctuations. For this we simulate the model repeatedly at different levels of autocorrelation, while keeping the variance of the stochastic fluctuations constant (see Supplementary Information for details).

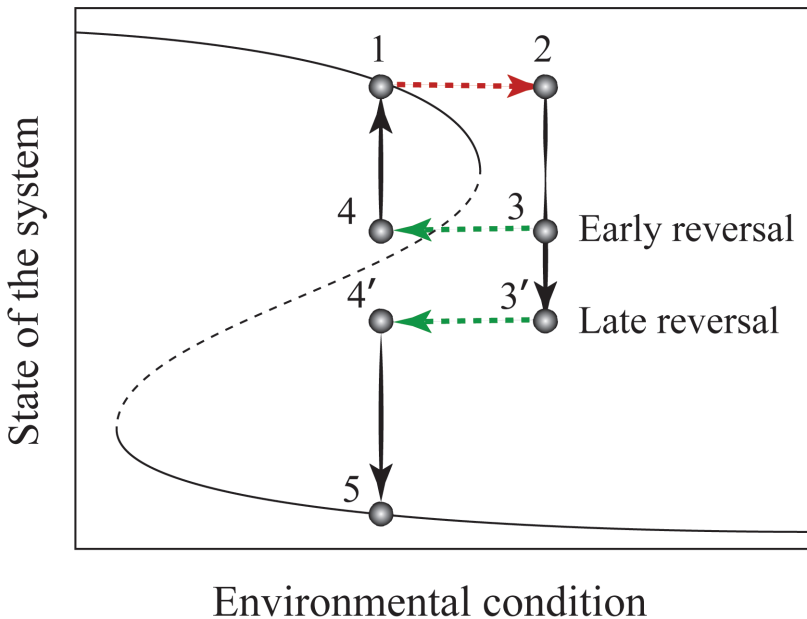


**Figure 5.1. Schematic representation of how the duration of a climate event may determine whether it invokes a transition to an alternative attractor.** The s-shaped equilibrium of the depicted system has a classical catastrophe fold where the dashed part of the curve represents unstable (saddle) points whereas the other branches of the curve represent alternative stable points. Starting from an initial stable state (point 1) at the upper branch we imagine a stepwise change in an environmental condition (red dashed arrow) bringing the system instantaneously to point 2 from where its state starts to change in response to the new condition (black arrow, where the thickness schematically represents the speed of change). If the conditions are reverted to the original early enough (point 3) the system is brought back into the attraction basin of the original attractor (4) from which it will return to its initial state (1). By contrast, if the reversal of conditions happens later (point 3') it may leave the system below the dashed part of the equilibrium curve representing the border between the alternative basins of attraction, implying a transition to the other equilibrium state (4' → 5).

## CHAPTER 5

Our first simulation approach is to increase the harvest rate continuously and very slowly over the 10,000 time steps of the simulations. In the absence of stochastic forcing this causes the system to switch directly after the bifurcation point of the deterministic model (inflection point of the dashed curve in Figure 5.3). With the addition of stochastic forcing to the model, the shift becomes less predictable, especially when the forcing regime is time-correlated (Figs. 5.3 and 5.4). Autocorrelation of the stochastic forcing causes the system to shift on average at a lower harvest rate as compared to forcing with white noise of the same variance (Figure 5.3). In addition to the transient simulations with a gradually changing driver (the harvest rate) we tested how a certain regime of stochastic fluctuations affects the probability of invoking a critical transition under constant parameter values. This analysis confirms that higher temporal autocorrelation can result in a markedly elevated likelihood that the system tips to the alternative state (Figure 5.4b). While we show that autocorrelation alone increases the probability of invoking a transition, in reality, an increase in autocorrelation is often accompanied by a change in variance. As both variance and autocorrelation influence the likelihood of invoking a shift, an increase in both of them has an even stronger effect on the chances that the noise brings the system past the unstable point (Figure 5.5).

In addition to the overharvesting model, we analysed two models that are commonly used to study alternative stable states in ecosystems (Stephen R. Carpenter et al., 1999; Dakos, van Nes, Donangelo, Fort, & Scheffer, 2009; Ludwig, Jones, & Holling, 1978; May, 1977; J H Steele & Henderson, 1984), and two models that are linked to two of our

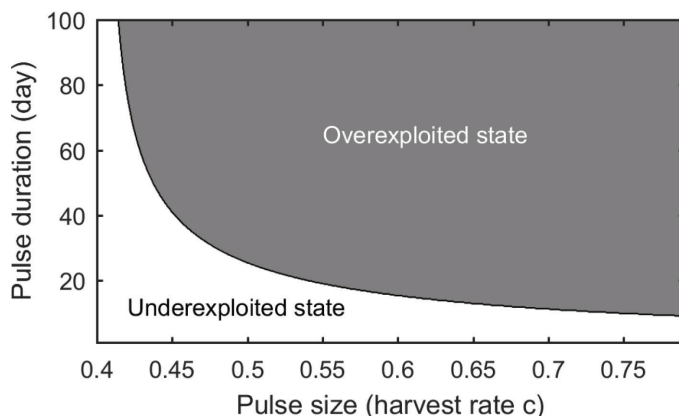


**Figure 5.2.** *The relationship between the duration and size of a perturbation in the conditions for invoking a state shift. The initial value of the driver (harvest rate  $c$ ) is 2.2 and the bifurcation point of the unperturbed version of the classical overexploitation model is situated at  $c=2.6$  (see methods for details).*



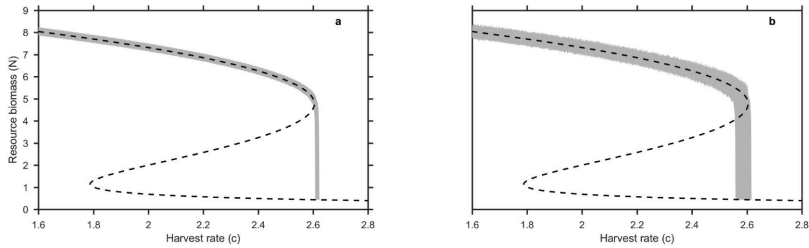


**Figure 5.3.** The simulated fate of biomass subject to a gradual slow increase of the harvest rate under a white noise versus a time-correlated stochastic forcing regime in a classical overexploitation model. For white noise ( $\alpha=0$ , panel a) the system collapses close to the fold (a saddle-node bifurcation) of the equilibrium curve of the underlying deterministic system (dashed line). By contrast, when the system is subject to time-correlated (red) noise of the same variance ( $\alpha=0.9$ , panel b) the collapse happens earlier on average and the unpredictability of the harvest rate at which the collapse happens is larger, as reflected by the broader band of the grey area between the 5<sup>th</sup> and 95<sup>th</sup> percentile of the ensemble of runs.

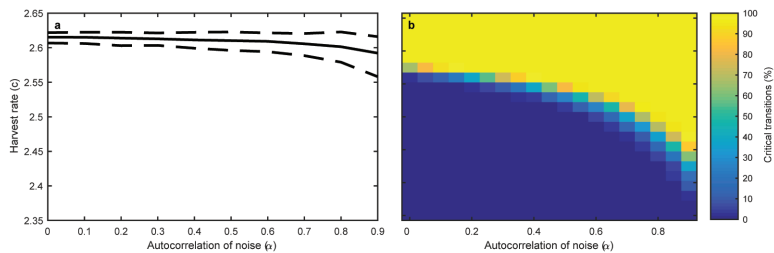


**Figure 5.4.** The effect of temporal autocorrelation of a stochastic forcing regime on the likelihood of collapse of the biomass system. In the simulations used for panel a, the control parameter ( $c$ ) is raised smoothly in 10,000 time steps from a low value ( $c=1.6$ ) in the direction of the tipping point of the deterministic version ( $c=2.6$ ) until the fish stock collapses. The mean value of  $c$  for which this shift happens decreases with the autocorrelation of the fluctuations (solid curve), while the variation across runs increases (dashed lines are the 5<sup>th</sup> and 95<sup>th</sup> percentile). For panel b, the harvest rate ( $c$ ) is kept constant within each of the 1,000 simulation runs used to measure the probability of collapse for different combinations of temporal autocorrelation of the noise regime and harvest rate. The colour scale represents the percentage of runs in which the biomass collapsed. The results for this example system illustrate that temporal autocorrelation of environmental fluctuations may strongly affect the likelihood of collapse.

## CHAPTER 5

examples of systems that are likely affected by future changes in climate variability: a model describing tree-cover dynamics as a function of precipitation (van Nes et al., 2014), and a model describing the interaction between corals reefs, herbivores and macroalgae (van de Leemput, Hughes, van Nes, & Scheffer, 2016). We analysed the five models with both multiplicative (i.e. state-dependent) and additive (state-independent) stochastic forcing. All those additional analyses gave qualitatively similar results, indicating the robustness of the patterns we showed (see supplementary information).

Our central result of a higher probability of shifting in a more time-correlated environment can be understood intuitively as the effect of a longer duration of extreme events (Figs. 5.1 and 5.2). Indeed, in simple red-noise time series, the length of ‘events’ where the value stays above a threshold (for instance the 90th percentile) is longer if the temporal autocorrelation of the time series is larger (Figure S5.3). As harsh conditions last longer, the chance increases that the fluctuations push the system for a long enough period across an irreversible threshold (the unstable equilibrium in our models) to shift to the other stable state. On the other hand, there can also be long periods of ‘favourable’ conditions in such time correlated environments, increasing the uncertainty of the transition time (the variance in Figs. 5.3 and 5.4).

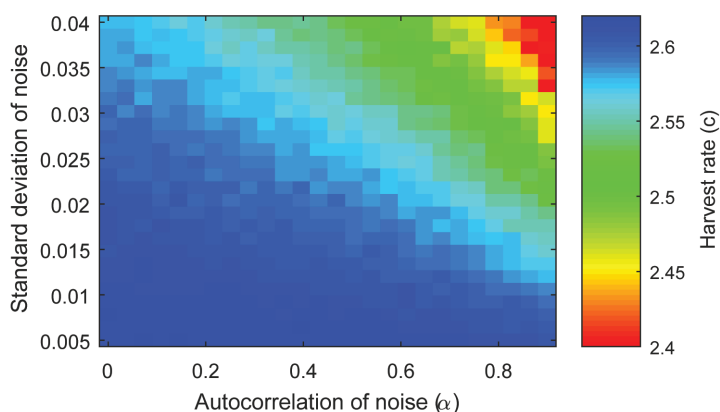


**Figure 5.5.** Combined effects of the autocorrelation and standard deviation of the fluctuations on the value of the driver at which the system shifts. Combined effects of temporal autocorrelation and standard deviation of fluctuations on the critical mean level of the harvest rate ( $c$ ) at which a transition is invoked in a large set of simulations similar to those represented in Fig. 3. (see methods for details).

## EMPIRICAL EVIDENCE

We now turn to a discussion of five examples illustrating the relevance of reddening of climate variability. The examples are chosen to illustrate the effects of the duration of extreme periods on a wide range of systems: two examples from ecosystems, two examples from society and one example from a tipping element of the climate system itself (Table 5.1). The duration of extreme events is predicted to promote the chances that a system is pushed across a tipping point (Figs. 5.1 and 5.2). Moreover, the duration is closely linked to the temporal autocorrelation (Figure 5.6) which we have shown to boost the likelihood of critical transitions over a wide range of assumptions (Figs. 5.3, 5.4 and 5.5 and supplementary material).

### TROPICAL FORESTS

Models and observations suggest that global warming will lead to more extreme rainfall regimes, with more extreme rainfall events but also longer dry periods between them (Allan & Soden, 2008; Goswami, Venugopal, Sengupta, Madhusoodanan, & Xavier, 2006; Groisman & Knight, 2008; Groisman et al., 2005). In the wet tropics increased interannual climate variability is associated with a lower probability of closed forest, most likely due to the effects of droughts (Holmgren, Hirota, van Nes, & Scheffer, 2013). Hot and dry periods can cause massive tree mortality (Allen et al., 2010) induced by water stress (da Costa et al., 2010; Nepstad, Tohver, Ray, Moutinho, & Cardinot, 2007; Rowland et al., 2015) and fire (Brando et al., 2014), which are dependent on the duration of the drought (Malhi et al., 2009). As a result of the tree mortality and fire (van Nes et al., 2018), the forests may slide into a stable fire-dominated savanna state from which recovery is difficult (Hirota, Holmgren, Van Nes, & Scheffer, 2011; Malhi et al., 2009; A Carla Staver, Archibald, & Levin, 2011; Zemp et al., 2017). By contrast, in parts of the dry tropics, large interannual climate variability is associated with positive effects on tree cover (Holmgren et al., 2013). Detailed case studies in the drylands of South America suggest an explanation. Rare wet episodes can cause massive recruitment of trees that can escape from the control by herbivores (Holmgren & Scheffer, 2001; Marten Scheffer et al., 2008), allowing a forest to form. Beyond a critical size, trees become less vulnerable to herbivores and fires (A. Carla Staver, Bond, Stock, van Rensburg, & Waldram, 2009; Ann Carla Staver & Bond, 2014). In addition, their roots are better able to reach deep groundwater (Bond, 2008). Therefore, the growth of the tree seedlings is a race against the clock and the duration of the wet period is critical to its effect. Once established, such dry forests can be self-stabilizing (Holmgren & Scheffer, 2001). Thus, there is broad empirical evidence that both in the dry and in the wet tropics critical

## CHAPTER 5

transitions between alternative states of tree cover are sensitively dependent on the duration of wet and dry anomalies.

### CORAL REEFS

One of the immediate threats to corals is rising sea surface temperatures (SST) as regional-scale coral bleaching is strongly associated with elevated sea surface temperatures (Hughes et al., 2017). Recent studies show that the monthly temperature variability and autocorrelation of SSTs increased in large parts of the North Pacific and North Atlantic between 1957 and 2002 (Boulton & Lenton, 2015; Lenton et al., 2017). Prolonged periods of higher SSTs as a result of reddening of the SSTs may have severe adverse effects for corals. Overheated corals expel most of their zooxanthellae and become pale or white (Hughes et al., 2003). While corals can recover from occasional short disturbances, stress accumulates over prolonged periods of elevated SSTs. Thus the damage increases with the duration of the extreme period (Hughes et al., 2017). Also, due to warming of the tropical oceans, coral reefs now live closer to their upper thermal limit and the chance that climate variability raises SSTs above these limits has increased (Eakin, Lough, & Heron, 2009). Importantly, reefs that are stressed and have suffered partial mortality are likely more vulnerable to a shift into an algae-covered state (Done, 1992; Knowlton, 1992; McCook, 1999). Thus, duration of warm extremes

**Table 5.1.** *Examples of systems in which the duration of extreme events has been shown to promote the chance of a critical transition.*

System	Critical Transition	Climatic driver	References
<b>Tropical rainforests</b>	Massive tree mortality	Duration of drought	(Allen et al., 2010; Gustafson & Sturtevant, 2013; Holmgren et al., 2013; McDowell et al., 2008)
<b>Dry lands</b>	Massive tree recruitment	Duration wet event	(Holmgren et al., 2013; Holmgren & Scheffer, 2001)
<b>Coral reefs</b>	Bleaching	Duration of SST anomaly	(Eakin et al., 2009; Hughes et al., 2017)
<b>Societies</b>	Violent conflict	Duration of Drought	(Kelley, Mohtadi, Cane, Seager, & Kushnir, 2015; Schleussner, Donges, Donner, & Schellnhuber, 2016; von Uexkull, Croicu, Fjelde, & Buhaug, 2016)
<b>Households</b>	Onset poverty trap	Duration of Drought	(Carter et al., 2007)
<b>West Antarctic Ice Sheet</b>	Cavitation triggering irreversible sliding	Duration of El Niño condition	(Smith et al., 2016)

## CLIMATE REDDENING PROMOTES THE CHANCE OF CRITICAL TRANSITIONS

promotes bleaching damage and the chances of shifting into an alternative state from which recovery is difficult.

### POVERTY TRAPS

People whose livelihoods depend directly on natural resources and ecosystem services are particularly vulnerable to climate change and changes in weather variables (Barnett & Adger, 2007). For example, the herds of pastoralists in East Africa graze extensively and the growth of the forage mainly depends on rainfall. Consequently, drought can lead to substantial herd losses. The effect of drought on the livelihood of people depends mostly on its duration. For example, in 1981 the seasonal rainfall totals in Brazil were slightly above average, but longer periods of drought resulted in yield losses that year (Donald. A. Wilhite, 2000). Inter-household differences in the capacity to deal with these losses can lead to variability in income and wealth (John. G. McPeak & Christopher B. Barrett, 2001). The poverty trap as a critical minimal asset threshold, below which families are unable to build up stocks of assets over time (Barrett & Carter, 2013). When households are close to such a situation, losses as a result of weather variability can have permanent adverse consequences as they invoke a transition into a poverty trap. An example of the differential effects of a prolonged weather event on poverty is the three-year drought in Ethiopia in the late 1990s. Wealthy households were able to rebuild their assets, while the adverse effects for the low-income households lasted longer (Carter, Little, Mogues, & Negatu, 2007).

### HUMAN CONFLICT

The question of whether or not climate change has significantly contributed to recent conflict outbreaks is the subject of an ongoing academic debate (Adams, Ide, Barnett, & Detges, 2018; H. Buhaug et al., 2014; Halvard Buhaug, 2010; Burke, Miguel, Satyanath, Dykema, & Lobell, 2009; Cane et al., 2014; Hsiang & Burke, 2014; Hsiang, Burke, & Miguel, 2013; Hsiang & Meng, 2014; Raleigh, Linke, & O'Loughlin, 2014; Scheffran, Brzoska, Kominek, Link, & Schilling, 2012; Schleussner et al., 2016). Several studies have suggested that a large number of conflict outbreaks are associated with climate extremes (Burke et al., 2009; Hsiang et al., 2013; Hsiang, Meng, & Cane, 2011; Schleussner et al., 2016). Between 1980 and 2010, 23% of the armed-conflict outbreaks in ethnically fractionized countries and 9% of the armed-conflicts globally, coincided with prolonged droughts (Schleussner et al., 2016). These findings point towards increased risks for conflict outbreaks in drought-prone areas such as Northern Africa and Levant (Field

## CHAPTER 5

et al., 2012). For example, in Syria, the 3-year drought of 2007-2010, in combination with existing water and agricultural insecurity, caused massive agricultural failures and mass migration of farming families to urban areas (Werrell, Femia, & Sternberg, 2015). As many as 1.5 million people moved from rural to urban areas (Solh, 2010). Such migration may cause tension and conflict in receiving areas (Barrett & Carter, 2013; Reuveny, 2007). In Syria, the influx of farming families, combined with the influx of 1.2-1.5 million Iraqi refugees between 2003 and 2007, resulted in a population shock in the peripheries of Syria's cities and further increased the strain on its resources (Erian, Katlan, & Babah, 2011). This rapid demographic change exacerbated a number of factors that contributed to unrest: unemployment, corruption, and inequality (United Nations High Commissions for Refugees, 2010). Although the context of each conflict is different and climate is always only one of many drivers, climate extremes likely have impacts by exacerbating pre-existing vulnerability. Systematic recent studies found that while under most conditions the relative effect of drought on conflict is modest, this is not true for agriculturally dependent groups in poor countries. Here, the duration of drought significantly increases the likelihood of sustained conflict as prolonged droughts threaten the food security, worsen humanitarian conditions and result in large-scale human displacement (von Uexkull et al., 2016). In summary, there is broad evidence that the duration of drought events may be important in triggering periods of large scale migration and conflict when there is a pre-existing vulnerability (Kelley et al., 2015; Schleussner et al., 2016).

### WEST ANTARCTIC ICE SHEET

Lastly, there is the possibility that internal variability of the climate triggers critical transitions in 'tipping elements' (Lenton et al., 2008) of the climate system that commit those elements to long-lasting change. A likely example is the retreat of the West Antarctic Ice Sheet (Smith et al., 2016). Parts of this ice sheet rest on a bedrock below sea level, where a ridge has been important in stabilizing the ice sheet. For decades, Pine Island Glacier and its associated ice sheet are among the fastest accelerating and thinning ice masses on Antarctica. A recent study indicates that the onset of the period of accelerated thinning happened in the 1940s, and was triggered by the longest-lasting El Niño event of the past century which occurred between 1939 and 1942. This event was already known to have had particularly strong impacts on Antarctic surface temperatures (Schneider & Steig, 2008). It now appears to have created an ocean cavity behind the ridge that induced subsequent phase of ongoing melting. Despite the fact that climate conditions returned to pre-1940s conditions, the process of glacial retreat and thinning has continued since the anomalously long climate event. Indeed, the

ongoing process is now unlikely to be reversible without a major change in conditions (Smith et al., 2016).

### PROSPECT

The transitions we have reviewed illustrate the potentially wide-ranging implications of our theoretical prediction that a reddening of climate fluctuations may promote the likelihood of inducing self-sustained shifts into alternative stable states of climate-sensitive systems. Clearly, there is a huge gap between our limited understanding of such real-world cases and the simple models we have analysed. Our initial theoretical analysis captures the essence of how the duration of an event may affect the likelihood of invoking a shift to an alternative attractor. Subsequently, our red-noise simulations illustrate that this basic conclusion may indeed be widened to include the effect of temporal correlation in regimes of permanent fluctuations. Clearly, we merely scratched the surface of the question of how timescale and magnitude of fluctuations may affect the scenarios we outlined. In any of the discussed systems, reality is much more complex than the schematic representation in the deterministic and stochastic parts of our models. For instance, our generated autoregressive noise is a strong simplification of the real spectrum of climate variability, which involves multiple variables, noise levels, and time scales. The most adequate model of such variability is system-specific and should capture the nature of the environmental fluctuations (in our study represented as additive and multiplicative noise), the magnitude of the fluctuations (Ovaskainen & Meerson, 2010), and the time scale on which autocorrelation is measured (Heino et al., 2000). Further exploration of the connection between our theoretical models and real-life cases will require deeper quantitative analyses: for example by applying more system-specific models and noise processes based on empirical data.

Unlike trends in mean climate and climate variance, trends in autocorrelation are not often studied. However, it is clear that climate autocorrelation may change markedly over time (Bathiany et al., 2016; Boulton & Lenton, 2015; Lenton et al., 2017). There can be different kinds of drivers for such systematic change in climate memory. The slowing down of Pacific fluctuations is likely due to deepening of the ocean mixed layer, increasing the heat capacity of this element (Boulton & Lenton, 2015), and a similar (but reversed) effect occurs for Arctic sea ice loss (Bathiany et al., 2016; Wagner & Eisenman, 2015). Such volume effects on slowness may well be common in the climate and are accompanied by a decrease in the variance of the fluctuations. A very different kind of mechanism that can cause an increased autocorrelation of fluctuations is the phenomenon of critical slowing down (Strogatz, 2014; Wissel, 1984). This can happen in

## CHAPTER 5

systems approaching a tipping point, or more precisely, a zero-eigenvalue bifurcation. Such slowing down has been shown for instance in models of the thermohaline circulation as it approaches a bifurcation point (Held & Kleinen, 2004; Kleinen, Held, & Petschel-Held, 2003; Lenton et al., 2009). Also, an increase in autocorrelation has been shown to precede various abrupt climate transitions in the paleoclimate, implying that tipping points may have been involved in these dramatic climatic shifts (Dakos et al., 2008). In the case of critical slowing down, the increase in autocorrelation of the fluctuations is accompanied by an increase in variance, as the strength of the restoring negative feedbacks decreases. As we have shown (Figure 5.5), such a simultaneous increase of variance and temporal correlation is a particularly powerful combination for driving a climate-sensitive system across a tipping point. Somewhat dazzlingly, this implies that the symptoms of a climate element approaching a tipping point (rising variance and temporal correlation) could themselves become a driver of catastrophic shifts in ecosystems and society.

Whatever the mechanism, systematic change in autocorrelation is an element of climatic change that warrants further attention in view of its potentially major implications for the systems that are affected by the climate. On the climate science side, understanding how global warming might affect autocorrelation will require more research into the ‘decadal oscillators’ and other poorly understood mechanisms of the climate system. Meanwhile, a better insight into the mechanisms that affect the resilience of social and ecological systems may help designing strategies to build a safe operating space (Rockström et al., 2009; M. Scheffer et al., 2015) in the face of altered climatic variability.



## SUPPLEMENTARY INFORMATION

## S5.1 METHODS

**Models.** To determine how systems could be affected by increased autocorrelation of the stochastic environmental variability, we adapted five well-studied models that can have alternative stable states. The (over)harvesting model by May (1977) describes the logistic growth of a resource  $N$  that is harvested following a sigmoidal functional response (May, 1977). The model describes the transitions from an underexploited to an overexploited state as the harvesting pressure increases and crosses a threshold. The second model describes the loss of phosphorus from the epilimnion and the sudden recycling under anoxic conditions in a eutrophic lake (Stephen R. Carpenter et al., 1999). At low nutrient input rates, the lake is oligotrophic because it loses nutrients to the sediment or hypolimnion. At increased nutrient input rates, there is a high recycling of nutrients from the sediment or hypolimnion as a result of lower oxygen levels and the lake may become eutrophic. The third model is a model with two state variables that describes the dynamics of aquatic vegetation and vertical light attenuation in shallow lakes (Marten Scheffer, 1998). The fourth model describes the dynamics of tree cover as a function of precipitation (van Nes et al., 2014) and the fifth model describes how the interaction between corals, macroalgae and herbivores affect the dynamics of corals reefs (van de Leemput et al., 2016).

**Perturbation experiment.** To study the effect of the size and duration of perturbations, we used the overharvesting model without stochastic forcing. The control parameter was kept constant ( $c = 2.2$ ). We started all simulations in the underexploited equilibrium state and performed a strong perturbation after 100 days by increasing the harvest rate with a specific amount for a specific duration. The equilibrium state of the system was determined at the end of a simulation of 1,000 days. This procedure was repeated for different perturbation sizes and perturbation durations (see Figure 5.2).

**Autocorrelation of noise.** We created autocorrelated time series of climate fluctuations of a hypothetical stochastic climate variable  $T_a$  using the following stochastic differential equation (called an Ornstein-Uhlenbeck process):

$$\frac{dT_a}{dt} = -\gamma T_a + \beta \frac{dW}{dt} \quad (5.1)$$

Where  $\beta$  is a parameter scaling the variance of the noise,  $dW/dt$  is a Wiener process with zero mean and unit variance.  $\gamma$  is  $\geq 0$  and corresponds to negative feedbacks that

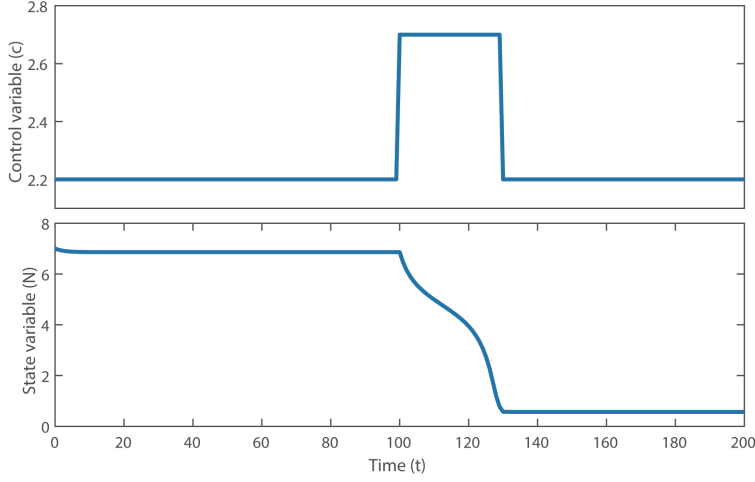


**Figure S5.1.** Example of how a pulse perturbation in the control variable can result in a shift. The upper panel is an example time series of a pulse in the control variable  $c$  with size 0.5 and a duration of 30 time steps. The lower panel shows the change in the state variable  $N$  as a result of the pulse in the control variable. In this example the pulse brings the system past the unstable equilibrium long enough for the system to switch to the alternative stable state.

act to restore any climate anomaly to the climate mean,  $T_a=0$ . The smaller  $\gamma$ , the larger the autocorrelation of  $T_a$ ;  $\gamma=0$  corresponds to an unbounded random walk (Brownian motion).

In general, the autocorrelation function of a time series with a sampling step  $\tau$  from an Ornstein-Uhlenbeck process is an exponentially decaying function:

$$\alpha(\tau) = e^{-\gamma|\tau|} \quad (5.2)$$

We solved the equation using an Euler-Maruyama scheme with time step 1. With this scheme and time step, the relation between  $\gamma$  and the autocorrelation  $\alpha$  of the discrete time series generated with this model can be described as  $\alpha(1) = 1-\gamma$  (sampling time step =1).

In our experiments we scale parameter  $\beta$  in a way to keep the expected variance of  $T_a$  at a constant value,  $\sigma$ , of 0.03 (see Figure S5.2). This corresponds to a rescaling based on the analytical relationship between autocorrelation and expected variance of the AR(1) process:

$$\alpha(1) = 1 - \gamma \quad (5.3)$$

This way we can study the effect of autocorrelation on critical transitions in isolation. In reality, the variance of a process can increase as a response to weakening feedbacks

(reduced  $\gamma$ , while  $\beta$  stays constant), which also can increase the risk of critical transitions. There are, however, also mechanisms that reduce the variance while increasing the persistence, for example changes in the effective heat capacity or inertia of a system (Bathiany et al., 2016; Boulton & Lenton, 2015; Wagner & Eisenman, 2015).

Subsequently we used the created time series of  $T_a$  to force a variety of ecosystem models and study the effect of the environmental autocorrelation (as controlled via parameter  $\gamma$  and independent of the variance) on the occurrence of critical transitions. Essentially, white noise is hence integrated twice: first atmospheric variability is integrated by slower components of the climate system like the ocean (Eq. 5.1), then the climate fluctuations are integrated by ecosystems (Di Lorenzo & Ohman, 2013).

Our default model, the stochastically forced (over)harvesting model (May, 1977) is given by the equation:

$$\beta = \sigma \sqrt{\frac{(1-\alpha^2)}{\Delta t}} \quad (5.4)$$

with resource amount  $N$ , a fixed density-dependent loss term  $a$  (0.1), the maximum harvest rate  $c$  as the control variable (1.6-2.8). An increase of the harvest rate  $c$  leads to a decrease in stability of the underexploited state and eventually, pushes the system to the overexploited state (approximately around  $c \approx 2.6$ ). Because the method is the same for all five models, we will focus on the (over)harvesting model to explain the procedure (see Table S5.1 for model equations, parameter settings and Supplementary Figures for results).

We ran the model with different data sets of  $T_a$  with the autocorrelation  $\alpha$  ( $\gamma$  of eq. 1 =  $(1-\alpha)/dt$ ), ranging from 0 to 0.9 with a step of 0.1. We started from equilibrium and slowly increased the grazing rate until the system transitioned to overexploitation. A transition is defined to have occurred when the system state passes the halfway value between the two alternative stable states. The control parameter was increased in small steps in a run of 10,000 time steps. We repeated this for 200 simulations and used 5<sup>th</sup>, 50<sup>th</sup> and 95<sup>th</sup> percentiles for Figure 3 and 4a. In all simulations the variance of the noise was scaled. In Table S5.1,  $T_{a1}$  refers to multiplicative noise and  $T_{a2}$  to additive noise, if the standard deviation was not the same for both.

To explore how the models respond to changes in the autocorrelation when the control parameter does not change, we repeated 1,000 runs of the (over)harvesting model while

## CHAPTER 5

keeping the control parameter  $c$  constant ( $c=2.35-2.65$  with step  $0.05$ ), with the same forcing regime as above (see Figure 5.4b). We repeated this with generated datasets with different values of the autocorrelation  $\alpha$ , ranging from  $0$  to  $0.9$  with a step of  $0.1$ . We determined for each ensemble of runs what percentage of the runs crossed a tipping point.

To study the influence of variance and autocorrelation together, we ran the model with different values for the autocorrelation ( $0-0.9$  with a step of  $0.036$ ) and the standard deviation ( $0.005-0.04$  with a step of  $0.0014$ ) of the stochastic forcing while increasing the control variable. Each run was repeated  $150$  times and the median value of the critical harvest rate was used for Figure 5.5.

Finally we illustrated the influence of autocorrelation of climatic variability on the duration of extreme events. We created  $1,000$  replicates of autocorrelated time series  $1,000$  time steps of one time unit (equation 1) for the different levels of autocorrelation ( $\alpha = 0-0.9$  with a step of  $0.009$ ), while keeping the variance constant. We defined an extreme event as the value of the  $90^{\text{th}}$  percentile or higher that lasts longer than two time units. For each autocorrelation level we determined the duration of the extreme events. We used the mean,  $5^{\text{th}}$ , and  $95^{\text{th}}$  percentile duration of the extremes for Figure S5.3.

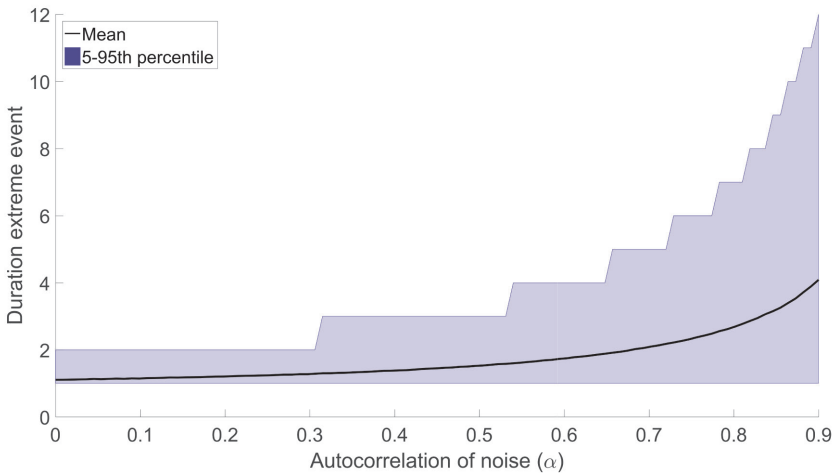


**Figure S5.3.** The expected duration of extreme events as a function of time correlation in simulated red-noise. Extreme events are defined as periods where the values exceed the  $90^{\text{th}}$  percentile for more than 2 time units. Results represent the distributions of the duration of extreme events in  $1,000$  replicate time series with a length of  $1,000$  time steps.

# CLIMATE REDDENING PROMOTES THE CHANCE OF CRITICAL TRANSITIONS

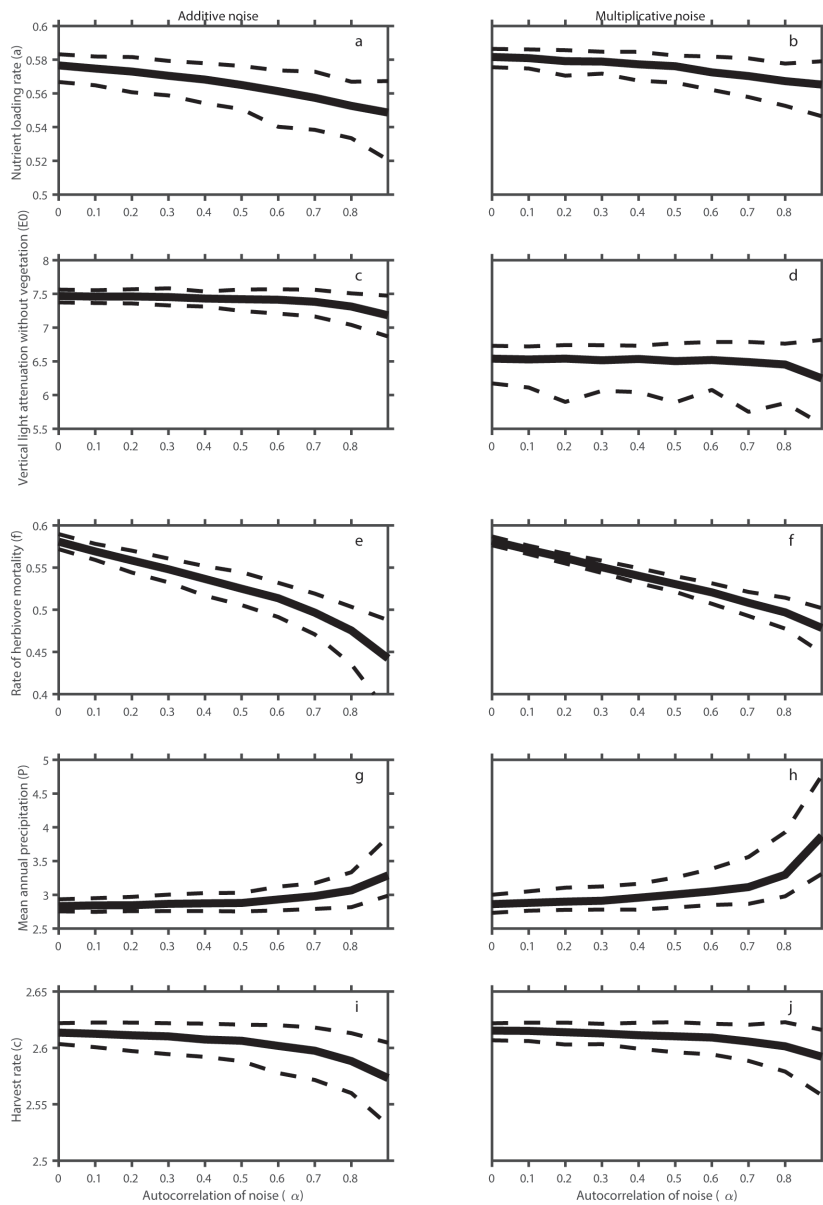


**Figure S5.2.** The empirical variance of the autocorrelated time series after rescaling (blue line) is close to the expected target variance (black dotted line) for all possible values of  $\alpha$ . We used time series with 10,000 time steps for this example. When this number is increased, the empirical result converges to the expected variance.

## CHAPTER 5

We implemented the models using the software package GRIND for MATLAB (accessed at <http://sparcs-center.org/grind>), which used a Runge-Kutta method with a variable time step to solve the differential equations with the use of C++.

### MULTIPLICATIVE NOISE

Environmental fluctuations can affect the state variable itself or one of the parameters. Both situations can be modelled by adding a stochastic term to the state variable (additive noise) or to one of the parameters (multiplicative noise). If one thinks of the dynamics of ecosystems and societies being affected by climatic variability, it makes more sense to use multiplicative noise, as the climatic conditions may generally be thought of as influencing parameters rather than state variables directly. For example, high temperatures do not directly remove corals or trees but they affect their growth or death rate. The rate of change of the state variable (amount of corals or trees) is usually a product of such rates with the state, which makes fluctuations in environmental drivers multiplicative in terms of stochastic systems. For that reason, the focus in the main text is on multiplicative noise. For the multiplicative simulations we added the noise term to a parameter that is likely to be influenced by changes in the environmental fluctuations.

In the (over)harvesting model we put the stochastic term on the mortality term. By doing so, the harvest model conceptualizes a change in mortality of the resource for a sustained period as a result of changes in environmental fluctuations. The stochastic term is added to the nutrient loss rate in the eutrophication model to conceptualize an increase or decrease in nutrient loss as a result of changes in precipitation. In the vegetation-turbidity model the situation where environmental fluctuations affect the vertical light attenuation by increasing the depth of the lake, is modelled. As mentioned in literature, sustained periods of high sea surface temperatures (SSTs) increase the mortality of corals reefs (Eakin et al., 2009). To conceptualize the effect of increased temporal correlation in environmental fluctuations such as SSTs, we added a stochastic term to the mortality rate of the corals. In the tree cover model we have added the stochastic term to the maximum loss rate due to fire, as longer periods of droughts may increase the area affected by forest fires.

# CLIMATE REDDENING PROMOTES THE CHANCE OF CRITICAL TRANSITIONS

Table S5.1. Model equations and parameter settings for models with multiplicative (a) and additive (b) noise

MODELS	STATE VARIABLES AND PARAMETERS		VALUE
<b>OVERHARVESTING MODEL (MAY 1977)</b>	$N$	Resource biomass (state)	
	$a$	Mortality term	0.1
	$c$	Maximum harvest rate (control)	1.6-2.8
	$T_{a1}$	Stochastic forcing with a mean of 0 and fixed standard deviation of	0.02
	$T_{a2}$	Stochastic forcing with a mean of 0 and fixed standard deviation of	0.06
a.) $\frac{dN}{dt} = N - (T_{a1} + 1) a N^2 - c \frac{N^2}{N^2 + 1}$			
b.) $\frac{dN}{dt} = N - a N^2 - c \frac{N^2}{N^2 + 1} + T_{a2}$			
<b>EUTROPHICATION MODEL (CARPENTER ET AL. 1999, EQ. 1)</b>	$N$	Nutrient concentration (state)	$\text{g m}^{-3}$
	$a$	Nutrient loading rate (control)	$0.1\text{-}0.9 \text{ g m}^{-3} \text{ day}^{-1}$
	$b$	Nutrient loss rate	$0.9 \text{ day}^{-1}$
	$c$	Maximum recycling rate	$1 \text{ g m}^{-3} \text{ day}^{-1}$
	$m$	Nutrient concentration at which recycling reaches half the	$1 \text{ g m}^{-3}$
	$p$	maximum rate Hill coefficient	8
	$T_a$	Stochastic forcing with mean 0 and a fixed standard deviation of	0.03
a.) $\frac{dN}{dt} = a - (T_a + 1) b N + c \frac{N^p}{N^p + m^p}$			
b.) $\frac{dN}{dt} = a - b N + c \frac{N^p}{N^p + m^p} + T_a$			
<b>VEGETATION-TURBIDITY MODEL (SCHEFFER 2009, APPENDIX 12)</b>	$V$	Vegetation cover (state)	
	$E$	Vertical light attenuation (state)	
	$e_0$	Vertical light attenuation without vegetation (control)	4.5-8
	$r_v$	Growth rate vegetation	0.05
	$r_e$	Growth rate vertical light attenuation	0.1
	$h_e$	Vertical light attenuation at which vegetation cover is reduced by half	2
	$h_v$	Vegetation cover at which vertical light attenuation is reduced by half	0.2
	$p$	Hill coefficient	4
	$T_{a1}$	Stochastic forcing with mean 1 and a fixed standard deviation of	0.15
	$T_{a2}$	Stochastic forcing with a mean of 0 and fixed standard deviation of	0.01
a.) $\frac{dE}{dt} = r_e E \left(1 - \frac{E h_v + V}{e_0 h_v}\right)$			
$\frac{dV}{dt} = r_v V \left(1 - V \frac{(h_e T_{a1})^p + E^p}{h_e^p}\right)$			
b.) $\frac{dE}{dt} = r_e E \left(1 - \frac{E h_v + V}{e_0 h_v}\right) + T_{a2}$			
$\frac{dV}{dt} = r_v V \left(1 - V \frac{h_e^p + E^p}{h_e^p}\right)$			

## CHAPTER 5

MODELS	STATE VARIABLES AND PARAMETERS		VALUE
<b>CORAL-MACROALGAE-HERBIVORE MODEL</b>  <b>(VAN DE LEEMPUT, 2016)</b>  $S = 1 - C - M$  <b>a.)</b>  $\frac{dC}{dt} = (i_c + b_c C) S (1 - \alpha M) - (T_{a1} + 1) d_c C$  $\frac{dM}{dt} = (i_m + b_m M) S \frac{g H M}{g \eta M + 1}$  $\frac{dH}{dt} = r H \left(1 - \frac{H}{(1 - \sigma) + \sigma C}\right) - f H$	$C$	Cover by corals (state)	0.7
	$M$	Cover by macroalgae (state)	0
	$H$	Herbivore abundance (state)	1
	$S$	Unoccupied space	
	$f$	Fishing pressure (control)	0-1
	$b_m$	Local expansion of existing adults of macroalgae	0.8
	$d_c$	Mortality rate of corals	0.1
	$i_c$	External import of propagules of coral	0.05
	$b_c$	Local expansion of existing adults of coral	0.3
	$\alpha$	Strength competition effect of macroalgae on coral recruitment	0.5
<b>b.)</b>  $\frac{dC}{dt} = (i_c + b_c C) S (1 - \alpha M) - d_c C + T_{a2}$  $\frac{dM}{dt} = (i_m + b_m M) S \frac{g H M}{g \eta M + 1}$  $\frac{dH}{dt} = r H \left(1 - \frac{H}{(1 - \sigma) + \sigma C}\right) - f H$	$i_m$	External import of macroalgae	0.05
	$g$	Grazing rate per herbivore	1
	$\eta$	Handling time of macroalgae by herbivores	1
	$r$	Growth rate of herbivores	1
	$\sigma$	Strength coral-herbivore feedback	0.6
	$T_{a1}$	Stochastic forcing with mean 0 and fixed standard deviation of	0.1
	$T_{a2}$	Stochastic forcing with mean 0 and fixed standard deviation of	0.01



# CLIMATE REDDENING PROMOTES THE CHANCE OF CRITICAL TRANSITIONS

MODELS	STATE VARIABLES AND PARAMETERS		VALUE
<b>TREE COVER MODEL</b>  <b>(VAN NES ET AL. 2014, EQ. 2)</b>  <b>a.)</b>  $\frac{dC}{dt} = (P / (h_p + P) r_m) C (1 - C / k)$ $- m_a C \left( \frac{h_a}{c + h_a} \right) - (T_{a1} + 1) m_f C (h_f^p / (h_f^p + C^p))$	C	Tree cover	75 %
	a	Tree cover below which there is an increased mortality due to an Allee effect	10 %
	f	Tree cover below which the fire mortality increases steeply	64 %
	p	The precipitation where the expansion rate is reduced by a half of its maximum	0.5 mm day <sup>-1</sup>
	k	Maximum tree cover	90 %
<b>b.)</b>  $\frac{dC}{dt} = (P / (h_p + P) r_m) C (1 - C / k) -$ $m_a C \left( \frac{h_a}{C + h_a} \right) - m_f C (h_f^p / (h_f^p + C^p)) + T_{a2}$	a	Maximum loss rate for increased mortality at low tree cover densities	0.15 yr <sup>-1</sup>
	f	Maximum loss rate due to fire	0.11 yr <sup>-1</sup>
	p	Exponent in Hill function for fire effect	7
	p	Mean annual precipitation (control)	5-1 mm day <sup>-1</sup>
	m	Maximum expansion rate of tree cover	0.3 yr <sup>-1</sup>
	a1	Stochastic forcing with mean 0 and fixed standard deviation of	0.1
	a2	Stochastic forcing with mean 0 and fixed standard deviation of	0.2

S5.2 SUPPLEMENTARY FIGURE

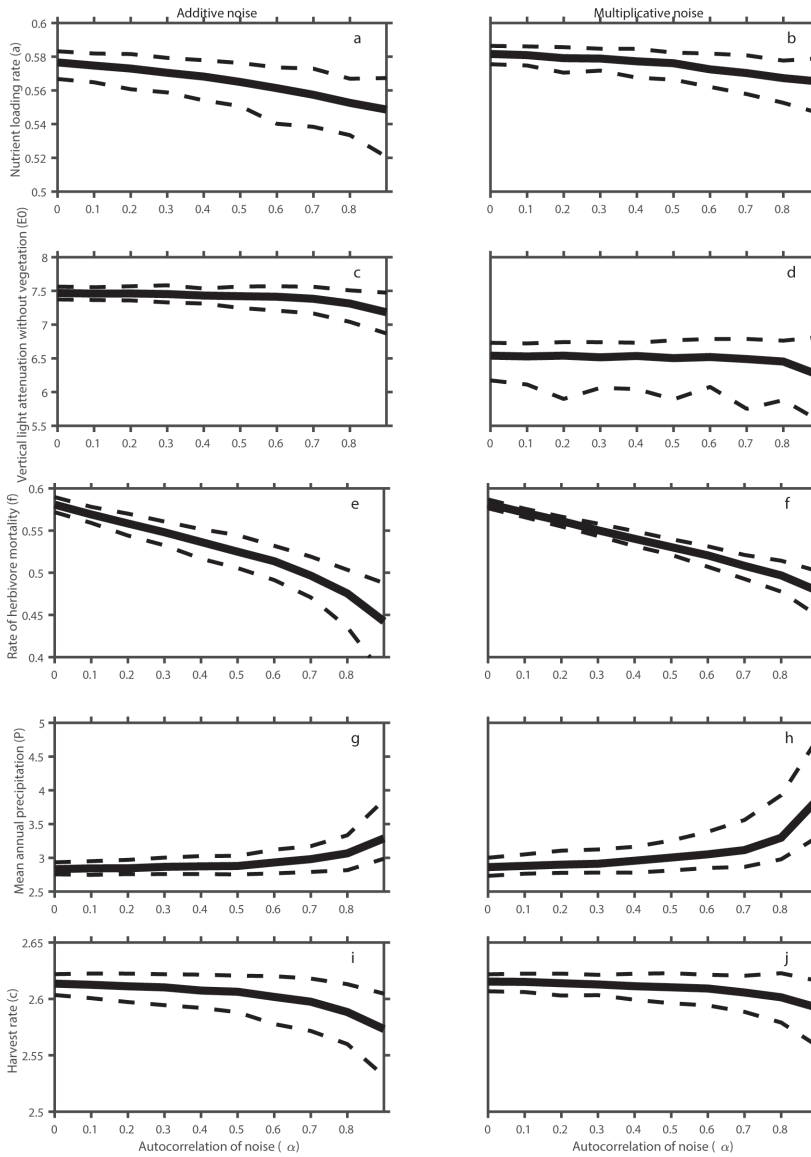


**Figure S5.4. Parameter ranges where shifts to the alternative state occur in five different models.** Parameter ranges where shifts to the alternative state occur in the eutrophication model (panel a and b), vegetation-turbidity model (panel c and d), coral cover model (panel e and f), the tree cover model (panel g and h) and the overharvesting model (panel i and j), depending on the autocorrelation of the environmental noise. The solid curve is the mean value of the control parameter for which the systems shifts to the alternative attractor and the dashed lines indicate the 5<sup>th</sup> and 95<sup>th</sup> percentile. The model runs of the left panels are with additive forcing regime, while the right panels are runs with the multiplicative forcing regime. Note that in the tree cover model the bifurcation parameter is decreased instead of increased as in the other models. Therefore, the direction of the curves is opposite to the curves of the other models.



# CHAPTER 6

## AFTERTHOUGHTS

Bregje van der Bolt

*“Time is relative;  
its only worth depends upon  
what we do as it is passing.”*

- Albert Einstein

### INTRODUCTION

Ecosystems and the climate may have tipping points: thresholds in environmental conditions at which an attractor becomes unstable and the system shifts to an alternative attractor. Such transitions can have long-term consequences, as they are difficult to reverse. Therefore, it is important to understand how and when these transitions might occur as climate change proceeds. In my thesis I asked how relative timescales of the rate of environmental change and variability may affect the occurrence and detectability of such critical transitions. The aim of my thesis was two-fold: I tried to unravel how changes in the relative timescales affect the probability of critical transitions, and how such changes affect the predictability of the transitions. In other words, I ask how climate change may affect the chance of critical transitions, and, as Vasilis Dakos put it poetically, how it may affect our ability to ‘*foresee the unexpected*’ (Dakos, 2011). Here I reflect on what I learned and what are the challenges that still lie ahead.

*In this chapter, when I use the word ‘system’, I refer to systems that are influenced by the climate and have alternative stable states. Such a system could either be part of the climate itself, or a system that is forced by the climate, such as social-ecological systems, agricultural systems and ecosystems. This means that that climate can both be the system, and the driver. For simplicity, I focus on ecosystems as systems that are forced by the climate, but the ideas also apply to other type of systems that are forced by the climate.*

### HOW ARE TIPPING POINTS AFFECTED BY CLIMATE CHANGE?

Under the ongoing climate change, critical transitions are projected to increase in systems that are forced by the climate. Drijfhout et al. (2015) found 37 regional abrupt changes in the CMIP5 model predictions of climatic change as radiative forcing of the planet rises. Climate models, however, have large uncertainties, especially in the strength of feedbacks (IPCC, 2013). Most models have not been able to simulate past abrupt change (Valdes, 2011) and do not account for several mechanisms that could give rise to abrupt change (Drijfhout et al., 2015). Therefore, it is likely that model simulations underestimate the number of critical transitions in the coming century.

As it is difficult to include all feedbacks in climate models, it would be useful to use climate data to measure the resilience. Resilience is the ability of a system to recover to the original state – or equilibrium – upon a disturbance (Holling, 1973). A way to quantify the resilience of a system is to estimate the intrinsic return rate to equilibrium.

Systems are permanently subject to natural perturbations from the environment. When one monitors the system and its relevant parameters, the system's dynamic responses to these perturbations can be captured and used to estimate the resilience of the system. A slow response rate is reflected by a change in the dynamical indicators of resilience (DIORs), such as the variance (Carpenter & Brock, 2006) and the temporal autocorrelation (Ives, 1995) of the system state.

A decrease in the resilience of the system before an abrupt shift is an indication that the abrupt shift might be the result of a self-reinforcing feedback that propelled the system to an alternative state (Scheffer, 2009). Reconstructed time series have been used to detect changes in resilience prior to several abrupt shifts in the past climate (Dakos et al., 2008). The typical way to monitor such changes in the resilience prior to a shift is to use a moving-window approach to determine the change in the DIORs (Dakos et al., 2012). This is, however, only possible under a limited set of conditions (Boettiger, Ross, & Hastings, 2013; Dakos, Carpenter, van Nes, & Scheffer, 2015). Sometimes these conditions are satisfied (**Chapter 2**). However, current anthropogenic forcing is causing much faster change in the Earth system than in the times of the past abrupt transitions for which the resilience indicators were determined (Joos & Spahni, 2008; Zeebe, Ridgwell, & Zachos, 2016). As a consequence, the intrinsic response rates of the system are relatively slow (compared to the external forcing).

## **THE EFFECT OF RELATIVELY FAST CLIMATE CHANGE ON TIPPING POINTS**

### **SLOW SYSTEMS CAN BE FAR FROM EQUILIBRIUM**

Traditionally, critical transitions from one state to another are thought of as sudden, rapid and difficult to reverse. Slowly responding systems, however, always show a gradual shift to the new state, regardless of whether a catastrophic, or non-catastrophic threshold is transgressed (Hughes, Linares, Dakos, van de Leemput, & van Nes, 2013). It may seem that such a slow system is in equilibrium, but in fact it is unstable and moving on a long transient trajectory to the alternative equilibrium. Especially in vicinity of the catastrophic threshold, long transient trajectories occur, as the dynamics are there slow by definition. This is sometimes referred to as the effect of a “ghost equilibrium” (Hastings et al., 2018; Van Geest, Coops, Scheffer, & van Nes, 2007).

When a system is on a long transient trajectory, it typically shows apparently stable

## CHAPTER 6

dynamics (Hastings et al., 2018). If such a system is only monitored on a short time scale, it would give the impression that it might remain in that state indefinitely, while this conclusion would be erroneous on a longer time scale. Consequently, systems may be committed to much greater change than can be observed from the present and the gradual change after they crossed a tipping point may go by unnoticed (Biggs, Carpenter, & Brock, 2009). Therefore, the analysis of the dynamical processes must be done across all relevant time scales (Hastings et al., 2018).

### TOO FAST TO TRACK: R-TIPPING

Another counter-intuitive consequence of slowness of the system may become apparent if environmental change is too fast for the system to track. This phenomenon is called rate-dependent tipping and has only been described recently (Ashwin, Wieczorek, Vitolo, & Cox, 2012) and can only occur in some rate-sensitive systems. Consequently, most of the theory on tipping points is based on systems in which rate-dependent tipping cannot occur. In rate-sensitive systems, however, rapid environmental change may induce a shift even if a change of the same magnitude in the conditions but at slower rates would not (Ashwin et al., 2012).

So-far, few studies describe rate-induced tipping in ecology and the climate (Scheffer, Van Nes, Holmgren, & Hughes, 2008; Siteur, Eppinga, Doelman, Siero, & Rietkerk, 2016; Wieczorek, Ashwin, Luke, & Cox, 2011). In **Chapter 4**, we showed that there can be rate-dependent tipping for a range of initial conditions in a model of cyanobacteria. The model has realistic parameter settings, suggesting that rate-dependent tipping might indeed occur in ecosystems dominated by cyanobacteria. However, the model is highly simplistic and obviously much remains to be done before we will have a good feel of the importance of this surprising phenomenon in nature.

### IMPLICATIONS FOR THE PREDICTABILITY OF CRITICAL TRANSITIONS

Currently, research on the predictability of rate-induced transitions is mostly lacking. Even though the equilibrium shifts in rate-induced tipping, the shape of the potential well remains constant (see Figure 4.1). Therefore, one would not expect signs of critical slowing down. Even so, both Ritchie and Sieber (2016) and Siteur et al. (2016) found that the prototype model for rate-induced tipping shows critical slowing down before the transition, albeit with a delay (Ritchie & Sieber, 2016). Nevertheless, it is not yet clear whether the currently used resilience indicators can give predictions for other systems than the model of rate-induced tipping used by these authors.

In slowly responding systems, the stability properties do change when the system moves towards the tipping point. Nevertheless, because the dynamics of such systems are already slow and because of statistical reasons, a relative decrease in the intrinsic response rate due to critical slowing down will be difficult to detect (**Chapter 3**). Moreover, the possibility of long transients implies that a system may spend much time too far from equilibrium to detect the critical slowing down of the equilibrium.

## EFFECTS OF SLOWER STOCHASTIC CHANGES IN CLIMATE ON TIPPING POINTS

Besides the effects of changes in the rate of environmental change, I explored the effect of changes in environmental variability on the chances of critical transitions. Already in 1985, John H. Steele noted that the character of environmental fluctuations may profoundly affect population shifts (Steele, 1985). Ever since, there has been a debate in population ecology about the question of how environmental variability may affect population dynamics and especially the risk of extinction (Heino, Ripa, & Kaitala, 2000; Mustin, Dytham, Benton, & Travis, 2013; Ripa & Lundberg, 1996; Ruokolainen, Linden, Kaitala, & Fowler, 2009; Schwager, Johst, & Jeltsch, 2006).

Intuitively, one may expect that a population that is able to cope with a single event of challenging environmental conditions, may still run into trouble when it is confronted with a series of subsequent events (Schwager et al., 2006). A corollary is that temporal autocorrelation in environmental variability could increase extinction risk. The effect of coloured (autocorrelated) environmental variability, however, is dependent on the noise generating process (Cuddington & Yodzis, 1999), driving not just autocorrelation but also the variance of the red noise (Heino et al., 2000). Depending on the noise generating process, the variance can either increase or decrease as the variability becomes more autocorrelated. I disentangled those effects, showing that regardless of the variance, the persistence of the fluctuations increases the chance of critical transitions (**Chapter 5**). In addition, I found that autocorrelated noise leads to large variation in the outcome, causing some simulation runs to transition to an alternative state much earlier than others, in line with the general finding that under red noise conditions, our ability to make accurate predictions is limited (Cuddington & Yodzis, 1999). In summary, changes in climate variability as a result of climate change will affect the chance of critical transitions as well as the predictability of such events in climate-sensitive systems that are not sensitive to rates of change.

For rate-sensitive systems, this is also the case, but here the rate of change in environmental conditions (shaping ‘the perturbation’) also influences the fate of the system. If the perturbation brings the system past a tipping point, the rate is not important, just as in systems that are insensitive to the rate of change; The fate of the system is determined by a combination of the size and the duration of the environmental pulse. In a system with rate-dependent tipping, however, the system may also shift if the perturbation does not bring the system past the tipping point. For those perturbations the rate of change is important. If the rate of change stays below a critical level, the system will be able to track the changing equilibrium (Figure 6.1, pink dot). On the other hand, if the rate of change is faster than the critical limit, the system is brought past the unstable equilibrium that marks the border between the two basins of attraction (Figure 6.1, orange dot). Whether the system collapses remains also dependent on the size and the duration of the pulse, but in a system without rate-dependent tipping, a pulse of similar magnitude would not result in rate-dependent tipping. Consequently, systems that can have rate-dependent tipping might be more sensitive to environmental perturbations.

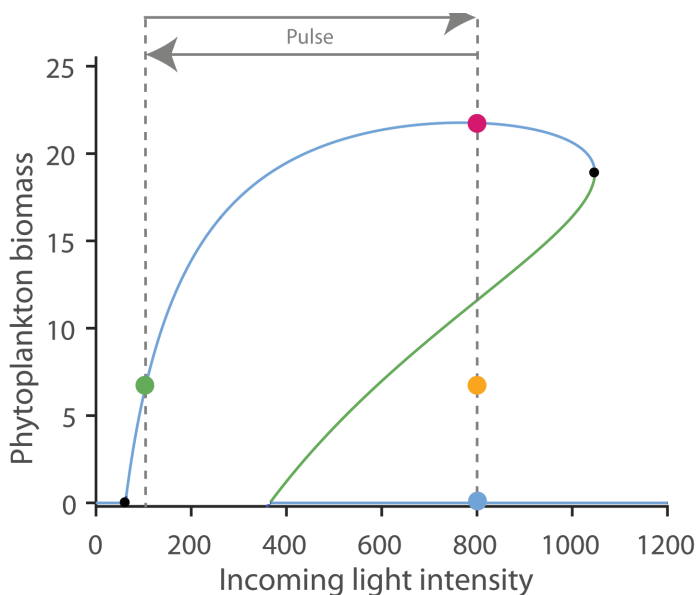


**Figure 6.1.** If a rate-sensitive system is subject to a pulse in the conditions, the rate of change of the pulse affects the response of the system. If the light intensity is increased from 100 to 800 with a rate that is below the critical rate, the system is able to track the changing equilibrium and reaches a high biomass state (pink dot) after which the biomass decreases again to the low biomass state (green dot) as the light intensity decreases. If the rate of the pulse is above the critical rate, however, the system crosses the unstable equilibrium (green line). The system is now in free fall (orange dot) and will move to the collapsed state (blue dot). If the pulse lasts long enough, the system will collapse. However, if the conditions are restored in time, the system crosses the unstable equilibrium again and the system will recover to the low biomass state (green dot).



When the system is affected by a stochastic regime of pulses, increased temporal correlation causes a higher probability of shifting. Uncorrelated perturbations are very rapid, and the duration of the pulses are too short for the system to respond. When the fluctuations are time-correlated, however, the duration of the fluctuations is long enough to cause an increase in the driver that the system can respond to. As a result, the system is more likely to collapse.

## TWO SIDES OF THE SAME COIN

To sum up, slower stochastic fluctuations in the climate increase the probability of tipping for both rate- and bifurcation-induced tipping. Furthermore, the moment of tipping becomes less predictable and the system can shift further away from the tipping point of the deterministic system. Systems with rate-tipping are more sensitive to pulses, because they can shift at lower absolute magnitudes of change. Therefore, these systems are likely more sensitive to perturbations in the environmental conditions and extreme events need not to be as ‘extreme’ for rate-dependent tipping to occur as for bifurcation-tipping.

Furthermore, increased rates of environmental change make it more difficult to observe the indicators of critical slowing down and increase the probability of rate-induced tipping. Although slowness of the intrinsic response rates of a system makes it difficult to observe the dynamics of a critical transition, their delayed responses might also provide a window of opportunity to navigate the system back to the original equilibrium (Hughes et al., 2013). For example, consider the phytoplankton population from **Chapter 4**. If the light intensity is instantaneously increased from 100 to 800, the system is brought past the unstable equilibrium (green line, Figure 6.2a). If the system responds fast, after 400 time steps the population will be in the new, collapsed state (green line, Figure 6.2b). The slow system (purple line, Figure 6.2b), however, still has a biomass of  $\sim 4$ . If one would notice after 400 time steps that the system is past the unstable equilibrium, and decrease the light intensity from 800 to 400, the system would be brought past the unstable equilibrium again (orange arrow, Figure 6.2a). As a result, the system would recover to the high biomass state. Taking the same measure for the fast system, does not bring the system past the unstable equilibrium as its biomass already decreased too far, and as a consequence, the system will not recover. This example illustrates how relevant it is for all three types of tipping to be able to distinguish between equilibrium and transient dynamics (see Chapter 5 for a similar example of bifurcation-induced tipping).

## CHAPTER 6

In conclusion, on the one hand, fast rates of change make it difficult to observe the underlying dynamics of climate-sensitive systems because these systems are likely not in equilibrium, but on the other hand, fast rates of change also give us the opportunity to restore environmental conditions in time to prevent a shift.

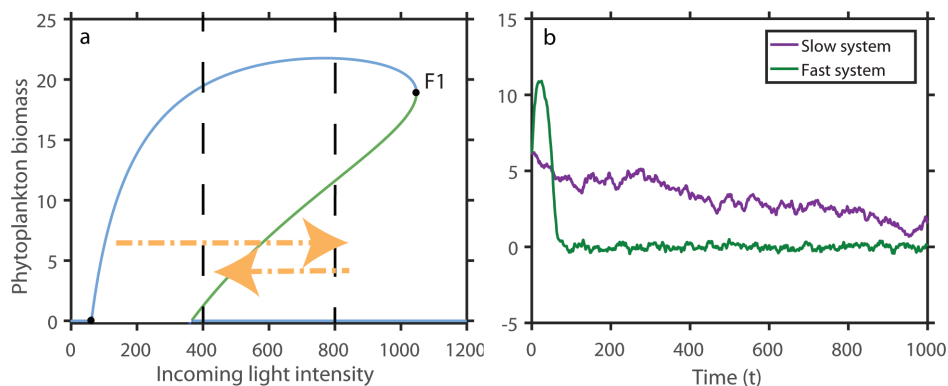


**Figure 6.2.** a) If you start from a phytoplankton equilibrium biomass of 6 for a light intensity of 100, and instantaneously increase the light intensity to 800, the system is brought across the unstable equilibrium (green line). If the light intensity is decreased to 400 before the system collapses, the system is brought past the unstable equilibrium and able to return to a high biomass state. b) Transient dynamics of a rate-induced shift to another stable state for systems with different response rates relative to the rate of change of the driver. The fast system (green line) shifts abruptly after the rate of change of the driver brings the system past the unstable equilibrium, but in a slowly responding system (purple line), the transient to the other state unfolds slowly.

## FORESEEING TIPPING POINTS: SLOWING DOWN AS CAUSE AND SYMPTOM

My results imply that climate change can affect both the occurrence and the predictability of critical transitions. Nevertheless, we still lack an understanding of how this will play out in reality. In a general sense, the dynamics of a nonlinear system are the result of an interplay between external influences and internal dynamics (Figure 6.3). In order to untangle the different effects of climate change, we need to account for the appropriate time scales and external influences in our data collection and construction of models. However, untangling system dynamics from external influences is not always straightforward.

For instance, a time-correlated environment can cause regime-like shifts in population dynamics in a system without alternative stable states (Doney & Salliey, 2013). But increased time-correlation of the environmental variability also increases the probability of tipping in systems with alternative stable states (Chapter 5). Therefore, it is difficult

to distinguish between external and internal mechanisms based on time-series analysis (left part, Figure 6.3). Untangling shifts from noise is further complicated by the fact that systems with alternative stable states may shift further away from the bifurcation point in a time-correlated environment compared to an environment without time-correlation (**Chapter 5**). As a result, in a strongly time-correlated environment, transitions will be more difficult to anticipate on the basis of the resilience indicators. In addition, the mere signal of large correlated environmental variability can overshadow indicators of critical slowing down in a bistable system that is approaching a threshold (Perretti & Munch, 2012). Obviously, a reddening environment can also result in false

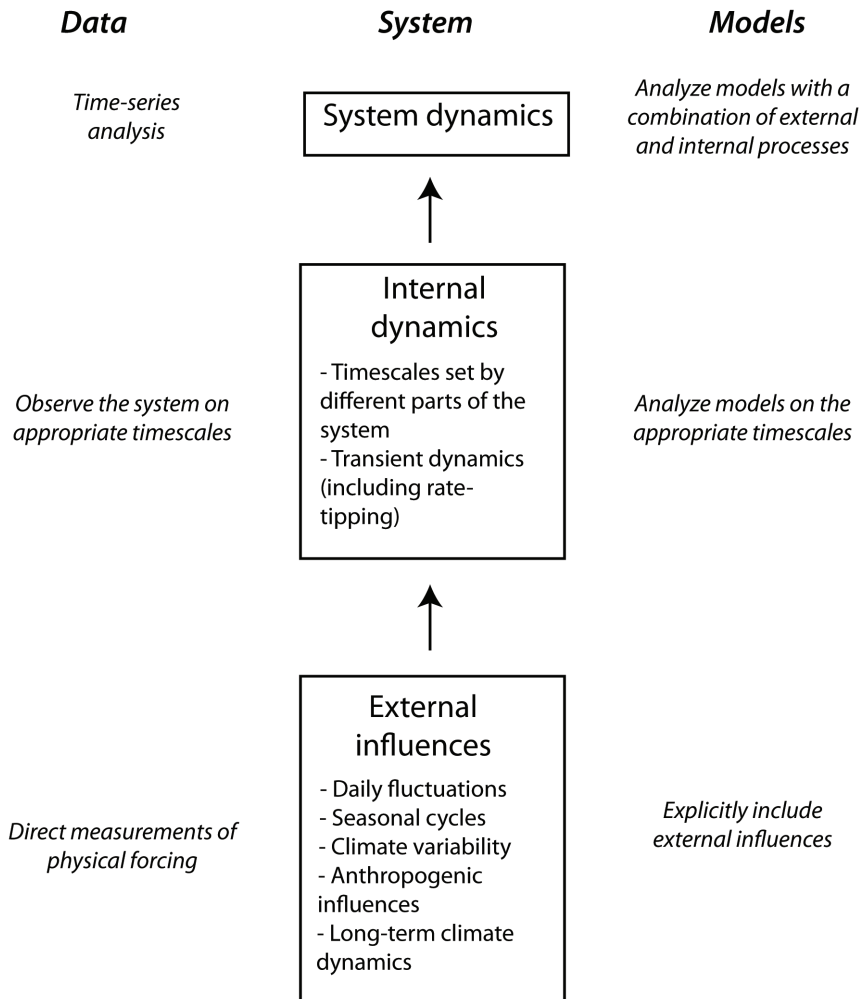


**Figure 6.3.** Summary of the relationships among aspects of timescales, dynamics, and implications for understanding. Actions on the left relate to data, and the actions on the right are directed towards modelling. Based on Fig. 1 from Hastings (2010).

CHAPTER 6

positives if its imprint on system dynamics is mistaken for a sign of critical slowing down. Consequently, the intertwined effects of internal dynamics and external forcing make it inherently difficult to distinguish between a system with alternative stable states that is, or is not, approaching a threshold, or a system without alternative stable states that is merely integrating its environment (Figure 6.4).

It should also be noted that while critical slowing down in elements of the climate can be an indicator of a loss of resilience of the climate system, the resulting rising variance and temporal correlation in climatic fluctuations may by themselves trigger a transition in climate-sensitive systems (**Chapter 5**). Consequently, observing indicators of critical slowing down in a climate-sensitive system followed by a shift to a different state may have two different explanations. It could be that the ecosystem was losing resilience, and then shifted. Likewise, it could also be that rising variance and redness of climatic dynamics (possibly related to dwindling resilience of the climate element itself) actually drove the transition in the ecosystem.

To conclude, the role of environmental variability in rapid transitions can be three-fold: it can obscure the underlying mechanisms, it can inform us about the stability of the system, and it can drive critical transitions. Distinguishing between these three different roles as climate variability changes, remains a significant challenge.

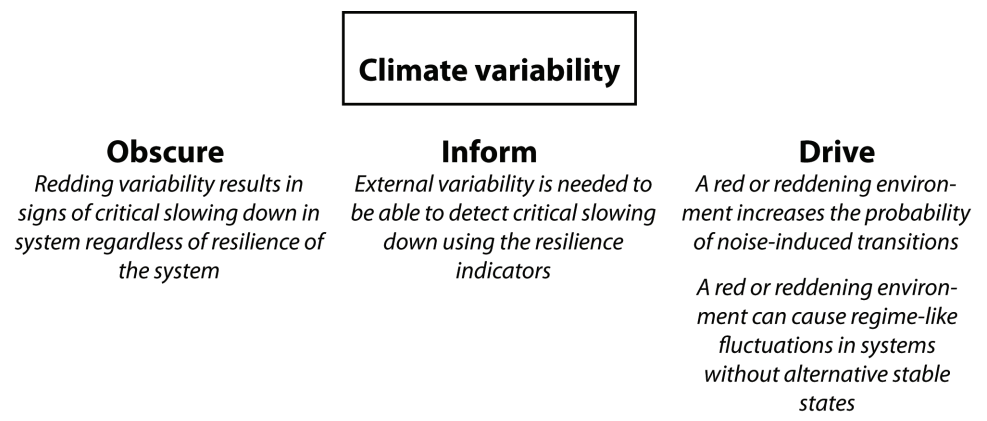


**Figure 6.4.** Climate variability can obscure the resilience indicators, is needed to use them (inform), and can drive (critical) transitions.

## BEWARE OF BIASES

The research on tipping points is no exception when it comes to the risk of being influenced by the systematic fallacies that tend to affect human reasoning. Two particular types of such fallacies stand out: the confirmation bias and the prosecutor's fallacy (Kahneman, 2011). The prosecutor's fallacy is an error in statistical reasoning and results from an invalid interpretation of a valid statistic. For example, suppose you are a cop and you pick up a suspect. The suspect has a match with the DNA found on the crime scene. Suppose that for a certain test the likelihood of such a match, purely by chance, is 1 in 20,000. One could think that the chance that your suspect is innocent, is therefore also 1 in 20,000. This is, however, not the case. Suppose you live in a city that has 600,000 inhabitants. In this city, you would expect 30 people to have DNA that also matches the sample found on the crime scene. Consequently, the suspect is 1 of 30 people who could have been at the crime scene and the odds are roughly 30 to 1 against your suspect being guilty.

A similar flaw in reasoning can occur in the interpretation of abrupt shifts in historical data. Not all sudden transitions are the result of crossing a tipping point: some systems may experience such transitions purely by chance (Scheffer & Carpenter, 2003). Claiming that the chance of such a transition is extremely low and that therefore the abrupt shift is probably a critical transition would be an example of the prosecutor's fallacy. In addition, these transitions owing to chance are likely to show trends in the resilience indicators, while time series of the same system that do not show a transition do not, even though the underlying dynamics are the same (Boettiger & Hastings, 2012). Selecting historical time series in which an abrupt shift occurred, therefore, introduces a bias towards detecting the resilience indicators (Boettiger & Hastings, 2012).

Confirmation bias is the tendency to seek or interpret evidence in ways that are partial to existing beliefs, expectations, or a hypothesis (Nickerson, 1998). In our field, this means that we tend to see evidence for alternative stable states everywhere. Abrupt shifts in time series, however, are not evidence of the existence of alternative stable states per se (Scheffer, 2009). Abrupt transitions can be caused by the integration of noise, a big stepwise change in the external conditions (Dakos et al., 2015) or can occur by chance alone (Boettiger & Hastings, 2012). Trends in the resilience indicators, on the other hand, can also be observed in systems that do not approach a critical transition (Boettiger et al., 2013; Kéfi, Dakos, Scheffer, Van Nes, & Rietkerk, 2013). Therefore, it is important to realize that trends in the resilience indicators could indicate that a system is losing resilience, but that other evidence is needed, such as the establishment of a

## CHAPTER 6

fold bifurcation in the system under study. The most convincing proof for alternative stable states can be achieved by manipulation in experimental systems (Dai, Vorselen, Korolev, & Gore, 2012; Veraart et al., 2012). But this is not possible for most natural systems. An alternative is to fit simplified models with alternative stable states to past abrupt shifts (Dakos et al., 2008). This might provide evidence for the existence of alternative stable states in systems that are not well-understood (Boettiger et al., 2013). In this case, however, sufficient alternative models need to be specified to make sure that one does not become subject to the confirmation bias and prosecutor's fallacy.

## PROSPECT

While avoiding these and other common cognitive fallacies requires permanent alertness and self-discipline, the more technical complications I discussed in these afterthoughts directly suggest concrete questions for future research:

- *As the current resilience indicators do not work in slow systems, are there other indicators that can be detected prior to a tipping point in slow systems?*
- *How could we distinguish transient from equilibrium dynamics?*
- *How long can a threshold or unstable equilibrium be crossed before the system is committed to long-lasting change?*

Answers to these questions are likely dependent on relative timescales and the complexity of the system dynamics (Figure 6.3). Therefore, system-specific approaches will be needed. More generally, an important limitation of my analysis is the focus on fold bifurcations in simple, models with the use of idealized noise processes. A next step could be to implement realistic time series of changing environmental variability in more realistic models with alternative stable states, such as a fisheries model, or a model of the Amazon rainforest.

The same is true for the findings on rate-dependent tipping. The modelled plankton system is rather stylized and simple. Rate-dependent tipping has not yet been observed in real ecosystems, but experimental studies do show rate-dependent outcomes (Bell & Gonzalez, 2009; Collins & de Meaux, 2009; Lindsey, Gallie, Taylor, & Kerr, 2013; Perron, Gonzalez, & Buckling, 2008), suggesting that rate-dependent tipping might be a relevant phenomenon. Nevertheless, grasping the potential for rate-dependent tipping in ecosystems will require a better understanding of how different species within an ecosystem respond to environmental change, and how these responses interact. From a

model perspective, we may explore whether more realistic ecosystem models also show rate-induced critical transitions, and if so, whether these systems have general features which can be used to distinguish rate-sensitive systems from ‘normal’ systems.

Another logical next step would be to develop resilience indicators for situations in which the currently used resilience indicators do not work. Besides resilience indicators for slowly responding systems, we need indicators for rate-induced tipping. Because there is no loss in stability, there is no reason to assume that the currently used resilience indicators can give predictions (Ashwin et al., 2012). This poses a great challenge for the coming years, because currently there is no way of knowing whether a system is rate-sensitive and if we are nearing a critical rate.

## AVOIDING TIPPING POINTS UNDER CLIMATE CHANGE

If anything, the findings of this thesis illustrate that we still have big challenges ahead. On the other hand, knowing that climate change might increase the chance of critical transitions, we may want to use the insights my work generated to help ‘avoid the unexpected’. There are, however, some fundamental problems that make it difficult to manage ecosystems under climate change. Preventing critical transitions in the climate is difficult in view of the large scientific uncertainties and the difficulties of developing and enforcing policies when many stakeholders are involved (Scheffer, 2009). Climate change requires global collective action, but this is difficult to achieve, because group effort will be systematically low in large, diffuse groups. This is known as the ‘*collective action problem*’ and is the result of low perceived effectiveness and noticeability (Magee, Brock, & Young, 1989). In addition, detection of a new problem depends on past experience (Klein, 2017), and because current rates climate change are unprecedented (Zeebe et al., 2016), detection of new problems as a result of climate change may take a long time. Once a problem is detected, there is often a delay in regulation due to inertia in the public opinion. Groups often lock into the same attitude, and therefore, are often rigid when it comes to responding to new problems or changing conditions (Scheffer, 2009). Consequently, public opinion might remain in a passive state for a very long time.

Furthermore, there are large scientific uncertainties in the effect of climate change on critical transitions. In addition to the uncertainties resulting from processes reflected upon in this last chapter, such as stochasticity, insufficient data and imprecise models, large uncertainties arise from the fact that the nature of system Earth is constantly changing. Such change includes interactions of the socio-ecological aspect of the

## CHAPTER 6

system (Chapin et al., 2009). The resulting uncertainty poses an important challenge for the management of ecosystems with alternative stable state. Assuming that there are tipping points when there are not may lead to unnecessary costs and devaluation of the theory of critical transitions. On the other hand, assuming that there are no tipping points when they are present may lead to unexpected shifts that are hard to reverse.

Given these large uncertainties, one approach is to manage ecosystems based on a precautionary principle. Johan Rockström and colleagues have developed a framework in which they identified and quantified planetary boundaries that must not be transgressed in order to remain in the stable Holocene state. The planetary boundaries are values of control variables that are either at a safe distance from thresholds (for processes that have thresholds), or at dangerous levels (for processes without thresholds) and are meant to provide a safe operating space for humanity (Rockström et al., 2009). As I have argued, sometimes the rate of change may be equally important as the absolute levels of environmental change. Thus in addition to such boundary values, we may need to define safe rates of change to stay within a safe operating space.

While the resilience indicators may help to assess the risks of critical transitions when the precise mechanisms are unknown, we will also need to understand the governing mechanisms if we want to manage critical transitions. For complex systems, such as the climate and ecosystems, there is no silver-bullet approach to get such insight. The strongest evidence for alternative stable states comes from replicated experiments, but such experiments are impossible for these complex systems. Consequently, we have to rely on data and models. Technological advances and geo-information tools make it possible to collect gigabytes of data. Including this data in the models that are designed to predict when critical transitions will happen, will drastically improve the performance of these models (Boettiger & Hastings, 2013).

### IT IS ALL RELATIVE

In this thesis, I looked at how climate change may affect the chance of critical transitions and our ability to foresee the unexpected. As reflected upon in this last chapter, it is difficult to untangle the different effects and consequences; A reddening environment can obscure, inform and drive critical transitions, and fast rates of change can obscure the resilience indicators, but also provide a window of opportunity to restore the conditions. While writing this last chapter, I realized that rather than falling into the trap of oversimplification we may need to embrace some of this complexity. Importantly, the relations I describe throughout this thesis are relative; Whether the



environment is time-correlated or not, the fluctuations are fast or slow, and the system is fast or slow. This means that it is impossible to make general rules up beforehand about whether resilience indicators can be observed or if conditions can be restored.

An extreme example of how time scales are relative when it comes to critical transitions, warning signals and the options for reversal are quantum jumps. Quantum jumps are transitions between two discrete energy levels of an atom and are usually assumed to occur instantaneously and at random (Bohr, 1913). The jump, however, is not really instantaneous and random. Researchers from Yale recently showed that quantum jumps are unpredictable on long timescales, but predictable on short timescales (Mineev et al., 2019). A few microseconds before the jump occurs, there is a period during which it is possible to observe a signal that warns of the upcoming jump. Furthermore, quantum jumps always take the same trajectory between the two energy levels. So while the starting point of the jump is random, the jump itself is predictable, allowing the researchers to reverse the quantum jumps mid-flight (Mineev et al., 2019).

If even extremely rapid quantum jumps in atoms can be caught using real-time monitoring and reversed, we should clearly not give up on a priori detecting and reversing critical transitions driven by climate change. Regardless of whether the dynamics are fast or slow in an absolute sense. Relative timescales, however, do need to be considered when interpreting resilience indicators. Especially in times when the scales are changing.

*The line it is drawn  
The curse it is cast  
The slow one now  
Will later be fast  
As the present now  
Will later be past  
The order is  
Rapidly fadin'  
And the first one now  
Will later be last  
For the times they are a-changin'.*

- Bob Dylan





**REFERENCES**

**SUMMARY**

**ACKNOWLEDGEMENTS**

**A FEW WORDS ABOUT THE AUTHOR**

**LIST OF PUBLICATIONS**

**SENSE CERTIFICATE**

## REFERENCES

- Adams, C., Ide, T., Barnett, J., & Detges, A. (2018). Sampling bias in climate–conflict research. *Nature Climate Change*, 1. <https://doi.org/10.1038/s41558-018-0068-2>
- Algeo, T. J., & Lyons, T. W. (2006). Mo–total organic carbon covariation in modern anoxic marine environments: Implications for analysis of paleoredox and paleohydrographic conditions. *Paleoceanography*, 21(1), n/a–n/a. <https://doi.org/10.1029/2004PA001112>
- Allan, R. P., & Soden, B. J. (2008). Atmospheric warming and the amplification of precipitation extremes. *Science (New York, N.Y.)*, 321(5895), 1481–. <https://doi.org/10.1126/science.1160787>
- Allen, C. D., Macalady, A. K., Chenchouni, H., Bachelet, D., McDowell, N., Vennetier, M., ... Cobb, N. (2010). A global overview of drought and heat-induced tree mortality reveals emerging climate change risks for forests. *Forest Ecology and Management*, 250(4), 660–684. <https://doi.org/10.1016/j.foreco.2009.09.001>
- Ashwin, P., Perryman, C., & Wiczeorek, S. (2017). Parameter shifts for nonautonomous systems in low dimension: bifurcation- and rate-induced tipping. *Nonlinearity*, 30(6), 2185–2210. <https://doi.org/10.1088/1361-6544/aa675b>
- Ashwin, P., Wiczeorek, S., Vitolo, R., & Cox, P. (2012). Tipping points in open systems: bifurcation, noise-induced and rate-dependent examples in the climate system. *Philosophical Transactions of the Royal Society of London A: Mathematical, Physical and Engineering Sciences*, 370(1962), 1166–1184.
- Barnett, J., & Adger, W. N. (2007). Climate change, human security and violent conflict. *Political Geography*, 26(6), 639–655. <https://doi.org/10.1016/j.polgeo.2007.03.003>
- Barrett, C. B., & Carter, M. R. (2013). The Economics of Poverty Traps and Persistent Poverty: Empirical and Policy Implications. *Journal of Development Studies*, 49(7), 976–990. <https://doi.org/10.1080/00220388.2013.785527>
- Bathiany, S., van der Bolt, B., Williamson, M. S., Lenton, T. M., Scheffer, M., van Nes, E. H., & Notz, D. (2016). Statistical indicators of Arctic sea-ice stability - prospects and limitations. *Cryosphere*, 10, 1631–1645. <https://doi.org/10.5194/tc-10-1631-2016>
- Bell, G., & Gonzalez, A. (2009). Evolutionary rescue can prevent extinction following environmental change. *Ecology Letters*, 12(9), 942–948. <https://doi.org/10.1111/j.1461-0248.2009.01350.x>
- Bestelmeyer, B. T., Ellison, A. M., Fraser, W. R., Gorman, K. B., Holbrook, S. J., Laney, C. M., ... Sharma, S. (2011). Analysis of abrupt transitions in ecological systems. *Ecosphere*, 2(12), art129. <https://doi.org/10.1890/ES11-00216.1>
- Bevis, M., Harig, C., Khan, S. A., Brown, A., Simons, F. J., Willis, M., ... Nylen, T. (2019). Accelerating changes in ice mass within Greenland, and the ice sheet's sensitivity to atmospheric forcing. *Proceedings of the National Academy of Sciences of the United States of America*, 116(6), 1934–1939. <https://doi.org/10.1073/pnas.1806562116>
- Biggs, R., Carpenter, S. R., & Brock, W. A. (2009). Turning back from the brink: detecting an impending regime shift in time to avert it. *Proceedings of the National Academy of Sciences of the United States of America*, 106(3), 826–831. <https://doi.org/10.1073/pnas.0811729106>
- Blaauw, M., & Christen, J. A. (2011). Flexible paleoclimate age–depth models using an autoregressive gamma process. *Bayesian Analysis*, 6(3), 457–474. <https://doi.org/10.1214/11-BA618>
- Bloemsma, M. R. (2015). *Development of a Modelling Framework for Core Data Integration using XRF Scanning*. Delft University of Technology. <https://doi.org/https://doi.org/10.4233/uuid:95a90787-edc7-4fif-9e6a-b2453effabdb>
- Boettiger, C., & Hastings, A. (2012). Early warning signals and the prosecutor's fallacy. *Proceedings of the Royal Society of London B: Biological Sciences*. Retrieved from <http://rspb.royalsocietypublishing.org/content/early/2012/10/09/rspb.2012.2085.short>
- Boettiger, C., & Hastings, A. (2013). From patterns to predictions. *Nature*, 493, 157. Retrieved from <https://doi.org/10.1038/493157a>
- Boettiger, C., Ross, N., & Hastings, A. (2013). Early warning signals: The charted and uncharted territories. *Theoretical Ecology*, 6(3). <https://doi.org/10.1007/s12080-013-0192-6>
- Bohr, N. (1913). On the Constitution of Atoms and Molecules. Part I. Binding of electrons by positive nuclei. *Philosophical Magazine*, 26(6), 1–25.
- Bond, W. J. (2008). What Limits Trees in C<sub>4</sub> Grasslands and Savannas? *Annual Review of Ecology, Evolution, and Systematics*, 641–659.

- Boulton, C. A., & Lenton, T. M. (2015). Slowing down of North Pacific climate variability and its implications for abrupt ecosystem change. *Proceedings of the National Academy of Sciences*, 112(37), 11496–11501.
- Box, G. E. P., Jenkins, G. M., Reinsel, G. C., & Ljung, G. M. (2015). *Time series analysis: forecasting and control*. John Wiley & Sons.
- Brando, P. M., Balch, J. K., Nepstad, D. C., Morton, D. C., Putz, F. E., Coe, M. T., ... Soares-Filho, B. S. (2014). Abrupt increases in Amazonian tree mortality due to drought-fire interactions. *Proceedings of the National Academy of Sciences of the United States of America*, 111(17), 6347–6352. <https://doi.org/10.1073/pnas.1305499111>
- Breitbart, D., LA, L., Oshlies, A., Grégoire, M., FP, C., DJ, C., ... Zhang, J. (2018). Declining oxygen in the global ocean and coastal waters. *Science (New York, N.Y.)* TA - TT -, 359(6371). <https://doi.org/10.1126/science.aam7240> LK - <https://wur.on.worldcat.org/oclc/7314509576>
- Buhaus, H., Nordkvelle, J., Bernauer, T., Böhmelt, T., Brzoska, M., Busby, J. W., ... von Uexküll, N. (2014). One effect to rule them all? A comment on climate and conflict. *Climatic Change*, 127(3–4), 391–397. <https://doi.org/10.1007/s10584-014-1266-1>
- Buhaus, Halvard. (2010). Climate not to blame for African civil wars. *Proceedings of the National Academy of Sciences of the United States of America*, 107(38), 16477–16482. <https://doi.org/10.1073/pnas.1005739107>
- Burke, M. B., Miguel, E., Satyanath, S., Dykema, J. A., & Lobell, D. B. (2009). Warming increases the risk of civil war in Africa. *Proceedings of the National Academy of Sciences of the United States of America*, 106(49), 20670–20674. <https://doi.org/10.1073/pnas.0907998106>
- Cane, M. A., Miguel, E., Burke, M., Hsiang, S. M., Lobell, D. B., Meng, K. C., & Satyanath, S. (2014). Temperature and violence. *Nature Climate Change*, 4(4), 234–235. <https://doi.org/10.1038/nclimate2171>
- Carpenter, S. R., & Brock, W. A. (2006). Rising variance: a leading indicator of ecological transition. *Ecology Letters*, 9(3), 311–318. <https://doi.org/10.1111/j.1461-0248.2005.00877.x>
- Carpenter, S. R. & Brock, W. A. (2006). Rising variance: a leading indicator of ecological transition. *Ecology Letters*, 9(3), 311–318.
- Carpenter, Stephen R., Ludwig, D., & Brock, W. A. (1999). Management of Eutrophication for Lakes Subject to Potentially Irreversible Change. *Ecological Applications*, 9(3), 751. <https://doi.org/10.2307/2641327>
- Carter, M. R., Little, P. D., Mogues, T., & Negatu, W. (2007). Poverty Traps and Natural Disasters in Ethiopia and Honduras. *World Development*, 35(5), 835–856. <https://doi.org/10.1016/j.worlddev.2006.09.010>
- Casford, J. S. ., Rohling, E. ., Abu-Zied, R. ., Fontanier, C., Jorissen, F. ., Leng, M. ., ... Thomson, J. (2003). A dynamic concept for eastern Mediterranean circulation and oxygenation during sapropel formation. *Palaeogeography, Palaeoclimatology, Palaeoecology*, 190, 103–119. [https://doi.org/10.1016/S0031-0182\(02\)00601-6](https://doi.org/10.1016/S0031-0182(02)00601-6)
- Chapin, F. S., Kofinas, G. P., Folke, C., Carpenter, S. R., Olsson, P., Abel, N., ... Stafford, D. M. (2009). Resilience-based stewardship: strategies for navigating sustainable pathways in a changing world. In *Principles of ecosystem stewardship* (pp. 319–337). Springer.
- Charmantier, A., McCreery, R. H., Cole, L. R., Perrins, C., Kruuk, L. E. B., & Sheldon, B. C. (2008). Adaptive Phenotypic Plasticity in Response to Climate Change in a Wild Bird Population. *Science*, 320(5877), 800–803. <https://doi.org/10.1126/SCIENCE.1157174>
- Chen, I.-C., Hill, J. K., Ohlemüller, R., Roy, D. B., & Thomas, C. D. (2011). Rapid range shifts of species associated with high levels of climate warming. *Science (New York, N.Y.)*, 333(6045), 1024–1026. <https://doi.org/10.1126/science.1206432>
- Collins, S., & de Meaux, J. (2009). Adaptation to different rates of environmental change in *Chlamydomonas*. *Evolution*, 63(11), 2952–2965. <https://doi.org/10.1111/j.1558-5646.2009.00770.x>
- Coumou, D., & Rahmstorf, S. (2012). A decade of weather extremes. *Nature Climate Change*, 2(7), 491. <https://doi.org/10.1038/nclimate1452>
- Courchamp, F., Clutton-Brock, T., & Grenfell, B. (1999). Inverse density dependence and the Allee effect. *Trends in Ecology & Evolution*, 14(10), 405–410. [https://doi.org/10.1016/S0169-5347\(99\)01683-3](https://doi.org/10.1016/S0169-5347(99)01683-3)
- Cuddington, K. M., & Yodzis, P. (1999). Black noise and population persistence. *Proceedings of the Royal Society of London. Series B: Biological Sciences*, 266(1422), 969–973. <https://doi.org/10.1098/rspb.1999.0731>
- da Costa, A. C. L., Galbraith, D., Almeida, S., Portela, B. T. T., da Costa, M., Silva Junior, J. de A., ... Meir, P. (2010). Effect of 7 yr of experimental drought on vegetation dynamics and biomass storage of an eastern Amazonian rainforest. *The New Phytologist*, 187(3), 579–591. <https://doi.org/10.1111/j.1469->

- Dai, L., Vorselen, D., Korolev, K. S., & Gore, J. (2012). Generic indicators for loss of resilience before a tipping point leading to population collapse. *Science (New York, N.Y.)*, 336(6085), 1175–1177. <https://doi.org/10.1126/science.1219805>
- Dakos, V. (2011). *Expecting the unexpected: indicators of resilience as early-warning signals for critical transitions*.
- Dakos, V., Carpenter, S. R., Brock, W. A., Ellison, A. M., Guttal, V., Ives, A. R., ... van Nes, E. H. (2012). Methods for detecting early warnings of critical transitions in time series illustrated using simulated ecological data. *PLoS One*, 7(7), e41010.
- Dakos, V., Carpenter, S. R., van Nes, E. H., & Scheffer, M. (2015). Resilience indicators: prospects and limitations for early warnings of regime shifts. *Philosophical Transactions of the Royal Society of London B: Biological Sciences*, 370(1659), 20130263. <https://doi.org/http://dx.doi.org/10.1098/rstb.2013.0263>
- Dakos, V., Scheffer, M., van Nes, E. H., Brovkin, V., Petoukhov, V., & Held, H. (2008). Slowing down as an early warning signal for abrupt climate change. *Proceedings of the National Academy of Sciences*, 105(38), 14308–14312. <https://doi.org/10.1073/pnas.0802430105>
- Dakos, V., van Nes, E. H., Donangelo, R., Fort, H., & Scheffer, M. (2009). Spatial correlation as leading indicator of catastrophic shifts. *Theoretical Ecology*, 3(3), 163–174. <https://doi.org/10.1007/s12080-009-0060-6>
- De Lange, G. J., Thomson, J., Reitz, A., Slomp, C. P., Speranza Principato, M., Erba, E., & Corselli, C. (2008). Synchronous basin-wide formation and redox-controlled preservation of a Mediterranean sapropel. *Nature Geoscience*, 1(9), 606–610. <https://doi.org/10.1038/ngeo283>
- deMenocal, P., Ortiz, J., Guilderson, T., & Sarnthein, M. (2000). Coherent high- and low-latitude climate variability during the holocene warm period. *Science (New York, N.Y.)*, 288(5474), 2198–2202. <https://doi.org/10.1126/SCIENCE.288.5474.2198>
- Dhooge, A., Govaerts, W., & Kuznetsov, Y. A. (2003). MATCONT: a MATLAB package for numerical bifurcation analysis of ODEs. *ACM Transactions on Mathematical Software (TOMS)*, 29(2), 141–164.
- Di Lorenzo, E., & Ohman, M. D. (2013). A double-integration hypothesis to explain ocean ecosystem response to climate forcing. *Proceedings of the National Academy of Sciences of the United States of America*, 110(7), 2496–2499. <https://doi.org/10.1073/pnas.1218022110>
- Diaz, R. J., & Rosenberg, R. (2008). Spreading dead zones and consequences for marine ecosystems. *Science (New York, N.Y.)*, 321(5891), 926–929. <https://doi.org/10.1126/science.1156401>
- Donald, A. Wilhite. (2000). Chapter 1 Drought as a Natural Hazard: Concepts and Definitions. In D. A. Wilhite (Ed.), *Drought: A Global Assessment, Vol. I* (pp. 3–18). London: Routledge.
- Done, T. J. (1992). Phase shifts in coral reef communities and their ecological significance. *Hydrobiologica*, (247), 121–132. [https://doi.org/10.1007/978-94-017-3288-8\\_13](https://doi.org/10.1007/978-94-017-3288-8_13)
- Doney, S. C., & Sailley, S. F. (2013). When an ecological regime shift is really just stochastic noise. *Proceedings of the National Academy of Sciences of the United States of America*, 110(7), 2438–2439. <https://doi.org/10.1073/pnas.1222736110>
- Drijfhout, S., Bathiany, S., Beaulieu, C., Brovkin, V., Claussen, M., Huntingford, C., ... Swingedouw, D. (2015). Catalogue of abrupt shifts in Intergovernmental Panel on Climate Change climate models. *Proceedings of the National Academy of Sciences of the United States of America*, 112(43), E5777–86. <https://doi.org/10.1073/pnas.1511451112>
- Dymond, J., Suess, E., & Lyle, M. (1992). Barium in Deep-Sea Sediment: A Geochemical Proxy for Paleoproductivity. *Paleoceanography*, 7(2), 163–181. <https://doi.org/10.1029/92PA00181>
- Eakin, C. M., Lough, J. M., & Heron, S. F. (2009). Climate Variability and Change: Monitoring Data and Evidence for Increased Coral Bleaching Stress (pp. 41–67). Springer Berlin Heidelberg. [https://doi.org/10.1007/978-3-540-69775-6\\_4](https://doi.org/10.1007/978-3-540-69775-6_4)
- Ebisuzaki, W. (1997). A Method to Estimate the Statistical Significance of a Correlation When the Data Are Serially Correlated. *Journal of Climate*, 10(9), 2147–2153. [https://doi.org/10.1175/1520-0442\(1997\)010<2147:AMTETS>2.0.CO;2](https://doi.org/10.1175/1520-0442(1997)010<2147:AMTETS>2.0.CO;2)
- Erian, W., Katlan, B., & Babah, O. (2011). Drought vulnerability in the Arab region: Special case study: Syria. *Background Paper Prepared for The*.
- Faassen, E. J., Veraart, A. J., Van Nes, E. H., Dakos, V., Lürling, M., & Scheffer, M. (2015). Hysteresis in an

- experimental phytoplankton population. *Oikos*.
- Field, C. B., Barros, V., Stocker, T. F., Dahe, Q., Dokken, D. J., Ebi, K., ... Midgley, P. M. (Eds.). (2012). *Managing the Risks of Extreme Events and Disasters to Advance Climate Change Adaptation*. Cambridge, UK and New York, USA: Cambridge University Press.
- Frankignoul, C., & Hasselmann, K. (1977). Stochastic climate models, Part II Application to sea-surface temperature anomalies and thermocline variability. *Tellus*, 29(4), 289–305. <https://doi.org/10.1111/j.2153-3490.1977.tb00740.x>
- Gerla, D. J., Mooij, W. M., & Huisman, J. (2011). Photoinhibition and the assembly of light-limited phytoplankton communities. *Oikos*, 120(3), 359–368. <https://doi.org/10.1111/j.1600-0706.2010.18573.x>
- Gijzel, S. M. W., van de Leemput, I. A., Scheffer, M., van Bon, G. E. A., Weerdesteyn, V., Eijssvogels, T. M. H., ... Melis, R. J. F. (2018). Dynamical Indicators of Resilience in Postural Balance Time Series Are Related to Successful Aging in High-Functioning Older Adults. *The Journals of Gerontology: Series A*. <https://doi.org/10.1093/gerona/gly170>
- Goswami, B. N., Venugopal, V., Sengupta, D., Madhusoodanan, M. S., & Xavier, P. K. (2006). Increasing trend of extreme rain events over India in a warming environment. *Science (New York, N.Y.)*, 314(5804), 1442–1445. <https://doi.org/10.1126/science.1132027>
- Grant, K. M., Grimm, R., Mikolajewicz, U., Marino, G., Ziegler, M., & Rohling, E. J. (2016). The timing of Mediterranean sapropel deposition relative to insolation, sea-level and African monsoon changes. *Quaternary Science Reviews*, 140, 125–141. <https://doi.org/10.1016/J.QUASCIREV.2016.03.026>
- Grant, K. M., Rohling, E. J., Bar-Matthews, M., Ayalon, A., Medina-Elizalde, M., Ramsey, C. B., ... Roberts, A. P. (2012). Rapid coupling between ice volume and polar temperature over the past 150,000 years. *Nature*, 491(7426), 744–747. <https://doi.org/10.1038/nature11593>
- Greenman, J. V., & Benton, T. G. (2003). The amplification of environmental noise in population models: causes and consequences. *The American Naturalist*, 161(2), 225–239.
- Groffman, P. M., Baron, J. S., Blett, T., Gold, A. J., Goodman, I., Gunderson, L. H., ... Wiens, J. (2006). Ecological Thresholds: The Key to Successful Environmental Management or an Important Concept with No Practical Application? *Ecosystems*, 9(1), 1–13. <https://doi.org/10.1007/s10021-003-0142-z>
- Groisman, P. Y., & Knight, R. W. (2008). Prolonged Dry Episodes over the Conterminous United States: New Tendencies Emerging during the Last 40 Years. *Journal of Climate*, 21(9), 1850–1862. <https://doi.org/10.1175/2007JCLI2013.1>
- Groisman, P. Y., Knight, R. W., Easterling, D. R., Karl, T. R., Hegerl, G. C., & Razuvaev, V. N. (2005). Trends in Intense Precipitation in the Climate Record. *Journal of Climate*, 18(9), 1326–1350. <https://doi.org/10.1175/JCLI3339.1>
- Gsell, A. S., Scharfenberger, U., Özkundakci, D., Walters, A., Hansson, L.-A., Janssen, A. B. G., ... Adrian, R. (2016). Evaluating early-warning indicators of critical transitions in natural aquatic ecosystems. *Proceedings of the National Academy of Sciences*. <https://doi.org/10.1073/pnas.1608242113>
- Gustafson, E. J., & Sturtevant, B. R. (2013). Modeling Forest Mortality Caused by Drought Stress: Implications for Climate Change. *Ecosystems*, 16, 60–74. <https://doi.org/10.2307/23501298>
- Hänggi, P., & Jung, P. (1995). Colored noise in dynamical systems. *Advances in Chemical Physics*, 89, 239–326. Retrieved from [https://www.researchgate.net/profile/Peter\\_Jung2/publication/227992407\\_Colored\\_Noise\\_in\\_Dynamical\\_Systems/links/00b4951fbeg6b827f5000000.pdf](https://www.researchgate.net/profile/Peter_Jung2/publication/227992407_Colored_Noise_in_Dynamical_Systems/links/00b4951fbeg6b827f5000000.pdf)
- Hänggi, P., Mroczkowski, T. J., Moss, F., & McClintock, P. V. E. (1985). Bistability driven by colored noise: Theory and experiment. *Physical Review A*, 32(1), 695–698. <https://doi.org/10.103/PhysRevA.32.695>
- Hasselmann, K. (1976). Stochastic climate models Part I. Theory. *Tellus*, 28(6), 473–485. <https://doi.org/10.1111/j.2153-3490.1976.tb00696.x>
- Hastings, A., Abbott, K. C., Cuddington, K., Francis, T., Gellner, G., Lai, Y.-C., ... Zeeman, M. Lou. (2018). Transient phenomena in ecology. *Science (New York, N.Y.)*, 361(6406), eaat6412. <https://doi.org/10.1126/science.aat6412>
- Heino, M., Ripa, J., & Kaitala, V. (2000). Extinction risk under coloured environmental noise. *Ecography*, 23(2), 177–184.
- Held, H., & Kleinen, T. (2004). Detection of climate system bifurcations by degenerate fingerprinting. *Geophysical Research Letters*, 31(23). <https://doi.org/10.1029/2004GL020972>
- Hennekam, R., Sweere, T., de Lange, G. J., & Reichart, G.-J. (2019). Trace metal analysis of sediment cores using a novel X-ray fluorescence core scanning method. *Quaternary International*, 514, 55–67. <https://doi.org/10.1016/j.quaint.2019.04.011>



doi.org/10.1016/J.QUAINT.2018.10.018

- Hirota, M., Holmgren, M., Van Nes, E. H., & Scheffer, M. (2011). Global resilience of tropical forest and savanna to critical transitions. *Science (New York, N.Y.)*, 334(6053), 232–235. <https://doi.org/10.1126/science.1210657>
- Holling, C. S. (1973). Resilience and stability of ecological systems. *Annual Review of Ecology and Systematics*, 4(1), 1–23.
- Holmgren, M., Hirota, M., van Nes, E. H., & Scheffer, M. (2013). Effects of interannual climate variability on tropical tree cover. *Nature Climate Change*, 3(8), 755–758.
- Holmgren, M., & Scheffer, M. (2001). El Niño as a window of opportunity for the restoration of degraded arid ecosystems. *Ecosystems*, 4(2), 151–159.
- Holmgren, M., Scheffer, M., & Huston, M. A. (1997). The interplay of facilitation and competition in plant communities. *Ecology*, 78(7), 1966–1975. [https://doi.org/10.1890/0012-9658\(1997\)078\[1966:TIOFAC\]2.0.CO;2](https://doi.org/10.1890/0012-9658(1997)078[1966:TIOFAC]2.0.CO;2)
- Holt, R. D. (1990). The microevolutionary consequences of climate change. *Trends in Ecology & Evolution*, 5(9), 311–315. [https://doi.org/10.1016/0169-5347\(90\)90088-U](https://doi.org/10.1016/0169-5347(90)90088-U)
- Horsthemke, W., & Lefever, R. (1984). Noise-Induced Transitions in Physics, Chemistry, and Biology. In *Noise-Induced Transitions* (pp. 164–200). Springer Berlin Heidelberg. [https://doi.org/10.1007/3-540-36852-3\\_7](https://doi.org/10.1007/3-540-36852-3_7)
- Hsiang, S. M., & Burke, M. (2014). Climate, conflict, and social stability: what does the evidence say? *Climatic Change*, 123(1), 39–55. <https://doi.org/10.1007/s10584-013-0868-3>
- Hsiang, S. M., Burke, M., & Miguel, E. (2013). Quantifying the influence of climate on human conflict. *Science*, 341(6151), 1235367.
- Hsiang, S. M., & Meng, K. C. (2014). Reconciling disagreement over climate-conflict results in Africa. *Proceedings of the National Academy of Sciences of the United States of America*, 111(6), 2100–2103. <https://doi.org/10.1073/pnas.1316006111>
- Hsiang, S. M., Meng, K. C., & Cane, M. A. (2011). Civil conflicts are associated with the global climate. <https://doi.org/10.1038/nature10311>
- Hughes, T. P., Baird, A. H., Bellwood, D. R., Card, M., Connolly, S. R., Folke, C., ... Roughgarden, J. (2003). Climate change, human impacts, and the resilience of coral reefs. *Science (New York, N.Y.)*, 301(5635), 929–933. <https://doi.org/10.1126/science.1085046>
- Hughes, T. P., Kerry, J. T., Álvarez-Noriega, M., Álvarez-romero, J. G., Anderson, K. D., Baird, A., ... Wilson, S. K. (2017). Global warming and recurrent mass bleaching of corals. *Nature*, 543, 373–377. <https://doi.org/10.1038/nature21707>
- Hughes, T. P., Linares, C., Dakos, V., van de Leemput, I. A., & van Nes, E. H. (2013). Living dangerously on borrowed time during slow, unrecognized regime shifts. *Trends in Ecology & Evolution*, 28(3), 149–155. <https://doi.org/10.1016/j.tree.2012.08.022>
- Huntingford, C., Jones, P. D., Livina, V. N., Lenton, T. M., & Cox, P. M. (2013). No increase in global temperature variability despite changing regional patterns. *Nature*, 500(7462), 327–330. Retrieved from <http://dx.doi.org/10.1038/nature12310>
- IPCC. (2013). *Climate Change 2013: The Physical Science Basis. Contribution of Working Group I to the Fifth Assessment Report of the Intergovernmental Panel on Climate Change*. (V. B. and P. M. M. (eds. . Stocker, T.F., D. Qin, G.-K. Plattner, M. Tignor, S.K. Allen, J. Boschung, A. Nauels, Y. Xia, Ed.). Cambridge, United Kingdom and New York, NY, USA: Cambridge University Press.
- Ives, A. R. (1995). Measuring resilience in stochastic systems. *Ecological Monographs*, 217–233.
- Jilbert, T., & Slomp, C. P. (2013). Rapid high-amplitude variability in Baltic Sea hypoxia during the Holocene. *Geology*, 41(11), 1183–1186. <https://doi.org/10.1130/G34804.1>
- John. G. McPeak, & Christopher B. Barrett. (2001). Differential Risk Exposure and Stochastic Poverty Traps among East African Pastoralists on JSTOR. *American Journal of Agricultural Economics*, 83(3), 674–679. Retrieved from <http://www.jstor.org/stable/1245098>
- Joos, F., & Spahni, R. (2008). Rates of change in natural and anthropogenic radiative forcing over the past 20,000 years. *Proceedings of the National Academy of Sciences of the United States of America*, 105(5), 1425–1430. <https://doi.org/10.1073/pnas.0707386105>
- Kanekar, N., Lee, Y.-J., & Aruin, A. S. (2014). Frequency analysis approach to study balance control in individuals with multiple sclerosis. *Journal of Neuroscience Methods*, 222, 91–96. <https://doi.org/10.1016/j.jneumeth.2014.05.001>



- Karssenber, D., Bierkens, M. F. P., & Rietkerk, M. (2017). Catastrophic Shifts in Semiarid Vegetation-Soil Systems May Unfold Rapidly or Slowly. *The American Naturalist*, 190(6), E145–E155. <https://doi.org/10.1086/694413>
- Keeling, R. F., Körtzinger, A., & Gruber, N. (2010). Ocean Deoxygenation in a Warming World. *Annual Review of Marine Science* TA - TT -, 2, 199–229. <https://doi.org/10.1146/annurev.marine.010908.163855> LK - <https://wur.on.worldcat.org/oclc/4761087023>
- Kéfi, S., Dakos, V., Scheffer, M., Van Nes, E. H., & Rietkerk, M. (2013). Early warning signals also precede non-catastrophic transitions. *Oikos*, 122(5), 641–648.
- Kelley, C. P., Mohtadi, S., Cane, M. A., Seager, R., & Kushnir, Y. (2015). Climate change in the Fertile Crescent and implications of the recent Syrian drought. *Proceedings of the National Academy of Sciences*, 112(11), 3241–3246. <https://doi.org/10.1073/pnas.1421533112>
- Kemp, W. M., Testa, J. M., Conley, D. J., Gilbert, D., & Hagy, J. D. (2009). Temporal responses of coastal hypoxia to nutrient loading and physical controls. *Biogeosciences*, 6(12), 2985–3008. <https://doi.org/10.5194/bg-6-2985-2009>
- Klein, G. A. (2017). *Sources of power: How people make decisions*. MIT press.
- Klein Goldewijk, K., Beusen, A., Van Dreht, G., & De Vos, M. (2011). The HYDE 3.1 spatially explicit database of human-induced global land-use change over the past 12,000 years. *Global Ecology and Biogeography*, 20(1), 73–86. <https://doi.org/10.1111/j.1466-8238.2010.00587.x>
- Kleinen, T., Held, H., & Petschel-Held, G. (2003). The potential role of spectral properties in detecting thresholds in the Earth system: application to the thermohaline circulation. *Ocean Dynamics*, 53(2), 53–63. <https://doi.org/10.1007/s10236-002-0023-6>
- Knowlton, N. (1992). Thresholds and multiple stable states in coral reef community dynamics. *Integrative and Comparative Biology*, 32(6), 674–682. <https://doi.org/10.1093/icb/32.6.674>
- Lenton, T. M. (2011). Early warning of climate tipping points. *Nature Climate Change*, 1(4), 201–209.
- Lenton, T. M. (2013). Environmental Tipping Points. *Annual Review of Environment and Resources*, 38(1), 1–29. <https://doi.org/10.1146/annurev-environ-102511-084654>
- Lenton, T. M., Dakos, V., Bathiany, S., & Scheffer, M. (2017). Observed trends in the magnitude and persistence of monthly temperature variability. *Scientific Reports*, 7(1), 5940. <https://doi.org/10.1038/s41598-017-06382-x>
- Lenton, T. M., Held, H., Kriegler, E., Hall, J. W., Lucht, W., Rahmstorf, S., & Schellnhuber, H. J. (2008). Tipping elements in the Earth's climate system. *Proceedings of the National Academy of Sciences*, 105(6), 1786–1793. <https://doi.org/10.1073/pnas.0705414105>
- Lenton, T. M., Myerscough, R. J., Marsh, R., Livina, V. N., Price, A. R., & Cox, S. J. (2009). Using GENIE to study a tipping point in the climate system. *Philosophical Transactions of the Royal Society of London A: Mathematical, Physical and Engineering Sciences*, 367(1890).
- Levin, L. A. (2018). Manifestation, Drivers, and Emergence of Open Ocean Deoxygenation. *Annual Review of Marine Science* TA - TT -, 10, 229–260. <https://doi.org/10.1146/annurev-marine-121916-063359> LK - <https://wur.on.worldcat.org/oclc/7287636563>
- Lindsey, H. A., Gallie, J., Taylor, S., & Kerr, B. (2013). Evolutionary rescue from extinction is contingent on a lower rate of environmental change. *Nature*, 494(7438), 463–467. <https://doi.org/10.1038/nature11879>
- Lisiecki, L. E., & Raymo, M. E. (2005). A Pliocene-Pleistocene stack of 57 globally distributed benthic  $\delta^{18}O$  records. *Paleoceanography*, 20(1), n/a-n/a. <https://doi.org/10.1029/2004PA001071>
- Long, S. P., Humphries, S., & Falkowski, P. G. (1994). Photoinhibition of photosynthesis in nature. *Annu. Rev. Plant Physiol. Plant Mol. Biol.*, 45, 633–662. Retrieved from <https://www.annualreviews.org/doi/pdf/10.1146/annurev.pp.45.060194.003221>
- Lourens, L. J., Wehausen, R., & Brumsack, H. J. (2001). Geological constraints on tidal dissipation and dynamical ellipticity of the Earth over the past three million years. *Nature*, 409(6823), 1029–1033. <https://doi.org/10.1038/35059062>
- Ludwig, D., Jones, D. D., & Holling, C. S. (1978). Qualitative Analysis of Insect Outbreak Systems: The Spruce Budworm and Forest. <https://doi.org/10.2307/3939>
- Magee, S. P., Brock, W. A., & Young, L. (1989). *Black hole tariffs and endogenous policy theory: Political economy in general equilibrium*. Cambridge University Press.
- Malhi, Y., Aragão, L. E. O. C., Galbraith, D., Huntingford, C., Fisher, R., Zelazowski, P., ... Meir, P. (2009).

- Exploring the likelihood and mechanism of a climate-change-induced dieback of the Amazon rainforest. *Proceedings of the National Academy of Sciences*, 106(49), 20610–20615.
- Mann, H. B. (1945). Nonparametric Tests Against Trend. *Econometrica*, 13(3), 245–259. <https://doi.org/10.2307/1907187>
- Mantua, N. J., Hare, S. R., Zhang, Y., Wallace, J. M., Francis, R. C., Mantua, N. J., ... Francis, R. C. (1997). A Pacific Interdecadal Climate Oscillation with Impacts on Salmon Production. *Bulletin of the American Meteorological Society*, 1069–1079. [https://doi.org/https://doi.org/10.1175/1520-0477\(1997\)078<1069:APICOW>2.0.CO;2](https://doi.org/https://doi.org/10.1175/1520-0477(1997)078<1069:APICOW>2.0.CO;2)
- Marino, G., Rohling, E. J., Rijpstra, W. I. C., Sangiorgi, F., Schouten, S., & Damsté, J. S. S. (2007). Aegean Sea as driver of hydrographic and ecological changes in the eastern Mediterranean. *Geology*, 35(8), 675. <https://doi.org/10.1130/G23831A.1>
- May, R. M. (1977). Thresholds and breakpoints in ecosystems with a multiplicity of stable states. *Nature*, 269(5628), 471–477.
- McCook, L. J. (1999). Macroalgae, nutrients and phase shifts on coral reefs: scientific issues and management consequences for the Great Barrier Reef. *Coral Reefs*, 18(4), 357–367. <https://doi.org/10.1007/s003380050213>
- McDowell, N., Pockman, W. T., Allen, C. D., Breshears, D. D., Cobb, N., Kolb, T., ... Yezpe, E. A. (2008). Mechanisms of plant survival and mortality during drought: why do some plants survive while others succumb to drought? *New Phytologist*, 178(4), 719–739. <https://doi.org/10.1111/j.1469-8137.2008.02436.x>
- Middelburg, J. J., & Levin, L. A. (2009). Coastal hypoxia and sediment biogeochemistry. *Biogeosciences*, 6(7), 1273–1293.
- Minev, Z. K., Mundhada, S. O., Shankar, S., Reinhold, P., Gutiérrez-Jáuregui, R., Schoelkopf, R. J., ... Devoret, M. H. (2019). To catch and reverse a quantum jump mid-flight. *Nature*, 570(7760), 200–204. <https://doi.org/10.1038/s41586-019-1287-z>
- Mustin, K., Dytham, C., Benton, T. G., & Travis, J. M. J. (2013). Red noise increases extinction risk during rapid climate change. *Diversity and Distributions*, 19(7), 815–824.
- Nepstad, D. C., Tohver, I. M., Ray, D., Moutinho, P., & Cardinot, G. (2007). Mortality of large trees and lianas following experimental drought in an Amazon forest. *Ecology*, 88(9), 2259–2269.
- Nickerson, R. S. (1998). Confirmation Bias: A Ubiquitous Phenomenon in Many Guises. *Review of General Psychology*, 2(2), 175–220. <https://doi.org/10.1037/1089-2680.2.2.175>
- Ovaskainen, O., & Meerson, B. (2010). Stochastic models of population extinction. *Trends in Ecology & Evolution*, 25(11), 643–652. <https://doi.org/10.1016/j.TREE.2010.07.009>
- Peeters, J. C. H., & Eilers, P. (1978). The relationship between light intensity and photosynthesis—A simple mathematical model. *Hydrobiological Bulletin*, 12(2), 134–136. <https://doi.org/10.1007/BF02260714>
- Perretti, C. T., & Munch, S. B. (2012). Regime shift indicators fail under noise levels commonly observed in ecological systems. *Ecological Applications*, 22(6), 1772–1779.
- Perron, G. G., Gonzalez, A., & Buckling, A. (2008). The rate of environmental change drives adaptation to an antibiotic sink. *Journal of Evolutionary Biology*, 21(6), 1724–1731. <https://doi.org/10.1111/j.1420-9101.2008.01596.x>
- Petchey, O. L. (2000). Environmental colour affects aspects of single-species population dynamics. *Proceedings of the Royal Society of London A: Mathematical, Physical and Engineering Sciences*, 267(1445), 747–754.
- Rahmstorf, S., Crucifix, M., Ganopolski, A., Goosse, H., Kamenkovich, I., Knutti, R., ... Weaver, A. J. (2005). Thermohaline circulation hysteresis: A model intercomparison. *Geophysical Research Letters*, 32(23), L23605. <https://doi.org/10.1029/2005GL023655>
- Raleigh, C., Linke, A., & O'Loughlin, J. (2014). Extreme temperatures and violence. *Nature Climate Change*, 4, 76–77. <https://doi.org/10.1038/nclimate2101>
- Reitz, A., Thomson, J., de Lange, G. J., & Hensen, C. (2006). Source and development of large manganese enrichments above eastern Mediterranean sapropel Si. *Paleoceanography*, 21(3). <https://doi.org/10.1029/2005PA001169>
- Reuveny, R. (2007). Climate change-induced migration and violent conflict. *Political Geography*, 26(6), 656–673. <https://doi.org/10.1016/j.polgeo.2007.05.001>
- Ripa, J., & Lundberg, P. (1996). Noise colour and the risk of population extinctions. *Proceedings: Biological Sciences*, 1751–1753.

- Ritchie, P., & Sieber, J. (2016). Early-warning indicators for rate-induced tipping. *Chaos: An Interdisciplinary Journal of Nonlinear Science*, 26(9), 093116. <https://doi.org/10.1063/1.4963012>
- Rockström, J., Steffen, W., Noone, K., Persson, Å., Chapin, F. S., Lambin, E. F., ... Foley, J. A. (2009). A safe operating space for humanity. *Nature*, 461(7263), 472–475. <https://doi.org/10.1038/461472a>
- Rodríguez-Sanz, L., Bernasconi, S. M., Marino, G., Heslop, D., Müller, I. A., Fernandez, A., ... Rohling, E. J. (2017). Penultimate deglacial warming across the Mediterranean Sea revealed by clumped isotopes in foraminifera. *Scientific Reports*, 7(1), 16572. <https://doi.org/10.1038/s41598-017-16528-6>
- Rohling, E. J., Marino, G., & Grant, K. M. (2015). Mediterranean climate and oceanography, and the periodic development of anoxic events (sapropels). *Earth-Science Reviews*, 143, 62–97. <https://doi.org/10.1016/J.EARSCIREV.2015.01.008>
- Rossignol-Strick, M. (1985). Mediterranean Quaternary sapropels, an immediate response of the African monsoon to variation of insolation. *Palaeogeography, Palaeoclimatology, Palaeoecology*, 49(3–4), 237–263. [https://doi.org/10.1016/0031-0182\(85\)90056-2](https://doi.org/10.1016/0031-0182(85)90056-2)
- Rowland, L., da Costa, A. C. L., Galbraith, D. R., Oliveira, R. S., Binks, O. J., Oliveira, A. A. R., ... Meir, P. (2015). Death from drought in tropical forests is triggered by hydraulics not carbon starvation. *Nature*, 528(7580), 119–122. <https://doi.org/10.1038/nature15539>
- Rudnick, D. L., & Davis, R. E. (2003). Red noise and regime shifts. *Deep Sea Research Part I: Oceanographic Research Papers*, 50(6), 691–699.
- Ruokolainen, L., Linden, A., Kaitala, V., & Fowler, M. S. (2009). Ecological and evolutionary dynamics under coloured environmental variation. *Trends in Ecology & Evolution*, 24(10), 555–563.
- Scheffer, M., Barrett, S., Carpenter, S. R., Folke, C., Green, A. J., Holmgren, M., ... Walker, B. (2015). Creating a safe operating space for iconic ecosystems. *Science*, 347(6228).
- Scheffer, Marten. (1998). *Ecology of Shallow Lakes: Population and Community Biology*. London: Chapman and Hall.
- Scheffer, Marten. (2009). *Critical Transitions in Nature and Society*. Princeton Studies in Complexity. Princeton University Press. <https://doi.org/10.5860/CHOICE.47-1380>
- Scheffer, Marten, Bascompte, J., Brock, W. A., Brovkin, V., Carpenter, S. R., Dakos, V., ... Sugihara, G. (2009). Early-warning signals for critical transitions. *Nature*, 461(7260), 53–59.
- Scheffer, Marten, Carpenter, S., Foley, J., Folke, C., & Walker, B. (2001). Catastrophic shifts in ecosystems. *Nature*, 413(6856), 591–596. <https://doi.org/doi:10.1038/35098000>
- Scheffer, Marten, & Carpenter, S. R. (2003). Catastrophic regime shifts in ecosystems: linking theory to observation. *Trends in Ecology & Evolution*, 18(12), 648–656. <https://doi.org/10.1016/J.TREE.2003.09.002>
- Scheffer, Marten, Carpenter, S. R., Dakos, V., & van Nes, E. H. (2015). Generic Indicators of Ecological Resilience: Inferring the Chance of a Critical Transition. *Annual Review of Ecology, Evolution, and Systematics*, 46(1), 145–167. <https://doi.org/10.1146/annurev-ecolsys-112414-054242>
- Scheffer, Marten, Van Nes, E. H., Holmgren, M., & Hughes, T. (2008). Pulse-driven loss of top-down control: the critical-rate hypothesis. *Ecosystems*, 11(2), 226–237.
- Scheffer, Marten, Westley, F., & Brock, W. (2003). Slow Response of Societies to New Problems: Causes and Costs. *Ecosystems*, 6(5), 493–502. <https://doi.org/10.1007/PL00021504>
- Scheffran, J., Brzoska, M., Kominek, J., Link, P. M., & Schilling, J. (2012). Climate Change and Violent Conflict. *Science*, 336(6083), 869–871. Retrieved from <http://science.sciencemag.org.ezproxy.library.wur.nl/content/336/6083/869.full>
- Schlesinger, M. E., & Ramankutty, N. (1994). An oscillation in the global climate system of period 65–70 years. *Nature*, 367(6465), 723–726. Retrieved from <http://dx.doi.org/10.1038/367723a0>
- Schleussner, C.-F., Donges, J. F., Donner, R. V., & Schellnhuber, H. J. (2016). Armed-conflict risks enhanced by climate-related disasters in ethnically fractionalized countries. *Proceedings of the National Academy of Sciences of the United States of America*, 113(33), 9216–9221. <https://doi.org/10.1073/pnas.1601611113>
- Schneider, D. P., & Steig, E. J. (2008). Ice cores record significant 1940s Antarctic warmth related to tropical climate variability. *Proceedings of the National Academy of Sciences of the United States of America*, 105(34), 12154–12158. <https://doi.org/10.1073/pnas.0803627105>
- Schwager, M., Johst, K., & Jeltsch, F. (2006). Does red noise increase or decrease extinction risk? Single extreme events versus series of unfavorable conditions. *The American Naturalist*, 167(6), 879–888.
- Siteur, K., Eppinga, M. B., Doelman, A., Siero, E., & Rietkerk, M. (2016). Ecosystems off track: rate-induced

- critical transitions in ecological models. *Oikos*, 125(12), 1689–1699. <https://doi.org/10.1111/oik.03112>
- Slomp, C. P., Thomson, J., & de Lange, G. J. (2002). Enhanced regeneration of phosphorus during formation of the most recent eastern Mediterranean sapropel (S1). *Geochimica et Cosmochimica Acta*, 66(7), 1171–1184. [https://doi.org/10.1016/S0016-7037\(01\)00848-1](https://doi.org/10.1016/S0016-7037(01)00848-1)
- Smith, J. A., Andersen, T. J., Shortt, M., Gaffney, A. M., Truffer, M., Stanton, T. P., ... Vaughan, D. G. (2016). Sub-ice-shelf sediments record history of twentieth-century retreat of Pine Island Glacier. *Nature*. <https://doi.org/10.1038/nature20136>
- Solh, M. (2010). Tackling the drought in Syria. *Nature Middle East*.
- Staver, A. Carla, Bond, W. J., Stock, W. D., van Rensburg, S. J., & Waldram, M. S. (2009). Browsing and fire interact to suppress tree density in an African savanna. *Ecological Applications*, 19(7), 1909–1919. <https://doi.org/10.1890/08-1907.1>
- Staver, A. Carla, Archibald, S., & Levin, S. A. (2011). The Global Extent and Determinants of Savanna and Forest as Alternative Biome States. *Science*, 334(6053), 230–232. <https://doi.org/10.1126/science.1210465>
- Staver, Ann Carla, & Bond, W. J. (2014). Is there a 'browse trap'? Dynamics of herbivore impacts on trees and grasses in an African savanna. *Journal of Ecology*, 102(3), 595–602. <https://doi.org/10.1111/1365-2745.12230>
- Steele, J. H., & Henderson, E. W. (1984). Modeling long-term fluctuations in fish stocks. *Science (New York, N.Y.)*, 224(4652), 985–987. <https://doi.org/10.1126/science.224.4652.985>
- Steele, John H. (1985). A comparison of terrestrial and marine ecological systems. *Nature*, 313(6001), 355–358.
- Steele, John H., & Henderson, E. W. (1994). Coupling between Physical and Biological Scales [and Discussion]. *Philosophical Transactions of the Royal Society B: Biological Sciences*, 343(1303), 5–9.
- Stommel, H. (1961). Thermohaline Convection with Two Stable Regimes of Flow. *Tellus*, 13(2), 224–230. <https://doi.org/10.3402/tellusa.v13i2.9491>
- Strogatz, S. H. (2014). *Nonlinear dynamics and chaos: with applications to physics, biology, chemistry, and engineering*. Westview press.
- Takahashi, S., & Murata, N. (2008). How do environmental stresses accelerate photoinhibition? *Trends in Plant Science*, 13(4), 178–182. <https://doi.org/10.1016/J.TPLANTS.2008.01.005>
- Thompson, J. M. T. (2011). Predicting Climate Tipping As a Noisy Bifurcation : a Review. *International Journal of Bifurcation and Chaos*, 21(2), 399–423. <https://doi.org/10.1142/S0218127411028519>
- Trenberth, K. E. (1984). Some Effects of Finite Sample Size and Persistence on Meteorological Statistics. Part I: Autocorrelations. *Monthly Weather Review*, 112(12), 2359–2368. [https://doi.org/10.1175/1520-0493\(1984\)112<2359:SEOFSS>2.0.CO;2](https://doi.org/10.1175/1520-0493(1984)112<2359:SEOFSS>2.0.CO;2)
- Tribouillard, N., Algeo, T. J., Lyons, T., & Riboulleau, A. (2006). Trace metals as paleoredox and paleoproductivity proxies: An update. *Chemical Geology*, 232(1–2), 12–32. <https://doi.org/10.1016/J.CHEMGEO.2006.02.012>
- United Nations High Commissions for Refugees. (2010). *Iraqi Refugees in Syria Reluctant to Return to Home Permanently: Survey*. Geneva: UB High Comm Refugees. Retrieved from [unhcr.org/4caf376c6.html](http://unhcr.org/4caf376c6.html)
- Valdes, P. (2011). Built for stability. *Nature Geoscience*, 4(7), 414–416. <https://doi.org/10.1038/ngeo1200>
- van de Leemput, I. A., Hughes, T. P., van Nes, E. H., & Scheffer, M. (2016). Multiple feedbacks and the prevalence of alternate stable states on coral reefs. *Coral Reefs*, 1–9. <https://doi.org/10.1007/s00338-016-1439-7>
- van de Leemput, I. A., van Nes, E. H., & Scheffer, M. (2015). Resilience of alternative states in spatially extended ecosystems. *PloS One*, 10(2), e0116859. <https://doi.org/10.1371/journal.pone.0116859>
- van der Bolt, B., van Nes, E. H., Bathiany, S., Vollebregt, M. E., & Scheffer, M. (2018). Climate reddening increases the chance of critical transitions. *Nature Climate Change*, 8(6), 478–484. <https://doi.org/10.1038/s41558-018-0160-7>
- Van Geest, G. J., Coops, H., Scheffer, M., & van Nes, E. H. (2007). Long Transients Near the Ghost of a Stable State in Eutrophic Shallow Lakes with Fluctuating Water Levels. *Ecosystems*, 10(1), 37–47. <https://doi.org/10.1007/s10021-006-9000-0>
- van Nes, E. H., Arani, B. M. S., Staal, A., van der Bolt, B., Flores, B. M., Bathiany, S., & Scheffer, M. (2016). What Do You Mean, "Tipping Point"? *Trends in Ecology & Evolution*, 31(12), 902–904. <https://doi.org/10.1016/j.tree.2016.09.011>
- van Nes, E. H., Hirota, M., Holmgren, M., & Scheffer, M. (2014). Tipping points in tropical tree cover: linking

- theory to data. *Global Change Biology*, 20(3), 1016–1021. <https://doi.org/10.1111/gcb.12398>
- van Nes, E. H., & Scheffer, M. (2007). Slow Recovery from Perturbations as a Generic Indicator of a Nearby Catastrophic Shift. *The American Naturalist*, 169(6), 738–747. <https://doi.org/10.1086/516845>
- van Nes, E. H., Staal, A., Hantson, S., Holmgren, M., Pueyo, S., Bernardi, R. E., ... Scheffer, M. (2018). Fire forbids fifty-fifty forest. *PLOS ONE*, 13(1), e0191027. <https://doi.org/10.1371/journal.pone.0191027>
- Vasseur, D. A. (2007). Populations embedded in trophic communities respond differently to coloured environmental noise. *Theoretical Population Biology*, 72(2), 186–196.
- Vasseur, D. A., & Yodzis, P. (2004). The color of environmental noise. *Ecology*, 85(4), 1146–1152.
- Veraart, A. J., Faassen, E. J., Dakos, V., van Nes, E. H., Lürling, M., & Scheffer, M. (2012). Recovery rates reflect distance to a tipping point in a living system. *Nature*, 481(7381), 357–359. <https://doi.org/10.1038/nature10723>
- Visser, M. E. (2008). Keeping up with a warming world; assessing the rate of adaptation to climate change. *Proceedings. Biological Sciences*, 275(1635), 649–659. <https://doi.org/10.1098/rspb.2007.0997>
- von Uexkull, N., Croicu, M., Fjelde, H., & Buhaug, H. (2016). Civil conflict sensitivity to growing-season drought. *Proceedings of the National Academy of Sciences of the United States of America*, 113(44), 12391–12396. <https://doi.org/10.1073/pnas.1607542113>
- Wagner, T. J. W., & Eisenman, I. (2015). False alarms: How early warning signals falsely predict abrupt sea ice loss. *Geophysical Research Letters*, 42(23), 10,333–10,341. <https://doi.org/10.1002/2015GL066297>
- Wang, R., Dearing, J. A., Langdon, P. G., Zhang, E., Yang, X., Dakos, V., & Scheffer, M. (2012). Flickering gives early warning signals of a critical transition to a eutrophic lake state. *Nature*, 492(7429), 419–422.
- Weltje, G. J., Bloemsa, M. R., Tjallingii, R., Heslop, D., Röhl, U., & Croudace, I. W. (2015). Prediction of Geochemical Composition from XRF Core Scanner Data: A New Multivariate Approach Including Automatic Selection of Calibration Samples and Quantification of Uncertainties (pp. 507–534). Springer, Dordrecht. [https://doi.org/10.1007/978-94-017-9849-5\\_21](https://doi.org/10.1007/978-94-017-9849-5_21)
- Werrell, C. E., Femia, F., & Sternberg, T. (2015). Did We See It Coming?: State Fragility, Climate Vulnerability, and the Uprisings in Syria and Egypt. *SAIS Review of International Affairs*, 35(1), 29–46. <https://doi.org/10.1353/sais.2015.0002>
- Wieczorek, S., Ashwin, P., Luke, C. M., & Cox, P. M. (2011). Excitability in ramped systems: the compost-bomb instability. In *Proceedings of the Royal Society of London A: Mathematical, Physical and Engineering Sciences* (Vol. 467, pp. 1243–1269). The Royal Society.
- Wissel, C. (1984). A Universal Law of the Characteristic Return Time near Thresholds. *Oecologia*, 65(1), 101–107. Retrieved from [http://www.jstor.org/stable/4217501?seq=1#page\\_scan\\_tab\\_contents](http://www.jstor.org/stable/4217501?seq=1#page_scan_tab_contents)
- Zeebe, R. E., Ridgwell, A., & Zachos, J. C. (2016). Anthropogenic carbon release rate unprecedented during the past 66 million years. *Nature Geoscience*, 9(4), 325–329. <https://doi.org/10.1038/ngeo2681>
- Zemp, D. C., Schleussner, C.-F., Barbosa, H. M. J., Hirota, M., Montade, V., Sampaio, G., ... Rammig, A. (2017). Self-amplified Amazon forest loss due to vegetation-atmosphere feedbacks. *Nature Communications*, 8, 14681. <https://doi.org/10.1038/ncomms14681>
- Ziegler, M., Tuenter, E., & Lourens, L. J. (2010). The precession phase of the boreal summer monsoon as viewed from the eastern Mediterranean (ODP Site 968). *Quaternary Science Reviews*, 29(11–12), 1481–1490. <https://doi.org/10.1016/j.quascirev.2010.03.011>
- Zwief, K. L., Hennekam, R., Donders, T. H., van Helmond, N. A. G. M., de Lange, G. J., & Sangiorgi, F. (2018). Marine productivity, water column processes and seafloor anoxia in relation to Nile discharge during sapropels S1 and S3. *Quaternary Science Reviews*, 200, 178–190. <https://doi.org/10.1016/j.quascirev.2018.08.026>



## SUMMARY

Complex systems in ecology and the climate can have tipping points. The term ‘tipping point’ is loosely defined as a threshold point in the conditions after which runaway change brings the system to a new stable state. Such a transition can have long-term dire consequences, and therefore it is of critical importance to understand why and when these transitions occur. Under the ongoing climate change, these critical transitions are projected to increase. However, little is understood about how relative timescales of the rate of environmental change and variability affect the occurrence and detectability of these critical transitions in nature and society. The aim of this thesis is to provide some insights in how differences in these timescales may affect critical transitions.

This thesis starts with the analysis of bistability of marine anoxic events in the Mediterranean Sea. Reconstructed time series have been used to detect changes in resilience indicators prior to several abrupt shifts in the past climate. This is, however, only possible under a limited set of conditions. For the past marine anoxic events in the Mediterranean Sea, these conditions are met. Recent technological advances made it possible to construct high-resolution and (almost) evenly spaced time series of past widespread anoxic events in the Mediterranean Sea. In **Chapter 2**, we analysed whether past transitions in the Mediterranean Sea could have been predicted using the resilience indicators autocorrelation and variance. We show that the repeated shifts into marine anoxia in the Mediterranean Sea had the character of critical transitions, because there was a gradual increase in the temporal autocorrelation and variance in the deep cores (>1600 meter depth) before the onset of most events. Our results imply that future widespread anoxia in marine systems might be recognizable using an appropriate statistical approach and high-resolution records.

These shifts to an anoxic state occurred relatively fast, but not all shifts to an alternative stable state unfold rapidly. Slowly responding systems show a gradual shift to the alternative state, once the tipping point has been passed. As the rate of the current environmental change is unprecedented, more system respond relatively slow to changes in the environment. The current resilience indicators are based on the theoretical finding that the system slows down close to the tipping point. But in these relatively slow systems, the recovery rates are always slow. Therefore, it is the question whether these resilience indicators flag that a relatively slow system is approaching a tipping point. In **Chapter 3**, we show that it is more difficult to quantify the resilience of a system that responds relatively slow. These results indicate that as the rates of environmental change keep increasing, it become more and more difficult to detect

whether systems are approaching a tipping point.

Another risk under current rates of environmental change is that the rate of change in the conditions triggers a shift to an alternative stable state, whereas a change of the same magnitude but at slower rates would not. Only few studies describe this so-called ‘rate-tipping’ in ecological systems, but understanding rate-tipping is needed to understand and predict ecosystem response to the ongoing rapid environmental change. Therefore, we show in **Chapter 4** that there can be rate-induced tipping for a range of initial conditions in a model of cyanobacteria with realistic parameter settings. A pulse in the environmental conditions, for example as a result of an extreme event, can cause a temporary collapse, depending on both the rate and the duration of the pulse. In addition, we showed that the type of environmental variability can influence the probability of inducing rate-tipping. These results imply that we need to incorporate critical rates of change in our ecosystems assessment and management.

In addition to affecting the probability of inducing rate-tipping, environmental variability itself can bring a system past a tipping point. The variability is different in different parts of the climate, but because of climate change, the climatic variability is changing systematically in different parts of the world. Therefore, we analysed in **Chapter 5** what the effect of changes in the memory of the climatic variability is on the chance of undergoing a critical transition. We show that chances of invoking such critical transitions are strongly affected by the climate memory as measured for instance by temporal autocorrelation in climatic variables. We illustrate the implications of this prediction with evidence from forests, corals reefs, poverty traps, violent conflict and ice-sheet instability. In all of these examples, the duration of anomalous dry or warm events increases the chance of invoking a critical transition. Our results imply that understanding the effects of altered climate variability requires research on climate memory.

In the **Afterthoughts** I conclude that fast rates of environmental change and changes in environmental variability can affect the detectability and predictability of critical transitions. While the exact impacts of climate change are likely system-specific, interacting timescales make it difficult to untangle system dynamics from external forcing. The relations I describe throughout this thesis, however, are relative. This means that it is impossible to make general rules about whether resilience indicators can be observed, or if the conditions can be restored. Therefore, we should not give up on a priori detecting and reversing critical transitions driven by climate change.

## ACKNOWLEDGEMENTS

Athletes around the world work in cycles of four years towards their ultimate goal: participating in the Olympic Games. In the last four years, I have worked towards my own Olympic Goal, and I made it. Now all that is left is the closing ceremony, and therefore, I would like to take the opportunity to thank everyone that made this journey possible.

First of all, I would like to thank my **coaches**, Egbert and Marten. Even though I had limited experience when I started, you always had faith in my ability to become a star athlete. As a coaching couple, you two are the perfect balance. Marten brought creativity, vision and passion to the table, while Egbert made sure that we had the proper tactics and materials. I have always known that you would not be the average coaches with training schemes, tests and dietary advice. Instead, you gave me the freedom to develop my own training regime, and to figure out what works for me. At times, this freedom was overwhelming, especially when the goal was still far away, but in the end, it made a strong, independent athlete that is able to deal with setbacks. Thanks you for the guidance throughout these four years.

An athlete would be nowhere without its **trainers**. When I joined the team, I was welcomed by Sebastian, who was my private trainer for a while. As the road to the Olympics progressed, his direct training moments decreased in frequency, but every time I needed some extra guidance, he was there. Where Sebastian was mostly responsible for my technical trainings, I could turn to Ingrid for some guidance on the process and the obstacles I encountered. In addition, she functioned as our team captain, by making sure that we would work and learn together as a team. While the role of Jeroen was maybe not like a traditional trainer, his presence made sure that I would not forget that there is more in life than just excelling at sports. He would always check-in to make sure that I was okay. I was lucky that in those first three years of my journey I had him as my mentor and roommate.

During all the games, I knew I could count on my **team mates**. As a newbie in the team, Marlies shared her tips with me, giving me the confidence I needed for a head start. Every good teams need a good defense, and I was lucky enough that I could always count on Merel, Sanne, Els and Hazimah. No matter how good the opponent, they were my safe guards. In addition, they made all the hours in between practices bearable and provided me with some '*psychological doping*' when needed: I could always ventilate my frustrations and doubts with you, thanks. Over the years, I had to try out different positions on the field. At times when everything felt completely new to me, Pablo made



sure that I quickly mastered some of the basic tactics. Even though I had often still no clue what I was supposed to be doing, those little tips were invaluable.

Every team has a player that is really talented, but is only twelve years old and that person often gets the honorary task of being the 'Benjamin': the one who has to make sure that all the water bottles are filled and the balls are counted at the end of every practice. Of course, this role was taken up by Arie. In addition, he supplied me with dropjes and made sure that every now and then we would take a water break (with beer).

My **managers** made sure that I did not have to worry too much about other things, so I was able to fully focus on becoming a better athlete. Nancy took on most of the work by booking my flights for training camps, taking care of all the financial stuff with external trainers, making sure that there was enough food on training days, and by brightening everyone's day as soon as she walked in (often with a bouquet of hand-picked flowers). When I had to switch housing in the middle of the process, Petra ensured that I knew enough about the contracts and gave invaluable tips on the decoration so I almost immediately felt at home. Both made my life as an athlete easier and a lot more pleasant than it otherwise would have been.

In order to become the absolute best in your field, you need to constantly evaluate your performance. My **video-operator**, Wolf, allowed me to assess my own performance. It can sometimes be tough to be directly confronted with your own shortcomings, but it is necessary if you want to keep improving. I dare to say that without his mirror, I might have had to wait for the next Olympics.

In those four years I also worked together with **athletes from different disciplines**. In my first year I made a quick detour into another discipline. Margot always made sure that I felt welcome and she spread her enthusiasm and love for her sport. In my last year, Rick supported me and showed me that training together with different athletes, even though the disciplines might be completely different, can be beneficial for both.

I would also like to thank all the **supporters**: Frits, John, Miguel, Bart, Edwin, Wendy, and others from the team. Without your work and occasional chat, I would not have been able to perform at the highest level.

Het is altijd handig om vrienden met een medische achtergrond te hebben – voornamelijk zodat je op een feestje met borrelnootjes in je hand al je kwaaltjes aan diegene voor kunt leggen – maar ook buiten feestjes om was Sanne voor mij onmisbaar.

Zij was mijn **fysiotherapeut** en zorgde ervoor dat ondanks de blessures die mij af en toe teisterde, ik iedere keer weer voldoende opgelapt werd om toch te presteren. Een paar weken voor de eindstreep viel ik tijdens een training en was het de vraag of ik überhaupt nog verder kon gaan. De gesprekken die ik toen bij haar op de behandelafel had, hebben mij door die laatste weken heen gesleept. Ik ben dan ook heel blij dat zij vandaag samen met Nancy met mij op het podium staat. Om mij bij te staan, maar ook om de erkenning te krijgen die zij beiden verdienen.

Nu het steeds duidelijker wordt dat voeding belangrijk is om op hoog niveau te presteren, ben ik extra blij dat ik de afgelopen jaren begeleid werd door het beste team van **sportdiëtisten** van de wereld. Niet alleen maakten zij de lekkerste gerechten, ze waren ook altijd opzoek naar verbetering en schuwden geen enkele regionale keuken. Zo kon ik putten uit de lange tradities van het traditionele Oostblok sportdieet, maar deelden zij ook geheime recepten uit het Midden Oosten en werd ik tijdelijk op een tapas-dieet gezet. Jolien, Maaïke, Charlotte en Laura, dankjewel. Zonder jullie was ik zeker niet verhoonger, maar door jullie soulfood en goede grappen heb ik de eindstreep gehaald.

Op momenten dat ik er mentaal even doorheen zat, kon ik altijd terecht bij mijn **sportpsychologen** Laurie, Lotte, Voes en Gabriëlle. Op de momenten dat ik er doorheen zat, gaven jullie mij het gereedschap om de knop om te zetten en weer verder te gaan. Dat ik het relatief lang uit heb kunnen houden zonder inzinkingen en stress, heb ik echt aan jullie te danken. Met Voes ging ik overigens ook nog een weekje op hoogtestage en dat was fantastisch.

Op de momenten dat ik er mentaal niet compleet doorheen zat, maar wel een licht dipje had wegens vermoeidheid of het gebrek aan leven, dan werd ik altijd opgevrolijkt door lieve berichtjes van mijn persoonlijke **cheerleaders**. Wybe, Dechen, Laas, Merel, Anouk, Paula, Ashley, Francien, Janine, Pascal, Lotte, Layla, Hiemke, Fleur, Karlijn en Saar, dankjewel!

Ook hielp het op die momenten om even te klagen met **andere topsporters**. Afgelopen jaren heb ik de ergernissen van het vele trainen en het alles opzij zetten voor dat ene doel kunnen delen met Anne, Lianne, Christiaan en Renske.

De tijden dat je als topsporter alleen maar sport beoefent zijn voorbij en bij het ontwikkelen van mijn imago heb ik veel hulp gehad van mijn **influencers**/grafische vormgevers Lou en Janine. Met zijn tweeën zijn ze voor een groot deel verantwoordelijk voor het uiterlijk van het werk wat nu voor je ligt.

Uiteraard wil ik ook **mijn ouders en mijn zusje** bedanken. Als ik terugkwam van trainingskamp dan kon ik altijd bij jullie terecht om bij te tanken. Jullie hebben mij al die jaren gesteund en mij de stabiele basis gegeven van waaruit ik mijn eigen pad kon vinden. Ook nu de trainingskampen voorlopig voorbij zijn, blijf ik graag bij jullie langskomen om ‘even snel de stad in te wandelen voor een kopje koffie’ of om op een andere manier de lokale economie draaiende te houden.

Ook **oma** wil ik bedanken, want afgelopen vier jaar ging ik één week per jaar op hoogtestage naar Limburg. Niet om de immense bergen daar te trotseren, maar wel om te debuten in haar handwerkclubje en om in alle rust te kunnen werken. Voor mijn uiteindelijk prestatie heb ik veel profijt gehad van alle stukken vlaai, de bloedworst met appeltjes (voor wat extra rode bloedcellen) en nog meer stukken vlaai.

Kevin, voor een ‘**thuisfront**’ was je erg weinig thuis, maar ja, iemand moet het werk doen natuurlijk. Je was de afgelopen jaren altijd bereid om mijn gemopper aan te horen als ik uitgeput thuiskwam na een loodzware training en als ik weer eens gevallen was, dan probeerde je mijn tranen te drogen en haalde je een pleister. Jij hebt nooit getekend voor het labiele monster waar ik af en toe in veranderde door de combinatie van overtraining, slaaptekort en te weinig eten, dus bedankt voor het feit dat je nooit je koffers hebt gepakt en weer terug bent gegaan naar het beloofde land.

Of ik de afgelopen jaren doping heb gebruikt? Jazeker. In het begin moest ik er absoluut niks van hebben, maar gaandeweg merkte ik dat niet kon concurreren zonder er ook zelf aan mee te doen. Zo heb ik enorme hoeveelheden koffie weggewerkt, nam ik hier en daar een reep chocola en genoot ik af en toe ter ontspanning van een lekker speciaalbiertje. Mijn favoriete **dopingdealers** – die ik echt iedereen kan aanbevelen, want ze leveren echt top spul – zijn Carel en Connie van de Vlaamsche Reus. Zij zijn altijd op de hoogte van de nieuwste ontwikkelingen in bierland, dus grote kans dat je niet gepakt wordt in een dopingtest, en als je op zaterdag koffie bij ze komt halen, dan krijg je er dus gewoon een zelfgebakken soesje bij. Hoogtepunt van de week.

*“Talent wins games, but teamwork and intelligence win championships.” - Michael Jordan*

## A FEW WORDS ABOUT THE AUTHOR

Bregje van der Bolt was born in 1991 in Utrecht in the Netherlands. At elementary school, she was not able to get her 'shoelace tying diploma', which explains the overcompensation she showed later in life. In 2008 she obtained her gymnasium degree cum laude at RSG Pantarijn in Wageningen. She started studying Medicine in Utrecht, but after her first year, she switched to University College in Maastricht, where she followed the track Life Sciences. In 2011, she studied a semester at Queen's University in Kingston, Canada. In 2012 she moved back to Wageningen to start with the master Environmental Sciences, in which she took the specialization track Environmental Systems Analysis. In addition, she did the minor 'Earth Systems and Climate Change', and the minor 'Tipping Points in Aquatic Ecology.' In 2013 she was selected for the Honours Programme of the Netherlands Research School for Socio-Economic and Natural Sciences of the Environment (SENSE). In 2015 she finished her MSc studies cum laude and started her PhD under the supervision of Egbert H. van Nes and Marten Scheffer in the Department of Aquatic Ecology and Water Quality Management in Wageningen.

Bregje is interested in studying (complex) problems from a systems perspective. She has a broad scientific background, which allows her to collaborate with scientists from different disciplines and build bridges between these disciplines.



## LIST OF PUBLICATIONS

**Bregje van der Bolt**, Egbert H. van Nes, Sebastian Bathiany, Marlies E. Vollebregt, and Marten Scheffer. Climate reddening increases the chance of critical transitions. *Nature Climate Change*, 8:478–484, 2018.

Egbert H. van Nes, Babak M.S. Arani, Arie Staal, **Bregje van der Bolt**, Bernardo M. Flores, Sebastian Bathiany, and Marten Scheffer. What do you mean, tipping point? *Trends in Ecology and Evolution*, 2016.

Sebastian Bathiany, **Bregje van der Bolt**, Mark S. Williamson, Tim M. Lenton, Marten Scheffer, Egbert H. van Nes, and Dirk Notz. Statistical indicators of Arctic sea-ice stability—prospects and limitations. *The Cryosphere Discussions*, 2016.



*Netherlands Research School for the  
Socio-Economic and Natural Sciences of the Environment*

# D I P L O M A

*for specialised PhD training*

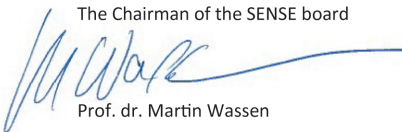
The Netherlands research school for the  
Socio-Economic and Natural Sciences of the Environment  
(SENSE) declares that

***Bregje van der Bolt***

born on 5 April 1991 in Utrecht, The Netherlands

has successfully fulfilled all requirements of the  
educational PhD programme of SENSE.

Wageningen, 10 January 2020

The Chairman of the SENSE board  
  
Prof. dr. Martin Wassen

the SENSE Director of Education  
  
Dr. Ad van Dommelen

*The SENSE Research School has been accredited by the Royal Netherlands Academy of Arts and Sciences (KNAW)*



K O N I N K L I J K E N E D E R L A N D S E  
A K A D E M I E V A N W E T E N S C H A P P E N



The SENSE Research School declares that **Bregje van der Bolt** has successfully fulfilled all requirements of the educational PhD programme of SENSE with a work load of 41.5 EC, including the following activities:

#### SENSE PhD Courses

- o Environmental research in context (2015)
- o Research in context activity: 'Initiating, developing and delivering highly accessible communications on complex societally relevant scientific insights, such as tipping points in the climate' (2015-2018)

#### Other PhD and Advanced MSc Courses

- o Urbino Summer School, Università degli studi di Urbino Carlo Bo (2015)
- o Critical Transitions in Complex Systems: mathematical theory and applications, CRITICS summer school (2016)
- o Bayesian Statistics, PE&RC and SENSE (2017)
- o Basic course in climate time series analysis, Climate Risk Analysis (2017)
- o Scientific writing, Wageningen In'to Language (2017)
- o Consumer-Resource Interactions in Times of Global Environmental Change, PE&RC graduate school and SENSE (2018)
- o Brain based teaching, Wageningen University (2018)

#### Communication your science

- o Scientist in the classroom (2017-2018)
- o Popular science article "Ga niet over één nacht ijs", Nature today (2018)
- o Pitch for Radio programme 'Voor de dag', National broadcast service NPO4 (2018)
- o Art/Science Cross-pollination, WUR and Rietveld Academy (2018)

#### Management and Didactic Skills Training

- o Supervising MSc student with thesis entitled 'Rate-tipping in ecosystem models' (2019)
- o Teaching in the BSc course 'Modelling Biological Systems (2016)' and the MSc course 'Marine Systems' (2018)
- o Guest lecturer in MSc course 'Complexity in ecological systems (2017-2018)
- o Developer of MSc course 'Trending topics in biology and chemistry of soil and water' (2017-2018)

#### Oral Presentations

- o *Climate reddening increases chance of critical transitions*. NESSC-NAC, 13-14 April 2018 Veldhoven, The Netherlands
- o *Climate reddening increases chance of critical transitions*. EGU, 8-11 April 2018, Vienna, Austria

SENSE coordinator PhD education

Dr. ir. Peter Vermeulen

The research described in this thesis was carried out under the programme of the Netherlands Earth System Science Centre (NESSC), financially supported by the Ministry of Education, Culture, and Science (OCW). Printing of this thesis was financially supported by the Aquatic Ecology and Water Quality Management Group of Wageningen University.

**Cover design and artwork:** Lou van Reemst

**Layout:** Bregje van der Bolt & Janine van Bon

**Printed by:** Digiforce || Proefschriftmaken



